2017-07-12

Transport Properties in Porcine Meniscus Fibrocartilage

Kelsey L. Kleinhans
University of Miami, kelseylynn231@live.com

UNIVERSITY OF MIAMI

TRANSPORT PROPERTIES IN PORCINE MENISCUS FIBROCARTILAGE

By

Kelsey L. Kleinhans

A DISSERTATION

Submitted to the Faculty
of the University of Miami
in partial fulfillment of the requirements for
the degree of Doctor of Philosophy

Coral Gables, Florida

August 2017

UNIVERSITY OF MIAMI

A dissertation submitted in partial fulfillment of
the requirements for the degree of
Doctor of Philosophy

TRANSPORT PROPERTIES OF PORCINE MENISCUS FIBROCARTILAGE

Kelsey L. Kleinhans

Approved:

_____ Alicia Jackson, Ph.D. Assistant Professor of Biomedical Engineering	_____ Fotios Andreopoulos, Ph.D. Associate Professor of Biomedical Engineering
_____ Chun-Yuh Charles Huang, Ph.D. Associate Professor of Biomedical Engineering	_____ Francesco Travascio, Ph.D. Assistant Professor of Industrial Engineering
_____ Weiyong Gu, Ph.D. Professor, Chair of Mechanical and Aerospace Engineering	_____ Guillermo Prado, Ph.D. Dean of the Graduate School

KLEINHANS, KELSEY L. (Ph.D., Biomedical Engineering)
Transport Properties of Porcine Meniscus Fibrocartilage (August 2017)

Abstract of a dissertation at the University of Miami.

Dissertation supervised by Professor Alicia Jackson.
No. of pages in text. (164)

The knee meniscus is a complex structure that has been the focus of important and extensive research for many years. The most common areas of study include meniscal structure, meniscal tears, regeneration, and the biomechanical and anatomical forces endured by the meniscus. Although much research has been done regarding these tissues, more is needed in order to fully understand the role that menisci plays in the function and pathophysiology of the human knee. The fibrocartilaginous meniscus plays an essential role in distributing the majority of the load and maintaining not only congruency, but also lubrication in the knee joint. Degeneration of the knee meniscus is commonplace, yet its pathophysiology has not been fully explained.

Because the meniscus is a nearly avascular tissue which lacks blood vessels for the delivery of nutrients, one area of study needing further research is the transport of fluids and solutes through meniscal tissues. In this dissertation, custom experimental methods are used to characterize the transport of solutes and fluids in meniscus fibrocartilage. For each study, we investigated the effects of mechanical strain, tissue anisotropy, and tissue region on the transport behavior in porcine meniscus tissue.

Using a direct permeation experiment, hydraulic permeability was investigated to determine its strain- and/or direction-dependent behavior in porcine meniscus fibrocartilage. Our measured permeability values ($1.53\text{-}1.87\times10^{-15}$ m^4/Ns) are similar to

those in the literature for meniscus tissues. Results indicate that hydraulic permeability is anisotropic, being significantly greater in the circumferential direction than in the axial. Additionally, it was found that with increased compressive strain, there was a significant decrease in hydraulic permeability for all groups studied.

Strain-dependent and anisotropic (i.e., direction-dependent) transport of glucose in porcine meniscus fibrocartilage was investigated using customized chambers to measure the diffusion and partition coefficients. Results indicate that both diffusivity and partitioning of glucose in porcine menisci significantly decrease with increasing compressive strain. Furthermore, diffusivity of glucose was found to be anisotropic, being significantly greater in the circumferential direction than the axial at all strain levels. Using the results from the partitioning and diffusion of glucose, we were able to calculate the effective diffusivity of porcine meniscus fibrocartilage.

Finally, the strain-dependent and anisotropic electrical conductivity and relative ion diffusion was investigated in porcine meniscus fibrocartilage using a four-wire method. Results indicate that the conductivity and diffusion of ions in the meniscus significantly decreases with increasing compressive strain. Additionally, the conductivity and diffusion of ions was found to be significantly anisotropic, being greater in the circumferential directions than the axial direction at all strain levels.

To our knowledge, this is the first study to quantitatively characterize the effects of strain, anisotropy, and region on transport properties in meniscus tissues. In particular, this is first study to measure glucose or ion diffusivity, glucose partitioning, or electrical conductivity in meniscus. The findings of this dissertation greatly enhance the knowledge of fluid and solute transport in the knee meniscus. Given that nutrient transport is critical

for meniscus survival, this information can provide important insight into the functions and mechanisms of meniscus disease and even help identify effective treatment solutions for osteoarthritis.

ACKNOWLEDGEMENTS

There are many people I would like to thank for their support and encouragement over the past years. Without their confidence in me and support of my dreams, this achievement would never have been possible.

I would like to start by thanking my advisor, Dr. Alicia Jackson, for giving me the opportunity to work in the biomechanics lab as a graduate student at the University of Miami. Thank you for always offering me great advice, answering my never-ending stream of questions, and supplying me with the necessary tools to become a better engineer. I am very grateful for the opportunity you provided me to move to Miami and work with you.

I would also like to thank the other members of my committee: Dr. Fotios Andreopoulos, Dr. Weiyong Gu, Dr. Chun-Yuh Charles Huang, and Dr. Francesco Travascio. I am very appreciative of the time you have spent and the advice you have provided while serving on my committee.

Additionally, I would like to extend my sincerest thanks to all of the members of the biomedical engineering department for making work enjoyable. I especially want to thank Lukas for putting up with all of my frustrated noises and for always doing whatever he could to help me succeed, particularly encouraging walks and chocolate when I'm having a bad day. Amaris, I want to thank you for your friendship and for giving me someone to follow by example and look up to as both an engineer and a person. You saved many of my bad days just by going with me on a walk outside and making me laugh. I would also like to thank the BME office staff: Christine, Vivian, Angie, and Melissa. I could always count on all of you to make me smile while I consumed cup after

cup of coffee. I feel as though this degree would not have been possible without all of you. Finally, to my favorite undergrads: Adam, Jeff, and Anthony, thank you guys for your consistent help and insights into why our experiments never seemed to run smoothly.

I have accomplished so many goals in life because of the support of my family: my parents, Kim and Rob, and my sister, Kara. I always enjoyed hearing your reports on my publications and I'm sorry for never taking your advice and naming the pigs we harvested. Thank you all so much for supporting me while I follow my dreams in Miami.

Lastly, I want to thank the two people who have been there for me in so many ways and made it possible for me to love my life in Miami: Liz, you are my best friend and I am so appreciative of your unyielding support and belief in me to succeed. I am constantly blown away by the encouragement you have always given me and never would have survived my move to Miami without meeting you. Sam, meeting you was the best "right swipe" of my life. Thank you for always encouraging me, supporting me, and loving me even through my most difficult days. I never could have achieved this without you guys; I love you both and dedicate this to the two of you.

TABLE OF CONTENTS

LIST OF FIGURES

LIST OF TABLES

CHAPTER 1. SPECIFIC AIMS

1.1 INTRODUCTORY REMARKS

The knee meniscus is a complex structure that has been the focus of important and extensive study for many years. The most common areas of research include meniscal structure, meniscal tears, regeneration, and the biomechanical and anatomical forces endured by the meniscus (Andriacchi et al., 2004; Makris et al., 2011; Sweigart and Athanasiou, 2005). Although much research has been done regarding these tissues, more is needed in order to fully understand the role that menisci play in the function and pathophsyiology of the human knee.

The fibrocartilaginous meniscus of the knee plays an essential role in distributing the majority of the load and maintaining not only congruency, but also lubrication in the knee joint (Makris et al., 2011; Newman et al., 1989; Proctor et al., 1989; Tissakht et al., 1996; Zhu et al., 1994). Degeneration of the knee meniscus is commonplace, yet its pathophysiology has not yet been fully explained. Because the knee meniscus is a nearly avascular tissue which lacks blood vessels in the inner region, termed the white zone, for the delivery of nutrients, one area of study needing further research is the transport of fluids and solutes through meniscal tissues.

This dissertation focuses on highlighting the transport of fluids and solutes through the meniscus extracellular matrix as an integral role in providing the necessary nutrients to cells (Makris et al., 2011). Transport may occur by diffusive processes or by

fluid flow (i.e., convection) through the extracellular matrix and is highly dependent upon tissue structure and composition as well as tissue loading conditions.

Clinical observation has long associated degeneration of the meniscus with the occurrence of osteoarthritis (OA) in the knee, although the mechanisms for linking the two are not well understood (Andriacchi et al., 2004; Berthiaume et al., 2005; Cooper et al., 1994; Fairbank, 1948; Lange et al., 2007; Makris et al., 2011). Given the large socio-economic impact and the high prevalence of OA, determining the role meniscus tissue plays in the onset and progression of the disease is a significant scientific pursuit that may greatly accelerate the development of novel OA treatment and management techniques.

1.2 SPECIFIC AIMS

The **long-term goals** of this project were to (**1**) better understand the pathophysiology involved in the development of knee meniscus injury and degeneration; and (**2**) identify effective treatment solutions for OA. The **overall goal of this research** was to further explore the roles of solute and fluid transport in the nutritional supply and mechanical functioning of the meniscus in order to more fully understand the origins of meniscal degradation. In order to address these goals, the following specific aims were pursued:

Specific Aim #1: To determine the hydraulic permeability of porcine knee meniscus tissues. An apparatus was designed and developed for characterizing the hydraulic

permeability of healthy knee meniscus tissues under varying levels of compressive strain (10%-20%). Anisotropy (axial vs. circumferential) and regional (central region vs. horn region) variations were investigated, as outlined above, and results were correlated with tissue water content and strain. Each sample specimen was compressed 10%-20% strains and includes one of three direction/region combinations: axial central, axial horn, or circumferential central.

Specific Aim #2: To determine the transport properties of glucose in porcine knee meniscus tissues. Using a one-dimensional steady-state diffusion experiment, the apparent diffusivity of glucose in knee meniscus tissues was determined. The glucose diffusivity was measured in healthy tissues under three levels of compressive strain (0%, 10%, and 20%). Additionally, the anisotropic (i.e., direction-dependent) behavior of glucose diffusivity was also examined (axial vs. circumferential) along with regional variation in the axial direction (i.e., central region vs. horn region). Furthermore, the partition coefficient of healthy knee meniscus tissues was determined. An apparatus was developed for measuring the partition coefficient of knee meniscus tissues. The tissues were taken in the axial direction from both the horn and central regions and were again compressed at varying levels of compressive strain (0%, 10%, and 20%). A relationship between glucose transport properties and tissue water volume content (or biochemical content) was established. Following both glucose diffusion and glucose partition coefficient, the effective diffusivity could be calculated using the results from both studies.

Specific Aim #3: To determine the relative ion diffusion coefficient of porcine knee meniscus tissues by using an electrical conductivity study. An apparatus was designed and developed for characterizing the electrical conductivity of healthy knee meniscus tissues under varying levels of compressive strain (0%, 10%, and 20%). Additionally, anisotropy (axial vs. circumferential) and regional variations (central region vs. horn region) were investigated, similar to Specific Aim #2, and results were correlated with tissue biochemical content (e.g., water volume fraction, glycosaminoglycan content). The tissues were taken from healthy pigs and pooled from both medial and lateral menisci. Each individual sample was compressed to one of the three compressive strain levels (i.e., 0%, 10%, or 20%). The electrical conductivity determined in this study was used to calculate the relative ion diffusion coefficient of Na^+ and Cl^- ions.

1.3 CONTENTS OF THIS DISSERTATION

The overall objective of this dissertation was to investigate the transport of fluid and solutes in the knee meniscus, in order to better understand the pathophysiology involved in the development of knee meniscus injury and degeneration. A background of the knee meniscus and its structure, composition, function, and transport properties is given in **Chapter 2**. In order to investigate the objectives of this work, new experimental techniques for investigating nutrient transport in the meniscus have been developed.

First, an experimental approach is developed for measuring the hydraulic permeability of porcine knee meniscus tissues in **Chapter 3**. This method is used to measure not only the permeability under various compressive strains, but also the anisotropic behavior in porcine knee meniscus tissues. Findings are discussed and compared to those in literature for other cartilaginous tissues.

In **Chapter 4**, an experimental method is developed for measuring the strain-dependent diffusion of glucose in meniscus tissues. This method is used to measure not only the diffusivity under various compressive strains, but also the anisotropic behavior of glucose diffusion in porcine knee meniscus tissues. The detailed methods and experimental findings are discussed; results are compared with those in literature.

In **Chapter 5**, a method is developed for determining the strain-dependent partition coefficient in knee meniscus tissues. This method is applied to measure the partition coefficient of glucose in porcine meniscus tissue under three levels of compressive strain. Details regarding the custom apparatus, experimental techniques, and results are fully described.

Chapter 6 investigates the effective diffusion coefficient by utilizing the data gathered in **Chapters 4** and **5**. Utilizing an equation calculated using results from the partition coefficient of glucose, we were able to calculate the relative diffusion coefficient using the apparent diffusivity found previously.

A new experimental approach is developed for measuring the electrical conductivity and relative ion diffusion coefficient in knee meniscus tissues in **Chapter 7**. A custom-chamber was developed to measure the resistance across tissues and used to

calculate both the electrical conductivity and relative ion diffusion coefficient in porcine knee meniscus tissues under three levels of compressive strain and in two directions.

Finally, in **Chapter 8**, the major findings of these investigations are summarized. Recommendations for future research initiatives in the field are also presented.

CHAPTER 2. BACKGROUND AND SIGNIFICANCE

2.1 FUNCTIONS OF THE KNEE MENISCUS IN BIOMECHANICS

Meniscus tissues exhibit anisotropic mechanical behavior when undergoing forces in shear, tension, and compression (Chia and Hull, 2008; Fithian et al., 1990; Gabrion et al., 2005; Leslie et al., 2000; Nguyen and Levenston, 2012; Proctor et al., 1989; Skaggs et al., 1994; Spilker et al., 1992; Sweigart et al., 2004; Tissakht and Ahmed, 1995). Along with playing a crucial role in load-bearing, the meniscus is also involved in load transmission, shock absorption, lubrication and nutrition of articular cartilage (Proctor et al., 1989). Everyday activities (e.g., walking, standing, running, etc.) compress the menisci, but due to the wedge shape of the tissue, these vertical compressive forces are able to be converted into horizontal hoop stresses, see **Figure 2-1**. Simultaneously, shear forces are also developed between the collagen fibers when the meniscus is deformed radially (Sweigart and Athanasiou, 2001).

Several studies have been completed researching the forces exerted on knee meniscus tissues, quantifying the properties of these tissues in human and animal models. According to these studies, the average meniscus resists axial compression with an aggregate modulus of 100-150 kPA (Sweigart et al., 2004). The tensile modulus is approximately 100-300 MPa circumferentially and approximately 10-30 MPa radially. The shear modulus was found to be approximately 120 kPa (Fithian et al., 1990). Studies have also shown that the meniscus absorbs approximately 40-90% percent of the load

during walking with 40-50% coming from the medial side and 60-70% coming from the lateral meniscus (Aagaard and Verdonk, 1999; Seedhom et al., 1974; Walker and Erkman, 1975). These properties of shock absorption protect the cartilaginous surfaces from both damaging effects and degeneration.

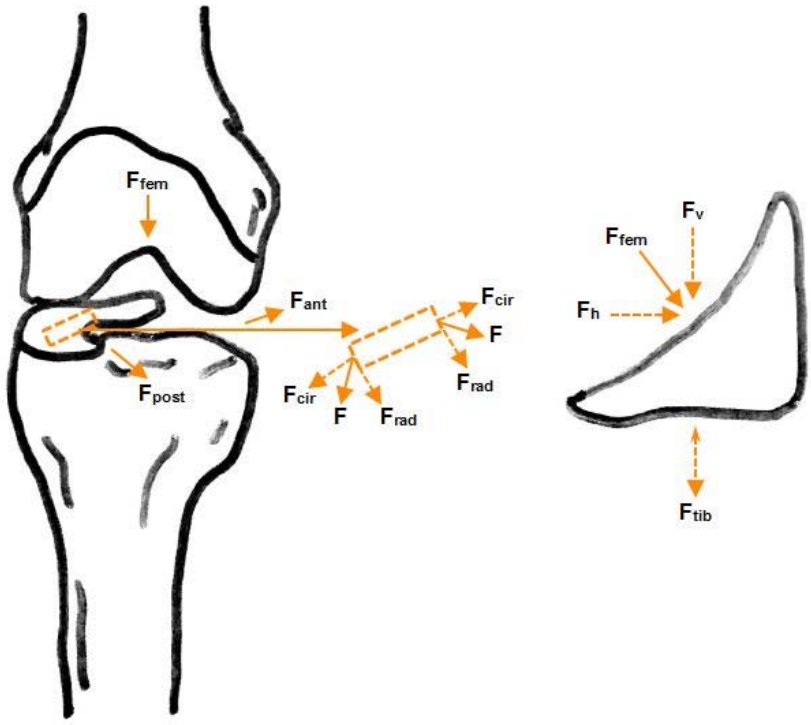

Figure 2-1 Free body diagram of the forces acting on the knee meniscus during loading (for simplicity, only the lateral meniscus is shown). Adapted from (Makris et al., 2011).

2.2 The Knee Meniscus

2.2.1 Anatomy

The knee joint is the largest joint in the body and is comprised of a medial and lateral meniscal component situated between the femoral condyle and the tibial plateau (Kohn

and Moreno, 1995). The complex tissue consists of cells, extracellular matrix (ECM) molecules, and region-specific innervation and vascularization. The lateral and medial menisci are critical components of a healthy knee joint, playing an essential role in the distribution of load, maintaining congruency, and lubrication (Makris et al., 2011; Newman et al., 1989; Proctor et al., 1989; Tissakht et al., 1996; Zhu et al., 1994).

As shown in **Figure 2-2**, the lateral and medial menisci are held in place by the anterior cruciate ligament, the posterior cruciate ligament, the transverse ligament, and the lateral and medial collateral ligaments (Kusayama et al., 1994; Makris et al., 2011). The surface of the healthy meniscus is smooth and glossy-like (Ghadially et al., 1978).

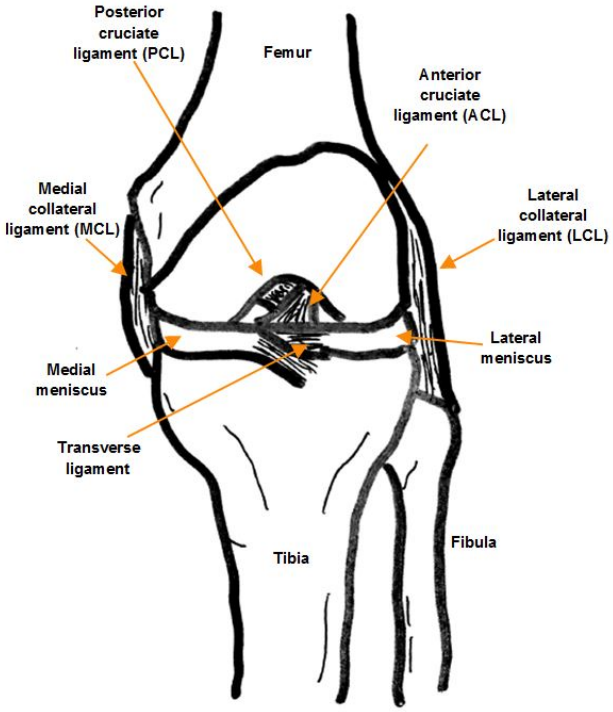

Figure 2-2 The knee meniscus is situated between the femur and the tibia. Crossing the meniscus are various ligaments, which aid in stabilizing the knee joint Adapted from **(Makris et al., 2011)**.

Medial and lateral menisci have very different dimensions: lateral menisci in humans are approximately 32.4-35.7 mm in length and 26.6-29.3 mm wide, while medial menisci measure approximately 40.5-45.5 mm long and 27 mm wide (Makris et al., 2011; McDermott et al., 2004; Shaffer et al., 2000). The lateral menisci display a greater variety in size, shape, thickness, and mobility than the medial, though both are roughly wedge-shaped and semi-lunar (Greis et al., 2002), see **Figure 2-3**. Due to the fact that the medial meniscus is weaker than the lateral under tensile load, the medial meniscus is damaged or diseased much more frequently than the lateral (Sweigart et al., 2004).

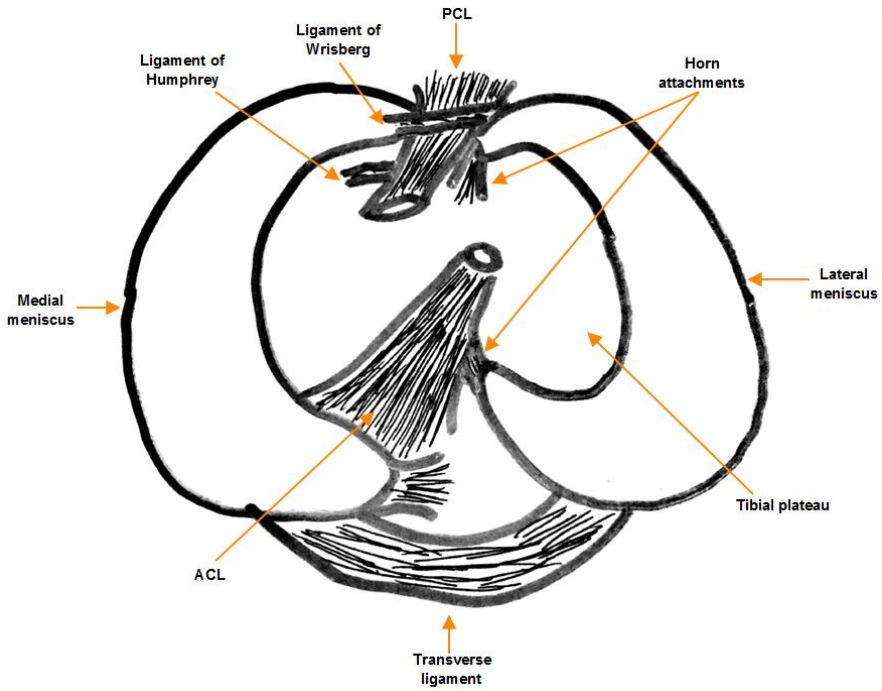

Figure 2-3 Anatomy of the meniscus: superior view of the tibial plateau Adapted from **(Makris et al., 2011)**.

One of the unique properties of knee meniscus tissue is its lack of full vascularization. During prenatal development until shortly after birth, the meniscus is fully vascularized (Makris et al., 2011). However, vascularization appears to almost

completely subside thereafter. Research has shown that at 10 years of age, vascularization is present in 10-30% of the tissue, and at maturity, only at the peripheral 10-25% of tissue (Clark and Ogden, 1983). This lack of vascularization in mature meniscal tissues points to the importance of diffusion for the transport of nutrients through the tissues with increasing age. The meniscus is known to have zones corresponding to different levels of vascularization known as the red-red zone, red-white zone, and the white-white zone. The red-red zone is fully vascular and has sufficient blood flow through which nutrients and fluid can be carried. The red-white zone is on the border of the vascularized tissue regions and has a generally sufficient flow of nutrients and fluids. Finally, the white-white zone is the mostly avascular region, with a very poor flow of nutrients and fluids (Brindle et al., 2001; Cannon and Vittori, 1992).

2.2.2 Biochemical Content

The knee meniscus is a biphasic composite material consisting of interstitial fluid and a porous, fiber-reinforced solid matrix. Water is the most abundant component of the knee meniscus, accounting for 63-75% of the total weight (Proctor et al., 1989). The majority of the rest of the tissue is made up of differing levels of collagen, glycosaminoglycans (GAG), DNA, adhesion glycoproteins, and elastin (Herwig et al., 1984; Proctor et al., 1989). Physiological conditions, including mechanical forces on the ECM and changes in the composition resulting from tissue degeneration, can greatly alter the physical signals at the cellular level within the tissue (Mow et al., 1999; Urban, 2000). The levels of these

components may also depend on age, prior injuries, and other pathological conditions (McDevitt and Webber, 1990; Sweigart and Athanasiou, 2001).

Type I collagen fibers are responsible for the dominant meniscal structural scaffolding (Brindle et al., 2001), while three other collagen fiber types in total compose the meniscus and are arranged to convert the compressive loads into circumferential stresses. In the outer layer, the fibers run radially, helping to reduce shearing or splitting. The middle layer consists of fibers running parallel or circumferentially to resist the circumferential stresses during weight bearing. Finally, the deep inner fibers are aligned parallel to the periphery (Brindle et al., 2001).

Proteoglycans (PGs) play important roles in the tissues, including hydration, compressive stiffness, and elasticity (Brindle et al., 2001). Meniscal shock absorption, one of the knee meniscus' primary roles, is dependent on the exudation of water out of the ECM (Brindle et al., 2001). As a viscoelastic tissue, meniscal tissues display creep properties and deform over time under loads of great frequency or duration.

2.2.3 MENISCUS PATHOPHYSIOLOGY

In the United States, meniscal tears represent the most common intra-articular knee injury, with the mean annual incidence increasing from 61 in 100,000 in 1985 to 8.27 in 1,000 inhabitants (Baker et al., 1985; Jones et al., 2012; Morgan et al., 1991) and the majority resulting in meniscectomy. With a male to female incident ratio between 2.5:1 and 4:1 (Baker et al., 1985), men are more prone to injuries (Bhattacharyya et al., 2003), although the overall incidence level peaks around 20-29 years of age for both sexes. With

a high prevalence of meniscal injuries, it has been reported that approximately 850,000 surgical procedures are performed on the meniscus each year (Arendt et al., 1999).

In older patients, meniscal lesions occur most often in middle-aged and elderly patients. Tears of this kind generally occur from long-term degradation and may lead to joint swelling, joint line pain, and mechanical blocking (Barrett et al., 1998). Along with general degradation, OA has been shown to have a high correlation to the prevalence of meniscal lesions (Englund et al., 2007). As vascularization has been shown to decrease with age, the successful application of meniscus repairs in older patients is much less promising than in younger age groups (Barrett et al., 1998; Eggli et al., 1995). This lack of vascularization decreases the levels of nutrients available to the inner areas of the knee meniscus, thus resulting in increased opportunity for degeneration and/or lesions and injuries.

2.3 Knee Meniscus and Osteoarthritis

Knee OA involves a complex chain of events that can be credited to either trauma or progressive degeneration (Abraham and Donahue, 2013). With increasing evidence, various joint structures have been identified as potential initiation pathways, including cartilage, bone, ligaments, synovial fluid, and the meniscus (McGonagle et al., 2010). Most importantly, the meniscus has been found to be crucial in maintaining joint health and in the role of preventing OA (Fairbank, 1948).

As previously stated, clinical observation has long associated degeneration of the meniscus with the occurrence of advanced OA in the knee. Studies have shown that impaired mechanical functioning of the meniscus can result in abnormal joint loading, which translates into excessive joint loads transmitted to the articular cartilage, thus resulting in a risk for the development of OA (Bedi et al., 2010; Bhattacharyya et al., 2003). Affecting over 15.8 million Americans, OA is the most common form of arthritis in humans (Pai et al., 1997). Several factors appear to correlate with the rate of progression in knee OA: pathogenic factors, impulsive loading, and the breakdown of protective, stabilizing mechanisms.

Studies have shown that one in four people over the age of 55 suffer from knee pain and by the age of 65, 30% of men and 40% of women have radiographic changes of knee OA (McAlindon et al., 1993). While studying the impact of age versus disease on proprioception, findings suggested that age-related declines in proprioception may precede the development of knee OA and, possibly, predispose its development (Pai et al., 1997). This idea that the deterioration of the knee joint may lead to a rapid progression of knee OA has many implications for the future care of patients suffering from OA. For example, there may be a need for preventative therapies that enhance proprioception and neuromuscular joint protection for high-risk elderly patients.

Future research is needed in order to fully understand the role the knee meniscus plays in the onset and progression of this disease. Determination of this role could lead to better OA treatment and management techniques and better inform innovative treatment strategies for tissue regeneration and/or repair.

2.4 NUTRITIONAL TRANSPORT IN THE KNEE MENISCUS

2.4.1 PATHWAYS OF TRANSPORT

Due to the limited blood supply in meniscus tissues, transport of fluid and solutes through the extracellular matrix plays an integral role in providing necessary nutrients to cells (Makris et al., 2011). However, few studies have investigated transport properties in knee meniscus tissues. Danzig *et al*. found that continuous passive motion does not significantly affect meniscal nutrition, indicating that diffusion is an important mechanism for transport of nutrients in the tissue (Danzig et al., 1987). Most recently, Travascio *et al.* measured the diffusion coefficient of fluorescein in meniscus fibrocartilage using fluorescence recovery after photobleaching (FRAP), and found an anisotropic trend (Travascio et al., 2009b).

Additionally, a study performed by Herwig et al. found that the changes in water content of human knee joint menisci are dependent on the stages of degeneration with a correlation coefficient of r=0.91 (Herwig et al., 1984), see **Figure 2-4**. Thus, since the degeneration of the knee meniscus is thought to be correlated with the onset of OA, the degeneration of the knee is also correlated to the diffusivity due to the changes in water content. The water content in this study by Herwig increased from about 70 to 85% wet weight of tissue with increasing degeneration. Also of note, this study did not find any age-detectable changes in water content (Herwig et al., 1984).

2.4.2 MECHANISMS OF TRANSPORT

In avascular cartilaginous tissues, diffusion is believed to be the main mechanism of transport for small solutes (Maroudas et al., 1975; Urban et al., 1978; Urban et al., 1982). To understand the transport mechanisms and pathways in knee meniscus, determining the diffusion coefficient (i.e., diffusivity, a measure of solute mobility) for small solutes (e.g., glucose) is important. Several investigators have examined the mechanical properties in meniscus fibrocartilage from human and animal sources. These studies have found that the meniscus exhibits anisotropic mechanical behavior in tension, compression, and shear loading conditions (Chia and Hull, 2008; Fithian et al., 1990; Gabrion et al., 2005; Leslie et al., 2000; Nguyen and Levenston, 2012; Proctor et al., 1989; Skaggs et al., 1994; Spilker et al., 1992; Sweigart et al., 2004; Tissakht and Ahmed, 1995). However, few studies have investigated transport properties in the meniscus. Recently, Travascio *et al.* used fluorescence recovery after photobleaching (FRAP) to measure the diffusion coefficient of fluorescein in meniscus fibrocartilage, finding an anisotropic trend (Travascio et al., 2009b). Moreover, Danzig et al found that continuous passive motion does not significantly affect meniscal nutrition, indicating that diffusion is an important mechanism for transport of nutrients in the tissue (Danzig et al., 1987). In this study, we compared the anisotropic transport of solutes and fluids under various levels of compressive strain and in various areas/components of the meniscus.

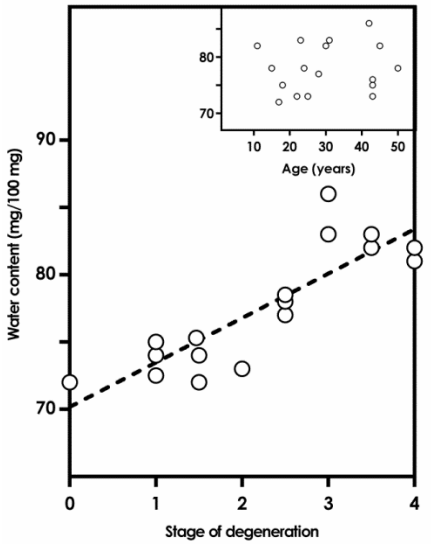

Figure 2-4 Changes of water content (g/100 g wet weight of tissue) of human knee joint menisci dependent on the stages of degeneration. Adapted from **(Herwig et al., 1984)**.

The solute concentration in a porous media relative to the concentration of solute in the surrounding fluid at equilibrium is known as the partition coefficient. Because it is one of the governing factors in determining the rate of movement of solutes between an external solution and the tissue, knowledge of this property is important and pertinent to our overall goals. Several studies have been done on the partitioning of small molecules, such as glucose, urea, and ions, and large molecules, such as myoglobin, serum albumin, and dextran, in cartilage tissues (Fetter et al., 2006; Maroudas, 1976; Nimer et al., 2003; Quinn et al., 2000; Roberts et al., 1996; Torzilli et al., 1998). However, this is the first study to our knowledge to report on the strain-dependent, region-specific glucose partitioning in meniscus fibrocartilage.

Furthermore, electrical conductivity is an important material property of biological tissues depending on ion diffusivity and ion concentration within the tissues.

These values are functions of the tissue composition and structure (Chammas et al., 1994; Eisenberg and Grodzinsky, 1988; Grodzinsky, 1983; Gu et al., 1998; Hasegawa et al., 1983; Helfferich, 1962; Maroudas, 1968). By using electrical conductivity to estimate the relative ion diffusivity in knee meniscus tissues and its relationship with tissue composition and structure, information can be gathered on ion transport in the meniscus. Previous studies have investigated the electrical conductivity in order to estimate the relative ion diffusivity in other cartilaginous tissues obtained from both human and animal sources (Jackson et al., 2009a; Kuo et al., 2011). Additionally, several studies have found a correlation between the electrical conductivity and the tissue water content with a decrease in water content associated with a decrease in conductivity (Gu et al., 2002; Jackson et al., 2009a; Jackson et al., 2006; Lai et al., 1991). However, to our knowledge, no study has reported on the anisotropic or inhomogeneous behavior of relative ion diffusivity or on the electrical conductivity in the knee meniscus. Such information is necessary to better clarify the transport environment in meniscus tissue and thus more clearly understand tissue pathology. In the present study, the electrical conductivity was measured and used to determine the relative ion diffusion coefficient in porcine knee meniscus.

Finally, an additional transport property that is important to cartilaginous tissues and knee meniscus tissues, in particular, is hydraulic permeability. This property governs the rate of fluid transport in cartilaginous tissues, thus influencing cellular nutrition and the viscoelastic behaviors of the tissue. Previous studies have looked at the effects of compressive strain (Chen et al., 2001; Frank and Grodzinsky, 1987; Jurvelin et al., 2003; Mow et al., 1984; Reynaud and Quinn, 2006) and anisotropy (Gu et al., 1999; Jurvelin et

al., 2003; Reynaud and Quinn, 2006) on hydraulic permeability in other cartilaginous tissues, such as the intervertebral disc, but to our knowledge few studies have looked at the anisotropic hydraulic permeability of knee meniscus tissues (Joshi et al., 1995; LeRoux and Setton, 2002; Mansour and Mow, 1976; Martin Seitz et al., 2013; Proctor et al., 1989). The effect of compressive strain on the hydraulic permeability of human knee meniscus was studied by Seitz et al., and found that on average, the mean permeability of the lateral and medial samples decreased with increasing strain (Martin Seitz et al., 2013). LeRoux and Setton studied the hydraulic permeability of canine meniscus tissues in tension and found that anisotropy did not significantly affect the results (LeRoux and Setton, 2002). In the present study, the hydraulic permeability of porcine knee meniscus tissues was determined using a direct permeation method, by applying a flow rate across the specimen and measuring the resulting pressure difference.

2.5 Effect of Mechanical Loading on Knee Meniscus

Previous studies have investigated the load bearing capabilities of the knee meniscus (Fairbank, 1948; Johnson et al., 1974; Krause et al., 1976; Morrison, 1969; Walker and Erkman, 1975). These studies found that the meniscus takes part in the load-bearing mode of the knee joint, by observing the joint after meniscectomy (Kurosawa et al., 1980).

One study in particular found that the maximum joint force during level walking was approximately 4 times the body weight of an individual (Morrison, 1969). Another study found that when the contact side is larger on the medial side than the lateral, the meniscus participates in load-bearing actions from small loads (Walker and Erkman, 1975). These studies, amongst others, outline the physical impacts the meniscus undergoes during daily activities and the importance of having healthy, functioning knee joints. Because the meniscus undergoes numerous forces during normal daily activities, it is important to understand the effects of mechanical loading on transport properties in the tissues. In these studies, we investigate the strain-dependent fluid and solute transport properties in porcine meniscus.

2.6 Significance and Clinical Relevance

Osteoarthritis is a debilitating joint disease that occurs in a large portion of the population over 60 years old (Berthiaume et al., 2005). An estimated 54 million adults in the United States are affected by some form of OA (Barbour et al., 2017), and this number is expected to jump to over 78.4 million by 2040. According to a 2009 study, medical care in the United States averages roughly $185.5 billion per year for OA patients (Kotlarz et al., 2009). Based on a 2005 study, in the United States alone, the costs of treatment were estimated to be roughly $16,146 per patient (White et al., 2008).

The research presented here attempts to begin clarifying the correlation between knee meniscus degeneration and the onset of OA. This impact is significant because it is

the first step in understanding the connection between the structure and function of the knee and developing possible treatments and/or preventative techniques. Research also helps determine the role of knee meniscus injuries due to compressive strains and/or degenerating tissues in leading to OA. Finally, a better understanding of the mechano-electrochemical properties elicits more information regarding the composition and structure of knee meniscus tissues which will be useful for tissue engineering approaches to meniscal treatment. Thus, important advances in the treatment and prevention of OA with regard to knee meniscus tissues are expected.

The following studies provide quantitative information regarding fluid and solute transport in meniscus tissue, which will help to offer important insight into the pathophysiology of meniscus degeneration and related OA in the knee, and will inform new strategies for the restoration of tissue function and disease treatment. Since meniscal degeneration is a common occurrence that results in a loss of proper joint biomechanics, this research will play a contributing role in understanding the onset of OA.

CHAPTER 3. MEASUREMENT OF STRAIN-DEPENDENT AND ANISOTROPIC HYDRAULIC PERMEABILITY IN KNEE MENISCUS TISSUES

3.1 INTRODUCTORY REMARKS

The transport of fluid within the knee meniscus is crucial to its viscoelastic behavior, cellular nutrition, and biomechanical properties. Therefore, it is necessary to investigate the kinetics of fluid flow in the meniscus in order to better understand the behaviors of both healthy and degenerated knee meniscus.

Hydraulic permeability is an important material property for hydrated soft tissues such as the knee meniscus. It governs the rate of fluid transport processes in cartilaginous tissues (Gu et al., 1993, 1998; Lai and Mow, 1980; Mow et al., 1980), which can influence cellular nutrition and tissue viscoelastic behaviors (Armstrong and Mow, 1982; Gu et al., 1993; Lai and Mow, 1980; Maroudas, 1979; Setton et al., 1993; Urban et al., 1977). Additionally, theoretical models have shown that the hydraulic permeability of charged hydrated tissues is related to water volume fraction, tissue fixed charge density, ion diffusion coefficients, and the frictional coefficient between water and the extracellular matrix (Armstrong and Mow, 1982; Gu et al., 1993; Lai and Mow, 1980; Maroudas, 1979). These, in turn, are functions of tissue structure (e.g., collagen fiber organization) and composition (e.g., water content).

Previously, the permeability coefficient has been studied in the IVD and other cartilaginous tissues from several species (e.g., bovine, human, porcine, etc.). For articular cartilage, values were found to be in the order of 10^{-15} m^4/Ns range (Ateshian et

al., 1997; Athanasiou et al., 1994; Athanasiou et al., 1995; Bursac et al., 1999; Froimson et al., 1997; Gu et al., 2003a; Jurvelin et al., 2003; Korhonen et al., 2002; Mansour and Mow, 1976; Mow et al., 1980; Reynaud and Quinn, 2006; Soltz and Ateshian, 2000; Wu et al., 2015; Yuan et al., 2011) and for knee meniscus, values were in the range of 0.81-6.2 x 10^{-15} m^4/Ns (Joshi et al., 1995; LeRoux and Setton, 2002; Martin Seitz et al., 2013; Proctor et al., 1989; Sweigart and Athanasiou, 2005). However, to our knowledge, limited information has been published regarding the strain-dependent, anisotropic, and region-specific permeability of healthy porcine knee meniscus tissues.

Therefore, the objectives of this study were to measure the hydraulic permeability coefficient of porcine meniscus tissues in two major directions (axial and circumferential), and to investigate the effects of location (medial vs lateral and horn vs central) on the permeability behavior of porcine meniscus. Knowing the hydraulic permeability of this tissue is important because many knee joint problems, such as OA, are associated with mechanical failure of the meniscus.

3.2 THEORETICAL APPROACH

Darcy's law describes the transport of fluid through a porous (permeable) material under a pressure gradient. This is shown by:

$$j_v = -k\frac{dp}{dx} \qquad \textbf{(3-1)}$$

where j_v is the flux of the fluid volume in the x-direction, p is the fluid pressure, and k is the hydraulic permeability. The flux is defined as the volume flow rate per unit area, while the volume flow rate is defined as the volume of transported fluid over time.

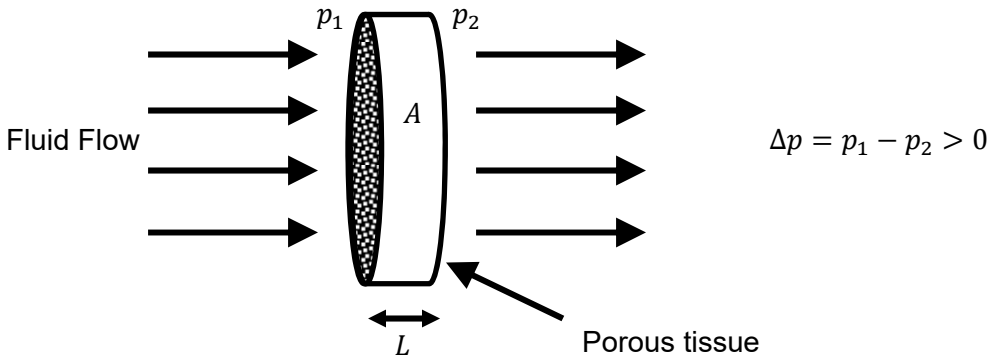

Figure 3-1 Schematic drawing of the fluid flow through a porous media (in this case, porcine meniscus tissue). The pressure difference across the tissue can be used along with the tissue thickness, tissue cross-sectional area, and fluid flow rate to calculate the hydraulic permeability.

The volumetric flow rate, Q, through the porous media is a function of the pressure difference across the sample, the cross-sectional area of the sample, A, and the thickness of the sample, L. It also depends on the hydraulic permeability of the sample:

$$Q = kA\frac{\Delta p}{L} \tag{3-2}$$

The volume flux of fluid flow through the porous media is the volume flow rate per area:

$$j_v = \frac{Q}{A} = k\frac{\Delta p}{L} \tag{3-3}$$

Therefore, the hydraulic permeability, k, can be determined by:

$$k = \frac{QL}{\Delta pA}, \quad \textbf{(3-4)}$$

where Q is the volumetric flow rate (volume per unit time), L is the sample thickness, Δp is the pressure difference across the sample, and A is the cross-sectional area of the tissue sample. Because the value of hydraulic permeability of cartilaginous tissue is very low, a precise measurement is always a challenge. The hydraulic permeability of a sample can be determined by applying a constant volumetric flow rate and measuring the pressure difference across the sample in a 1-D permeation test (Gu et al., 1999; Maroudas et al., 1968; Weiss and Maakestad, 2006).

3.3 Materials and Methods

3.3.1 Design of Experimental Apparatus

A custom-designed chamber was 3D printed using a Stratasys 3D Printer to be used in the hydraulic permeability experiments, see **Figure 3-2 - 3.5**. The customized chamber was used to measure hydraulic permeability by simultaneously applying a fluid flow across the sample and measuring the resulting fluid pressure difference. The chamber set up included two pressure transducers, a syringe pump, and a digital flow meter, as seen in **Figure 3-2 - 3.5**.

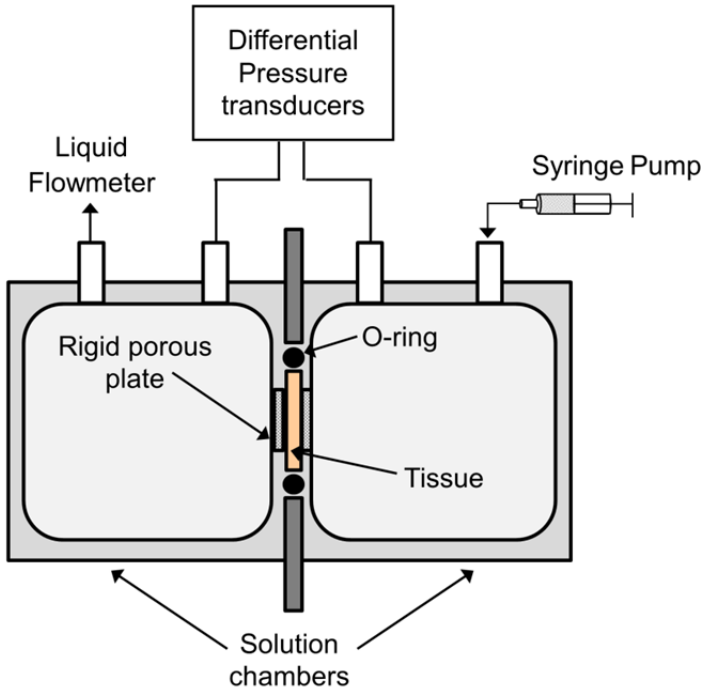

Figure 3-2 Schematic drawing of the parts of the hydraulic permeability experiment. The pressure transducers were connected to strain gage meters that were able to output the pressure on both sides of the tissue.

Figure 3-3 Photograph of the hydraulic permeability system including the syringe pump, the two pressure transducers and strain gage meters, the chamber, and the flow meter.

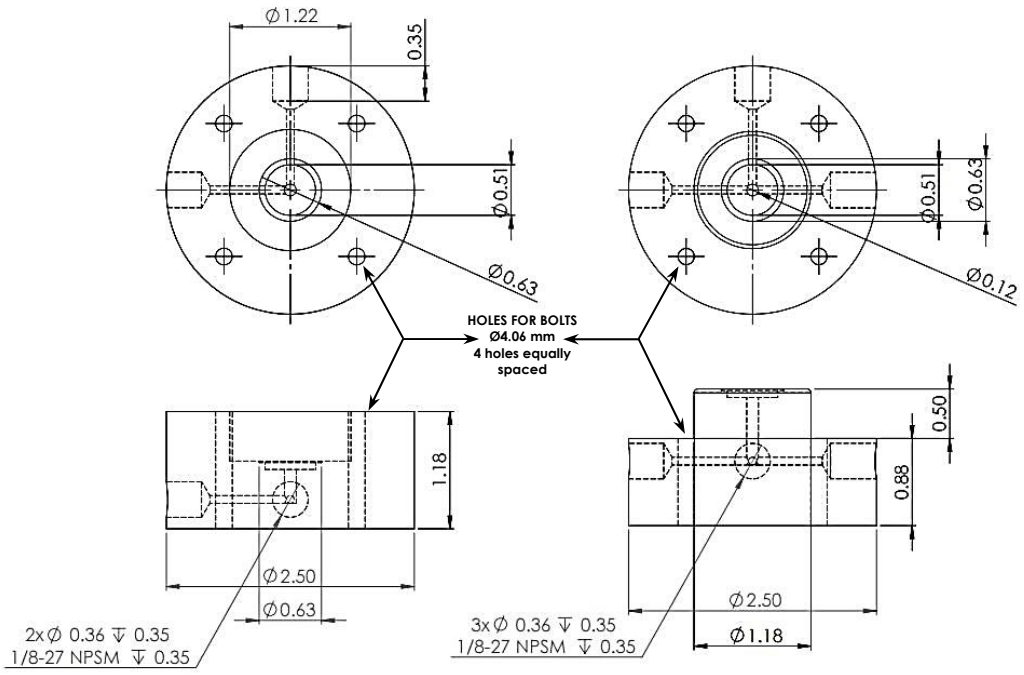

Figure 3-4 Engineering drawings for the permeability chamber used in this experiment.

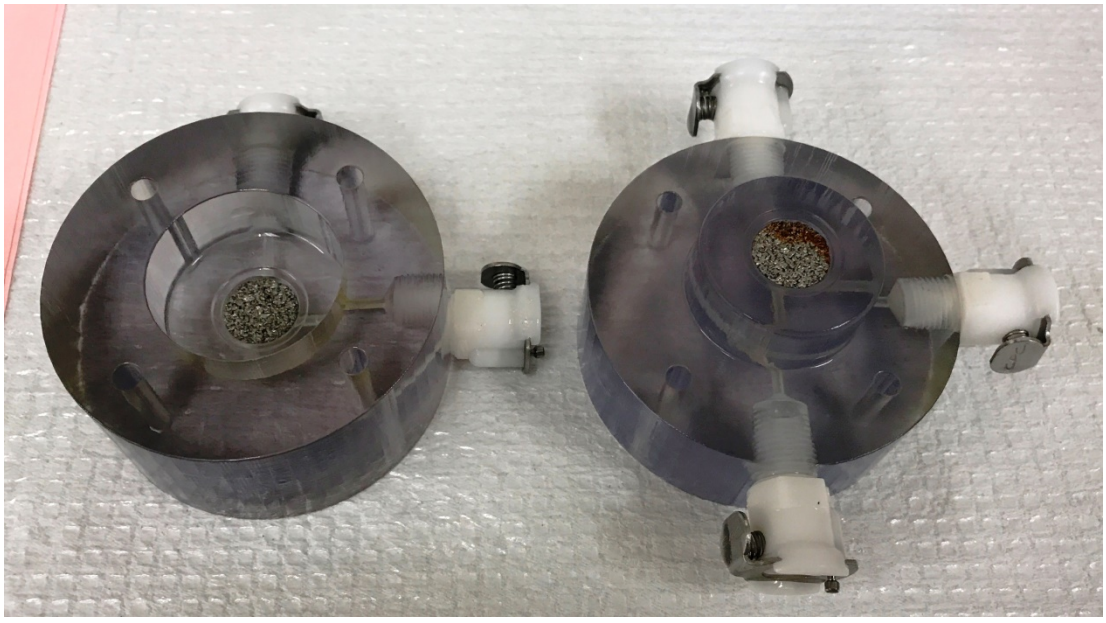

Figure 3-5 Photograph of the hydraulic permeability chamber showing both chamber halves open with no tissue.

3.3.2 SPECIMEN PREPARATION

Porcine knee meniscus samples were obtained from a frozen tissue bank (Animal Technologies, Tyler, Texas), see **Figure 3-6**. They were extracted from the knees of healthy pigs (approximately 100kg, 20-25 weeks old, male and female).

Figure 3-6 Photograph of a porcine knee meniscus tissue sample. Meniscus tissues were taken from both the left and right knees and both medial and lateral menisci were studied.

A total of 30 menisci were harvested from 15 knees. Cylindrical samples were excised in the axial central (AC), axial horn (AH), and circumferential central (CC) sections of both the medial and lateral components, n=15 for each group (6 groups = 3 locations/directions x 2 components), see **Figure 3-7**. Each specimen was cut to a diameter of 6mm and a thickness of approximately 1mm using a corneal trephine punch (Biomedical Research Instruments, Inc., Malden, MA) and sledge microtome (Model

SM2400, Leica Instruments, Nussloch, Germany) with freezing stage (Model BFS-30, Physitemp Instruments, Inc., Clifton, NJ). The height of the specimens was measured using a custom current-sensing micrometer that works by using a capacitive sensor to read the height of the tissue to the nearest 0.001mm. Each specimen was tested under static compressive strains varying from 10-20% (i.e., compressed to a final height of 0.9mm). Each group had 15 samples, for a total of 90 hydraulic permeability specimens.

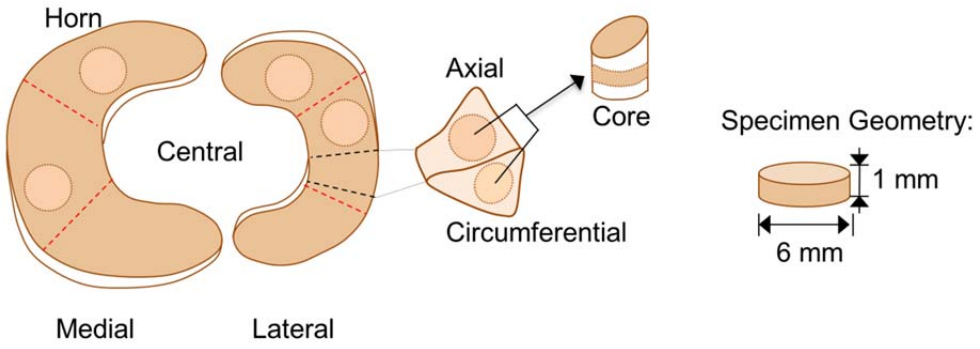

Figure 3-7 Schematic drawing of the meniscus tissues with the sections, direction, and sizes of specimens labeled.

3.3.3 Water Content Measurement

The water volume fraction of undeformed specimens was measured using a buoyancy method(Gu et al., 1996; Gu et al., 1997). The weight of the specimen in air, W_{wet}, and in phosphate buffered saline (PBS), W_{PBS}, were measured using a density determination kit of an analytical balance (Model ML104, Mettler Toledo, Columbus, OH) prior to experimentation, see **Figure 3-8**. Following permeability measurements, specimens were lyophilized and the weight of the dry specimen, W_{dry}, was measured.

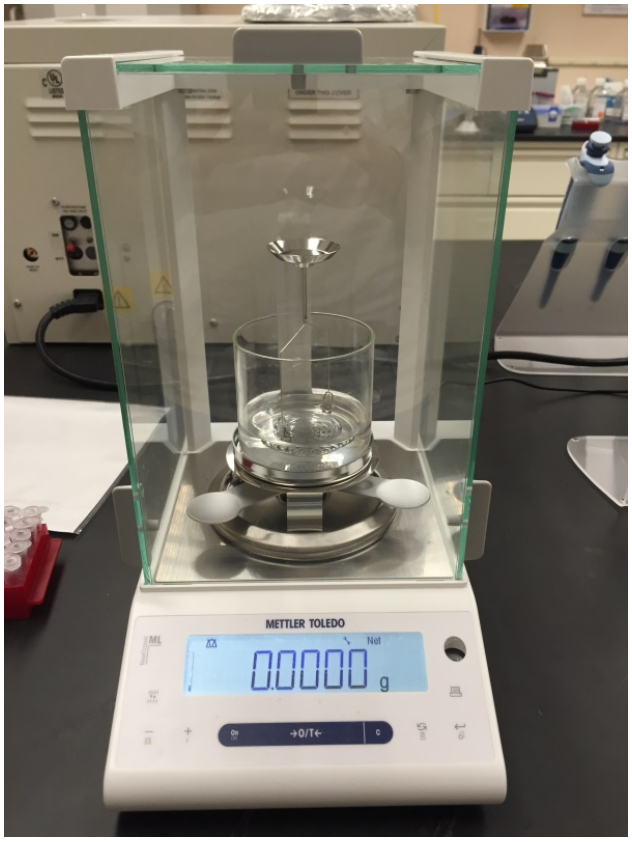

Figure 3-8 Photograph of the Density Determination Kit of an analytical balance. This balance was used to calculate the tissue water volume fraction of all specimens by taking the wet weight (in air), the weight in PBS, and the dry weight (post-lyophilization) and utilizing **Equation (3-5)**.

The volume fraction of water, ϕ_o^w, of the specimens was then calculated by:

$$\phi_o^w = \frac{W_{wet} - W_{dry}}{W_{wet} - W_{PBS}} \frac{\rho_{PBS}}{\rho_{H2O}}, \tag{3-5}$$

where ρ_{PBS} and ρ_{H2O} are the mass densities of PBS and water, respectively. The volume fraction of water in the compressed tissue (ϕ^w) can then be estimated based on the tissue dilatation, e (Lai et al., 1991):

$$\phi^w = \frac{\phi_o^w + e}{1 + e}, \quad \textbf{(3-6)}$$

wherein for one-dimensional confined compression, the relative volume change is related to deformation by $e(= J - 1)$ where J is the ratio of the current tissue volume to the undeformed tissue volume (Jackson et al., 2008; Lai et al., 1991). The dilatation is thus equal to the compressive strain (e.g., for 10% compressive strain, $e = -0.1$).

3.3.4 Measurement of Hydraulic Permeability

Prior to experiments, the samples were loaded in the chamber ensuring the proper compressive strain based on the size of the tissue chamber. Compression was necessary in order to seal the tissue within the o-ring. The hydraulic permeability was then measured by applying a flow rate of 7 μL/min across the sample using a high precision syringe pump (Cole Parmer Single-Syringe Infusion Pump EW-74900-00, Vernon Hills, IL). The flow rate was verified by a liquid flow meter (Sensirion SLG0150, Westlake Village, CA). The resultant pressure difference was measured via two pressure transducers (Omega Engineering Inc., Stamford, CT) and recorded. The hydraulic permeability was then calculated using **Equation (3-4)**.

3.3.5 Statistical Analyses

A total of 15 specimens were tested (n=15) for each of the six groups. Two independent variables were studied: direction and regional variation. Statistical significance between groups was determined by two-way repeated measures ANOVA analysis of variance tests

using IBM SPSS Statistics 22 (International Business Machines Corp., Armonk, NY) with alpha level set at $p<0.05$; sample size was set to n=15.

One-way ANOVA was also performed to determine if water volume fraction and height measurements differed significantly between the three test groups (AC, AH, and CC). Regression analysis was performed to determine if the relationships between permeability and water volume fraction and strain level were statistically significant.

3.4 RESULTS

A total of 90 specimens were measured, with an average uncompressed water volume fraction of 0.71 ± 0.04; results for all groups are shown in **Table 3-1** and **Figure 3-9**. The relationship between static compressive strain and hydraulic permeability for all groups is shown in **Figure 3-10**. There was a significant negative linear correlation between hydraulic permeability and compression level (AC: $R^2 = 0.7490$, AH: $R^2 = 0.6850$, CC: $R^2 = 0.5649$; $p<0.05$). In addition, hydraulic permeability was significantly greater in the circumferential direction than the axial direction for central specimens ($p<0.05$) in the lateral meniscus.

Location	Component	N	Strain (%)	φ^w	κ ($\times 10^{-15}$ m^4/Ns)
AC	Medial	15	12.02 ± 2.20	0.67 ± 0.04	1.65 ± 0.05
	Lateral	15	10.76 ± 2.71	0.68 ± 0.05	1.68 ± 0.07
AH	Medial	15	12.47 ± 2.43	0.68 ± 0.04	1.65 ± 0.06
	Lateral	15	11.24 ± 2.03	0.69 ± 0.04	1.67 ± 0.04
CC	Medial	15	11.56 ± 2.61	0.67 ± 0.06	1.70 ± 0.08
	Lateral	15	12.26 ± 2.52	0.67 ± 0.05	1.71 ± 0.07

Table 3-1 Results for hydraulic permeability in porcine knee meniscus tissues for the three groups tested (axial central (AC), axial horn (AH), circumferential central (CC)) and between the medial and lateral components of the tissues. All results are shown as mean ± standard deviation.

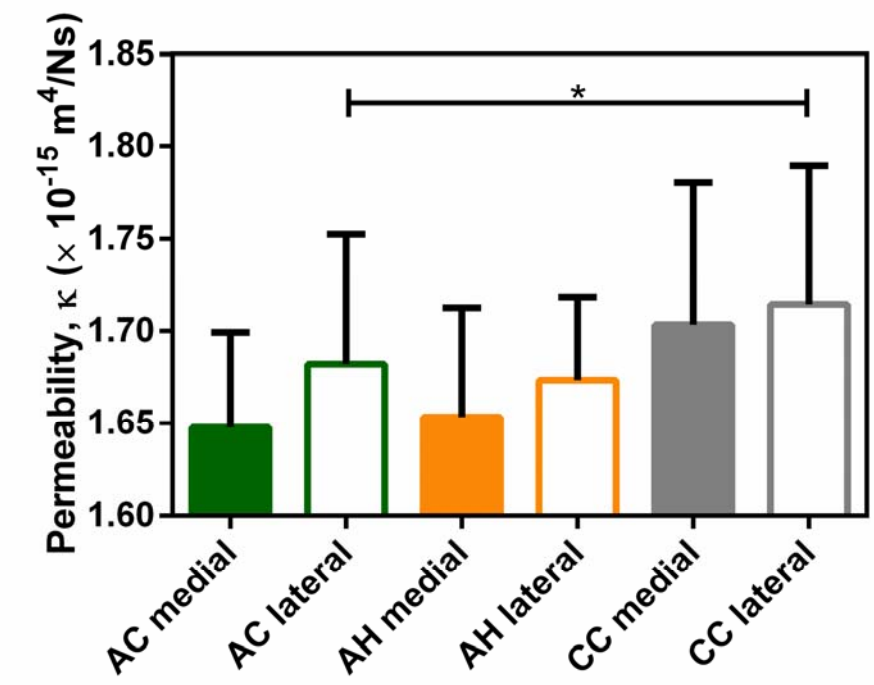

Figure 3-9 Results for hydraulic permeability in porcine knee meniscus tissues for all six groups investigated (AC medial and lateral, AH medial and lateral, and CC medial and lateral). For each group, n=15. Graph shows mean ± standard deviation.

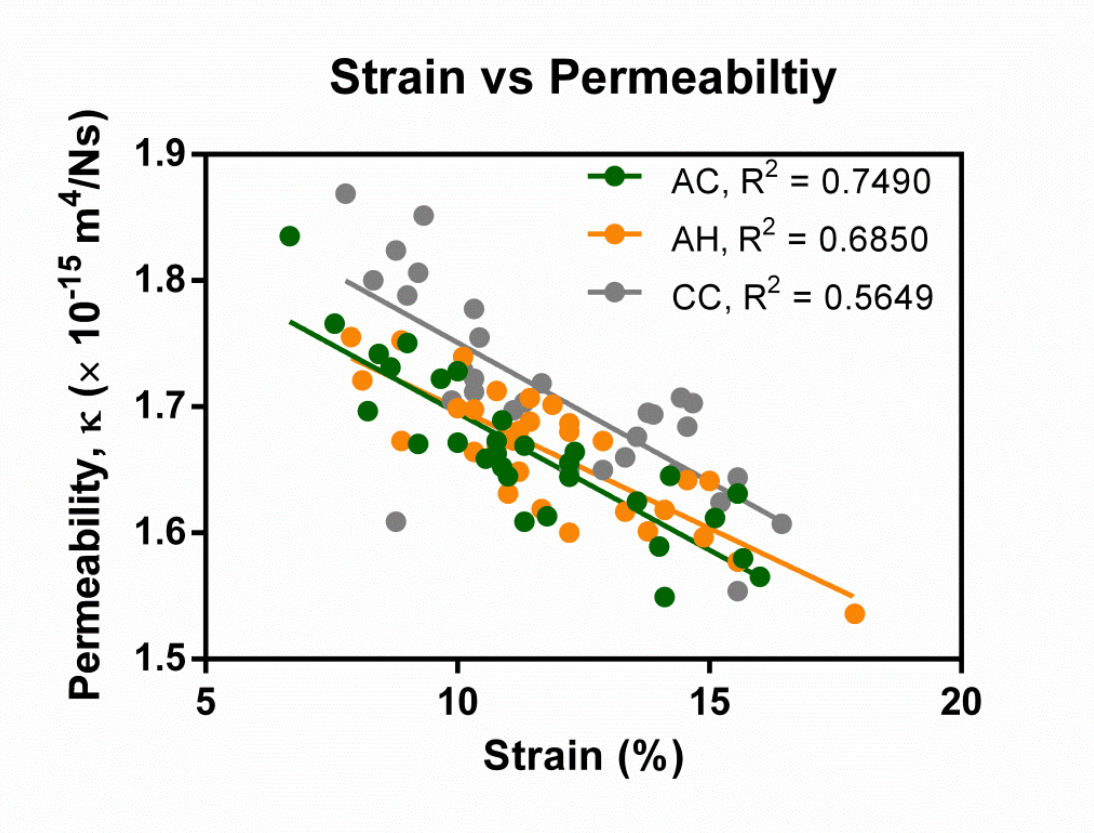

Figure 3-10 Relationship between static compressive strain (%) and hydraulic permeability, *κ,* in porcine meniscus tissues for the three directional groups investigated: axial central (AC), axial horn (AH), and circumferential central (CC). Significant correlation was detected for all groups, $p<0.05$; R^2 values are shown. For each group, 30 measurements were taken.

Additionally, the relationship between tissue water volume fraction and hydraulic permeability can be seen in **Figure 3-11**. Regression analysis for all groups showed a significant positive correlation between hydraulic permeability and tissue water volume fraction (AC: $R^2 = 0.4745$, AH: $R^2 = 0.3311$, CC: $R^2 = 0.4074$; $p<0.05$).

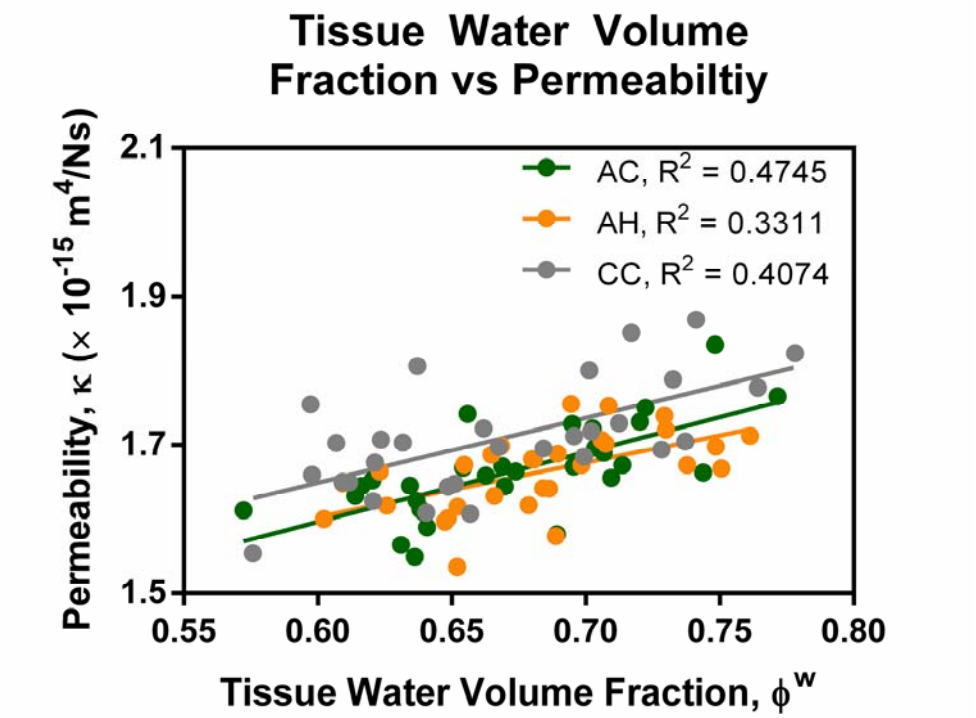

Figure 3-11 Relationship between tissue water volume fraction, ϕ^w, and hydraulic permeability, κ, in porcine meniscus tissues for the three groups investigated: axial central (AC), axial horn (AH), and circumferential central (CC). Significant correlation was detected for all groups, $p<0.05$; R^2 values are shown. For each group, 30 measurements were taken.

The statistical analysis results can be found in **Table 3-2**. Two-way repeated measures ANOVA showed a significant difference between axial central and circumferential central groups in the medial ($p=0.013$) component, but not the lateral ($p=0.210$) component. However, the direction of study was statistically significant ($p=0.009$) for the pooled groups. No statistically significant differences were found between the axial central and axial horn groups in either the medial ($p=0.770$) or lateral ($p=0.678$) groups, nor between the medial and lateral groups of the axial central ($p=0.200$), axial horn ($p=0.264$), or circumferential central ($p=0.641$) groups. Finally, there was no significant difference between the tissue water volume content or static compressive strain of any of the groups (ANOVA, $p<0.05$).

A. ***Medial vs. Lateral Component***

	P-values
Axial Central	0.200
Axial Horn	0.264
Circumferential Central	0.641

B. ***Axial Horn vs. Central Region***

	P-values
Medial	0.770
Lateral	0.678
Component	0.090
Region	0.894
Interaction	0.663

C. ***Axial Central vs. Circumferential Central***

	P-values
Medial	0.013*
Lateral	0.210
Component	0.226
Direction	0.009*
Interaction	0.495

Table 3-2 Statistical analysis for hydraulic permeability comparisons: (A) meniscal variation: medial vs. lateral component; (B) regional specific variation: axial horn vs. axial central (samples taken in the axial direction only); and (C) direction variation: axial central vs. circumferential central. Values shown are p-values; significant variation is highlighted and noted with a '*'. Two-way repeated measures ANOVA was performed using SPSS software.

3.5 DISCUSSION

The experimental results of this study show that the hydraulic permeability in porcine knee meniscus tissues is significantly correlated to both the level of compressive strain applied and the tissue water volume content. We also found a significant anisotropic trend when comparing axial and circumferential permeability in the central region of the tissue.

Compared to previous studies in literature, our values, ranging from 1.53-1.87×10^{-15} m^4/Ns, are comparable with other meniscal tissue samples, again ranging from approximately 0.81–6.2 ×10^{-15} m^4/Ns (Joshi et al., 1995; LeRoux and Setton, 2002; Martin Seitz et al., 2013; Proctor et al., 1989; Sweigart and Athanasiou, 2005; Sweigart et al., 2004), see **Table 3-3**. The wide spread of data is likely due to differences in measurement techniques used (e.g., direct permeation vs. confined compression vs. creep indentation) and different species and locations of test specimens. Furthermore, previous studies have shown that the measured value of permeability is dependent upon the pressure gradient applied to the tissue (Lai and Mow, 1980; Mow et al., 1980). Nonetheless, our results are within the range reported in the literature for human and animal meniscus tissues.

Tissue	κ ($\times 10^{-16} m^4/Ns$)	Reference
Human	1.99 ± 0.79	(Joshi et al., 1995)
Human	1.5-3.9	(Martin Seitz et al., 2013)
Human	1.32-2.74	(Sweigart et al., 2004)
Porcine	3.05-6.18	(Sweigart and Athanasiou, 2005)
Porcine	1.74	(Joshi et al., 1995)
Porcine	2.86-6.32	(Sweigart et al., 2004)
Porcine	1.53-1.87	Present Study
Bovine	0.81 ± 0.45	(Proctor et al., 1989)
Bovine	5.40-6.22	(Sweigart et al., 2004)
Canine	0.11	(LeRoux and Setton, 2002)
Canine	1.56-3.27	(Sweigart et al., 2004)
Lapine	0.89-4.00	(Sweigart et al., 2004)
Baboon	1.05-1.36	(Sweigart et al., 2004)

Table 3-3 Summary of experimental results for hydraulic permeability, κ, in meniscus tissues from various sources from literature.

3.5.1 Effect of Compression

The decrease in permeability as the compressive strain increases is likely due to changes in the compressed collagen fibers running along the tissues. In general, as a porous tissue is compressed, water can flow through the matrix of this tissue through the pores. The

rate of flow is directly related to the drag force between the tissue and fluid. As compressive strain is increased, the compaction of the collagen network provides an increased frictional resistance (or drag force) to the flow of interstitial fluid (Mansour and Mow, 1976). Although this study did not measure the effects of highly variable compression levels, we nonetheless found a significant negative correlation ($p<0.05$) between permeability and compression level using regression analysis, see **Figure 3-10**. These results are in agreement with previous studies done by this group investigating the effects of static compressive strain on other transport properties discussed in the subsequent chapters of this dissertation, including glucose diffusion coefficient, glucose partitioning, and electrical conductivity in porcine meniscus fibrocartilage (Kleinhans and Jackson, 2017; Kleinhans et al., 2015; Kleinhans et al., 2016). In the literature, previous studies performed in articular cartilage and the meniscus have also found similar results showing a decreasing permeability trend with increasing compression (Chen et al., 2001; Frank and Grodzinsky, 1987; Jurvelin et al., 2003; LeRoux and Setton, 2002; Mow et al., 1984; Reynaud and Quinn, 2006).

Over the small range of compressive strain levels applied in this study, we found a significant negative linear correlation between permeability and strain. However, it should be noted that previous studies have found a non-linear relationship when looking at a larger range of strain levels and associated tissue water volume fraction values (Gu et al., 2003b; Lai and Mow, 1980). Therefore, it is likely that the relationship between permeability and strain in meniscus tissue is also non-linear, and should be further investigated. This particular behavior is believed to play an important role in the

physiological functioning of cartilaginous tissues by preventing rapid and excessive fluid exudation from the tissue during loading.

Previously, Lai and Mow found that hydraulic permeability was exponentially dependent on the level of compressive strain applied (Lai and Mow, 1980) by **Equation 3-7**:

$$\kappa = \kappa_o e^{-M \cdot \epsilon_c}, \qquad \textbf{(3-7)}$$

where κ_o and M are material parameters that depend on the applied pressure. Specifically, κ is the apparent permeability found in this study, κ_o is the intrinsic permeability of uncompressed tissue, M is the dimensionless nonlinear interaction coefficient, and ϵ_c is the first invariant of the strain tensor (i.e., compressive strain). By curve-fitting this equation with our experimental data, we were able to solve for the intrinsic permeability, κ_o, and M, see **Figures 3-12** through **3-15**. Our values for intrinsic permeability (κ_o), which range from 1.905 x 10^{-15} m^4/Ns to 1.993 x 10^{-15} m^4/Ns, are similar to those found in the literature for articular cartilage (Lai and Mow, 1980). Note that the permeability measured using a permeation experiment is considered the apparent permeability given that it is dependent on the applied pressure difference across the tissue and non-uniform tissue compaction caused by the pressure-driven fluid flow (Holmes 1985). Therefore, the measured permeability is the averaged permeability across the tissue sample. Using **Equation 3-7**, we are able to predict the intrinsic hydraulic permeability of the tissue. The high correlation coefficients determined here indicate that this exponential model by Lai and Mow is able to accurately describe permeability behavior for meniscus tissues.

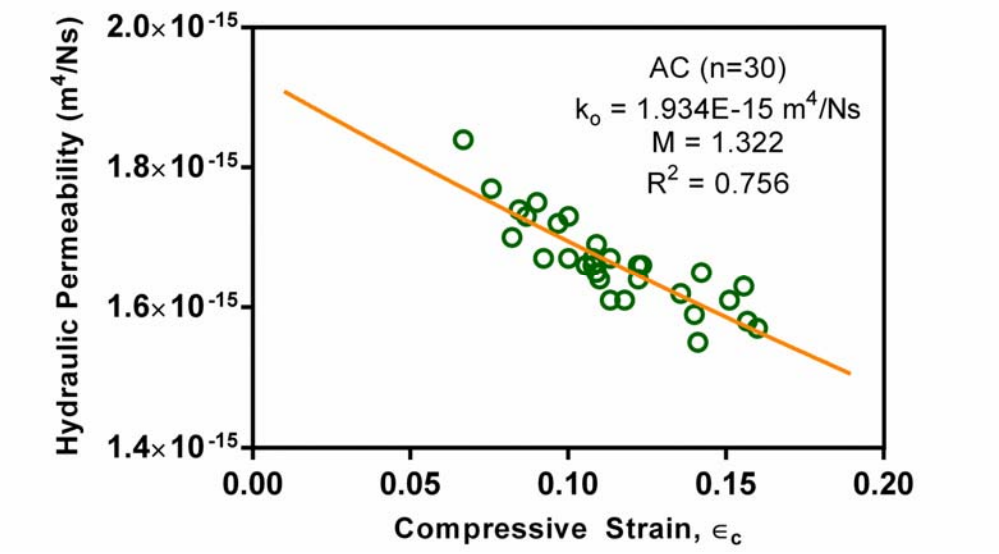

Figure 3-12 Results for curve fitting the hydraulic permeability of porcine meniscus tissues in the axial central (AC) region using **Equation 3-7**. The results for the curve-fit values of the intrinsic permeability, k_o and M are shown, along with the R^2 value.

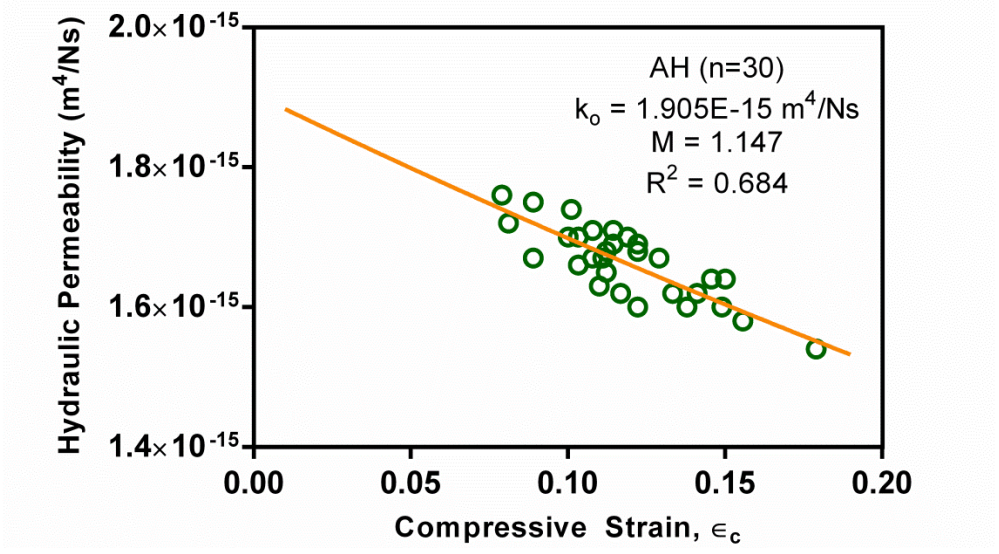

Figure 3-13 Results for curve fitting the hydraulic permeability of porcine meniscus tissues in the axial horn (AH) region using **Equation 3-7.** The results for the curve-fit values of the intrinsic permeability, k_o and M are shown, along with the R^2 value.

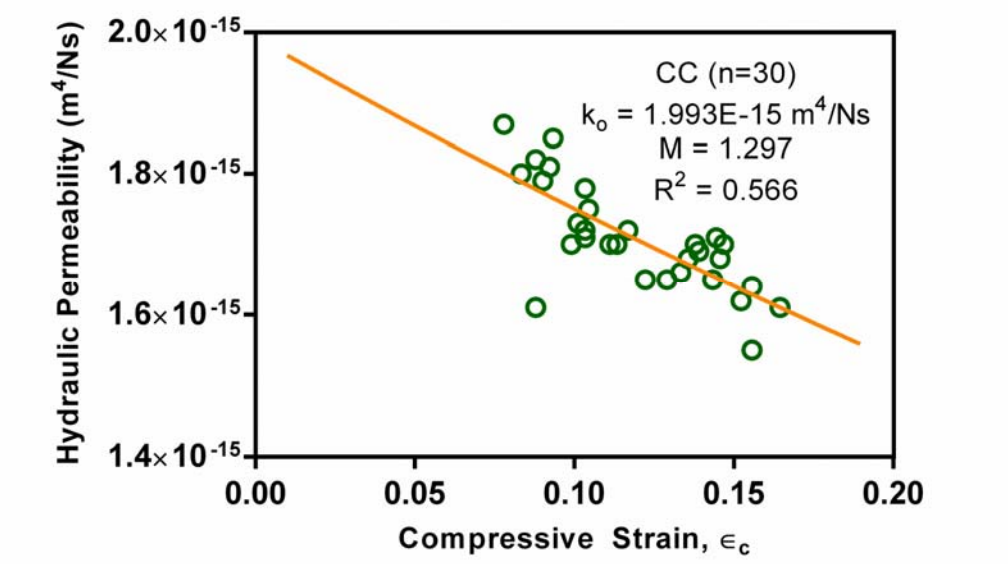

Figure 3-14 Results for curve fitting the hydraulic permeability of porcine meniscus tissues in the circumferential central (CC) region using **Equation 3-7**. The results for the curve-fit values of the intrinsic permeability, k_o and M are shown, along with the R^2 value.

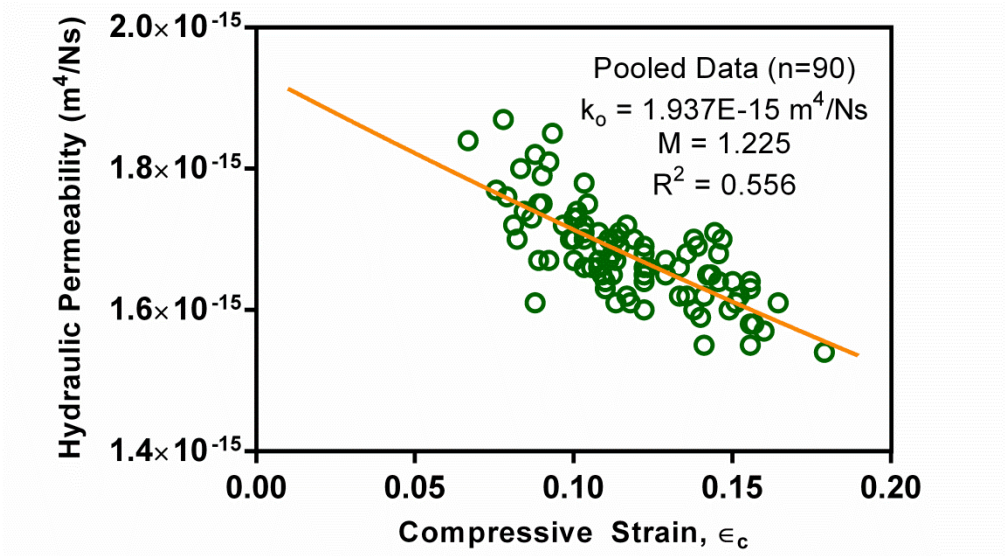

Figure 3-15 Results for curve fitting the hydraulic permeability of porcine meniscus tissues for all pooled data using **Equation 3-7**. The results for the curve-fit values of the intrinsic permeability, k_o and M are shown, along with the R^2 value.

3.5.2 Effect of Water Volume Content

In addition, as seen in **Figure 3-11**, it was found that the hydraulic permeability of the tissue is highly dependent upon the tissue water content, highlighted by a significant positive correlation ($p<0.05$). Regression analysis showed this significant relationship for all groups investigated. This was expected, given the relationship between strain level applied and tissue water volume fraction, as shown in **Equation 3-6**. As previously stated, as tissues are compressed, the water volume fraction decreases due to the exudation of water from the tissue during compression. This explains the positive correlation between hydraulic permeability and water content with a negative correlation between hydraulic permeability and level of compressive strain. Other studies have found similar results; for example Gu et al. also reported permeability increasing with increasing hydration and decreasing with increasing fixed charge density for other cartilaginous tissues (Gu et al., 1993; Gu and Yao, 2003).

3.5.3 Effect of Anisotropy

Our results also indicate that hydraulic permeability in porcine meniscus tissues is anisotropic (i.e., direction-dependent). It was found that the hydraulic permeability in the central region in the axial direction was significantly less than that in the circumferential direction. Additionally, the circumferential group has a very comparable slope to the axial horn and axial central groups, but was shifted higher than both other groups. This leads us to believe that the hydraulic permeability follows the same trends when compared to the water volume content, but at different levels between the directional

groups. Previous studies have found that hydraulic permeability was most anisotropic when tissues were statically compressed between 20-40% (Reynaud and Quinn, 2006) so we can predict that with an even higher level of compressive strain, we would see an even greater difference between axial and circumferential specimens.

Additionally, based on the results in **Table 3-1**, the specific resistance (reciprocal of permeability coefficient) to fluid flow in the axial direction is approximately 3% higher than in the circumferential direction. This suggests that the effective "pore" size in the axial direction is smaller than the "pore" size in the circumferential direction. This shows that an increase in water content, such as with degeneration or increased strain level, would therefore lead to a reduced "pore" size in the meniscus. Previous studies have found this to be true for other non-degenerative cartilaginous tissues, with differences as much as 25% greater in the circumferential direction (Gu et al., 1999).

3.5.4 Effect of Regional Variation

Finally, our results indicate that there is no statistically significant variation in the hydraulic permeability when comparing axial diffusion in different tissue regions (i.e., horn versus central regions) or different components (i.e., medial versus lateral components). Although results in the literature vary regarding tissue homogeneity, these findings are consistent with previous studies that showed transport in meniscus tissues is homogeneous (Kleinhans and Jackson, 2017; Kleinhans et al., 2015; Kleinhans et al., 2016; Proctor et al., 1989; Sweigart et al., 2004).

3.5.5 Experimental Limitations

There are several limitations to this project that should be noted for future reference. For example, due to the intricate system of tubing and channels in this project, the presence of even the smallest air bubbles could impact our results. Therefore, it was pertinent to remove all air bubbles prior to study; all attempts were made to eliminate air bubbles from the system prior to measurements. However, over time, it was not always possible to ensure 100% elimination of all air bubbles in channels and tubes that were not experiencing high levels of pressure and it was also impossible to see whether or not there were bubbles present in the inner areas of the 3D printed chamber due to its darker coloring. However, we believe that the stability of our results and the comparable range with the literature are evidence that our method and experimental setup is able to accurately measure hydraulic permeability.

Additionally, in order to seal the chamber completely, we were unable to measure the tissues at 0% compressive strain. In order to ensure no leakage, the minimal level of compressive strain required was 10%. In the future, finding a method to measure the tissues at 0% compressive strain would be helpful in understanding the true strain-dependent trends of hydraulic permeability and determine values for intrinsic (zero strain) permeability. Additionally, our tissues were compressed only over a narrow range between 10-20% strain levels. In the future, it would also be beneficial to expand this range of strain in order to get a more accurate depiction of how the hydraulic permeability is related to strain in the meniscus.

Furthermore, because our tissues came pre-harvested from a frozen tissue bank, we were not able to distinguish between anterior and posterior horn in the menisci. Therefore, in this study, samples were pooled from these two regions. However, some studies in literature show that the posterior and anterior horns are not homogeneous (Di Giancamillo et al., 2014; Killian et al., 2010; Sanchez-Adams et al., 2011); therefore, further investigation is necessary to better understand the region variation (if any) for fluid transport properties in the meniscus.

Moreover, in this study we focused on uniaxial, static compressive strain within the range of physiological meniscal strains occurring during daily activity (Chia and Hull, 2008; Eckstein et al., 2000; Martin Seitz et al., 2013; Quinn et al., 2000; Quinn et al., 2001; Yang et al., 2010). Our results, therefore, represent the hydraulic permeability under static conditions. As previously mentioned, the knee meniscus undergoes a variety of loading conditions during normal daily activity, including dynamic compression (Fithian et al., 1990; Kurosawa et al., 1980; Makris et al., 2011). Nonetheless, the results of this study provide important information regarding nutritional supply in the tissue and serve as a launching point for this proposed work.

Finally, as discussed in more detail in the future recommendations section of **Chapter 8**, future studies should investigate all three primary directions (axial, radial, and circumferential) in addition to posterior and anterior regions of the menisci and degenerated tissues. This data would be beneficial for better understanding the inhomogeneous, anisotropic, and degeneration-dependent behavior of fluid transport in the meniscus.

3.6 SUMMARY AND CONCLUSIONS

In summary, this study investigated the strain-dependent, anisotropic, and region-dependent hydraulic permeability in porcine meniscus fibrocartilage. It was found that the permeability coefficient is significantly affected by mechanical compression, which decreases as strain is increased. It was also found that the permeability in the circumferential direction, along the primary direction of the collagen fibers, is significantly greater than in the axial direction. Finally, there was no statistically significant difference in axial permeability comparing the central and horn regions of the meniscus in both the medial and lateral meniscal components. Given the importance of a healthy meniscus in the proper functioning of the knee joint, as well as the unknown role of the tissue in the onset and progression of OA, better understanding the transport environment within the tissue and the relationship with tissue pathophysiology is essential in the development of new strategies to treat and/or prevent tissue degeneration and related OA. This study provides baseline information on the structure-function relationships for fluid transport properties in the meniscus and provides important insight into the tissue viscoelastic behavior, load support, and biomechanical functioning.

CHAPTER 4. MEASUREMENT OF STRAIN-DEPENDENT AND ANISOTROPIC DIFFUSION OF GLUCOSE IN KNEE MENISCUS TISSUES

4.1 INTRODUCTORY REMARKS

The lack of full vascularization is a distinctive property of knee meniscus tissues. As previously reported, during prenatal development until shortly after birth, the meniscus is fully vascularized (Clark and Ogden, 1983; Makris et al., 2011). Over time, however, the majority of vascularization appears to subside (Clark and Ogden, 1983; Makris et al., 2011). Due to incomplete vascularization, the knee meniscus relies on the transport of fluid and solutes through the extracellular matrix (ECM) for providing the necessary nutrients to cells (Makris et al., 2011). Transport may occur by diffusive processes or by fluid flow (i.e., convection) through the ECM and is highly dependent upon tissue structure and composition as well as tissue loading conditions. It is believed that the main mechanism of transport for small solutes in avascular cartilaginous tissues is diffusion (Maroudas, 1975; Urban et al., 1978; Urban et al., 1982). To understand the transport mechanisms and pathways in knee meniscus, determining the diffusion coefficient (i.e., diffusivity, a measure of solute mobility) for small solutes (e.g., glucose) is important.

Numerous investigators have examined the mechanical properties in meniscus fibrocartilage from human and animal sources. Several studies have found that the meniscus exhibits anisotropic mechanical behavior in tension, compression, and shear

loading conditions (Chia and Hull, 2008; Fithian et al., 1990; Gabrion et al., 2005; Leslie et al., 2000; Nguyen and Levenston, 2012; Proctor et al., 1989; Skaggs et al., 1994; Spilker et al., 1992; Sweigart et al., 2004; Tissakht and Ahmed, 1995). Furthermore, the mechanical properties of meniscus tissues have been found to be strain-dependent (Bursac et al., 2009; Chia and Hull, 2008; Danso et al., 2014; LeRoux and Setton, 2002; Sanchez-Adams et al., 2011). However, few studies have investigated transport properties in knee meniscus tissues. Danzig *et al*. found that continuous passive motion does not significantly affect meniscal nutrition, indicating that diffusion is an important mechanism for transport of nutrients in the tissue (Danzig et al., 1987). Most recently, Travascio *et al.* measured the diffusion coefficient of fluorescein in meniscus fibrocartilage using fluorescence recovery after photobleaching (FRAP), and found an anisotropic trend (Travascio et al., 2009b). No previous study has reported on the anisotropic, strain-dependent, or inhomogeneous behavior of nutrient (i.e., glucose) diffusion in the knee meniscus. Such information is necessary to better elucidate the nutritional environment in meniscus tissue and thus more clearly understand tissue pathology.

It was hypothesized that the diffusion of glucose in porcine knee meniscus tissue is strain-dependent due to changes in the water content caused by compression. It was also hypothesized that glucose diffusion coefficient in the meniscus is anisotropic, due to the structure of the tissue. Finally, it was hypothesized that the diffusion of glucose in meniscus tissue does not vary with regional location (i.e., horn region versus central region), based on previous studies investigating the inhomogeneous behavior of hydraulic permeability in the meniscus (Proctor et al., 1989; Sweigart et al., 2004). Therefore, the

objective of this study was to test these hypotheses by measuring the apparent glucose diffusion coefficient of porcine knee meniscus in two directions (axial and circumferential), from two locations (horn and central), and under three levels of static compressive strain (0%, 10%, and 20%). Similar methods have been employed to determine solute diffusion coefficients in other cartilaginous tissues and intervertebral disc tissues (Jackson et al., 2012; Jackson et al., 2008; Maroudas et al., 1968; Maroudas et al., 1975; Yuan et al., 2009).

4.2 THEORETICAL APPROACH

In the present study, a one-dimensional steady-state diffusion experiment was utilized to determine the value of the apparent glucose diffusion coefficient in porcine knee meniscus. With this approach, a tissue specimen of known thickness is confined between two acrylic compartments of a diffusion chamber. High-glucose concentrated solution is introduced into the upstream, larger chamber, while a solution containing no glucose is introduced in the downstream, smaller chamber. Over time, the glucose gradually diffuses through the tissue, from the upstream to the downstream chamber. The concentration of solute diffusion in the downstream chamber is measured and used to calculate the apparent glucose diffusivity of the tissue specimen.

Using this method, we can assume that the upstream chamber solution is constant due to its high concentration of glucose and larger volume of solution versus that of the

smaller, downstream chamber. Additionally, since the solution downstream is replaced periodically for measurement with a fresh solution, we can assume the concentration in the downstream chamber is always close to zero. The apparent diffusion coefficient, D_{app} ($= KD_{eff}$, where K is the partition coefficient and D_{eff} is the effective diffusion coefficient), is derived from Fick's first law of diffusion:

$$J = -D\frac{dC}{dx} = -D_{app}\frac{\Delta C}{h}, \quad \textbf{(4-1)}$$

where J is the diffusive flux and C is the concentration. The concentration can also be estimated as the concentration difference, ΔC, across a tissue of thickness h. Furthermore, at steady state, we can assume that the distribution of solute within the tissue is linear (that is, $-dC/dx = \Delta C/h = (C_{up} - C_{down})/h$, where C_{up} is the concentration of solute in the upstream chamber). The diffusive flux is defined as the mass flow rate of solute, ΔQ, per unit area, A:

$$J = \frac{\Delta Q}{A} = \frac{V\,dC}{A\,dt}. \quad \textbf{(4-2)}$$

From this relationship, we can therefore derive the following:

$$\frac{V_{down}\,dC_{down}}{A\,dt} = -D_{app}\frac{\Delta C}{h}, \quad \textbf{(4-3)}$$

where C_{down} is the concentration of solute in the downstream chamber and V_{down} is the volume of solution in the downstream chamber. After integrating and solving for D_{app}, we have:

$$D_{app} = \ln\left(\frac{C_{up} - C_{down}(t_o)}{C_{up} - C_{down}(t)}\right)\frac{V_{down}h}{A(t - t_o)}. \quad \textbf{(4-4)}$$

where $C_{down}(t_o)$ is the concentration of solute in the downstream chamber at time t_o (initial time) and $C_{down}(t)$ is that at time t. When the tissue reaches steady-state (i.e., linear distribution of solute across the tissue), the apparent diffusion coefficient can be calculated directly from the concentration measurements from the downstream chamber.

In order to determine the strain-dependent diffusion coefficient of tissues, varying levels of compressive strain must be applied to the tissue specimens. This was accomplished by changing the size of the metal spacers between the chamber halves, thus resulting in a 1-D uniaxial strain applied to the tissue. Furthermore, the anisotropic behavior of the diffusion coefficient can be investigated by varying the orientation (i.e., direction) of the tissue specimens during preparation.

4.3 Materials and Methods

4.3.1 Design of Experimental Apparatus

A custom-made diffusion apparatus was constructed as shown in **Figure 4-1** and **Figure 4-2** to measure the strain-dependent diffusion coefficient of glucose in meniscus tissue based on previous studies (Jackson et al., 2012; Jackson et al., 2008; Yuan et al., 2009). The device consists of two cylindrical acrylic solution chambers divided by a specimen holder in the center. The volume of the larger, upstream chamber is 1000μL, while that of

the smaller, downstream chamber is 200µL. The diameters of the chambers allow for the volumes to have similar heights of solution, thus negating gravitational force as an additional driving force for transport across the tissue specimen.

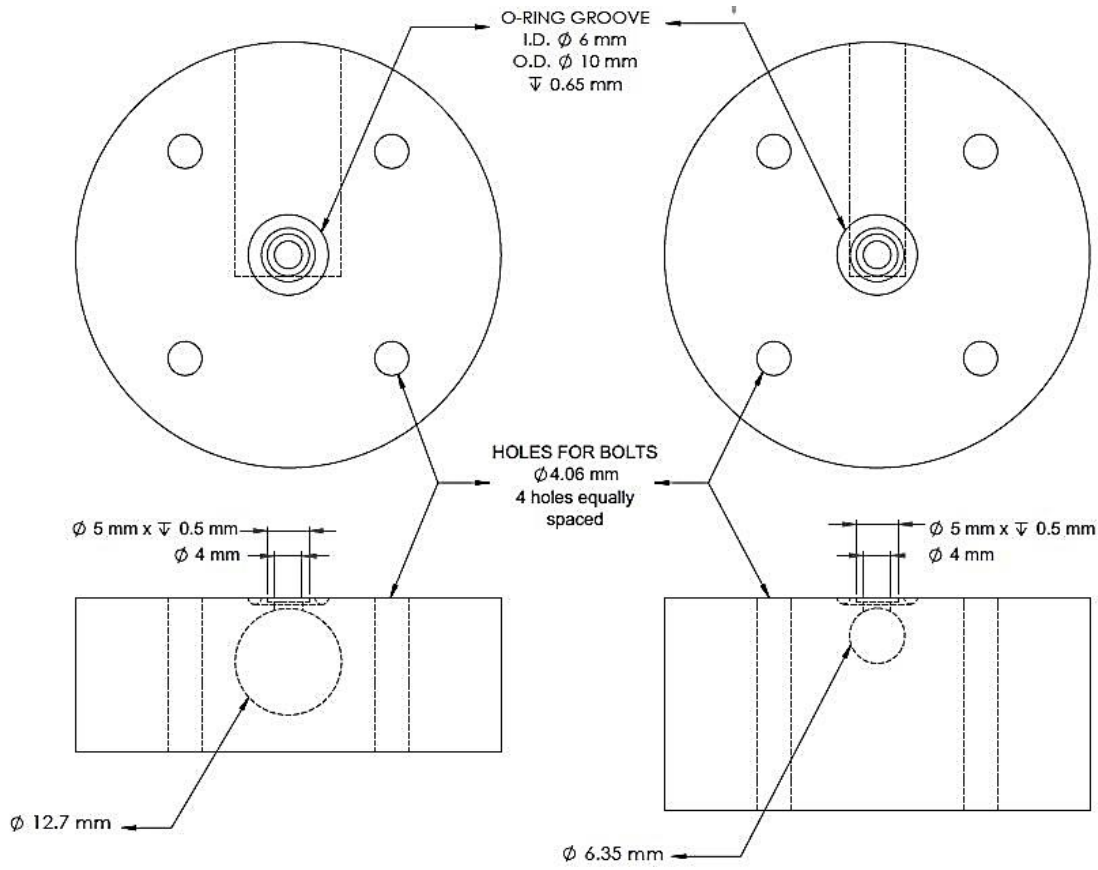

Figure 4-1 Engineering drawing showing the front and top views of the diffusion chamber halves.

The specimen is held between two semi-rigid polyethylene porous plates (hydrophilic polyethylene, 50-90µm pore size, Small Parts, Inc., Miami Lakes, FL) (diameter = 5mm) with 50% open area and sealed radially with an o-ring (Buna-N metric rubber, Small parts, Inc., Miami Lakes, FL) (inner diameter = 6mm, thickness = 2mm).

The 50% open area and 5 mm diameter of the porous plates were used to determine the area of diffusive flux across the tissue, in order to calculate the diffusion coefficient using **Equation (4-4)**. The level of compressive strain (0%, 10%, 20%) is controlled by adjusting the size of the spacer between the chamber halves to within 0.01 mm of the tissue size. Stirring bars (VWR International, Suwannee, GA) ensure that the solutions in the upstream and downstream chambers are continuously moving to allow homogeneous concentration and reduce boundary layer formation.

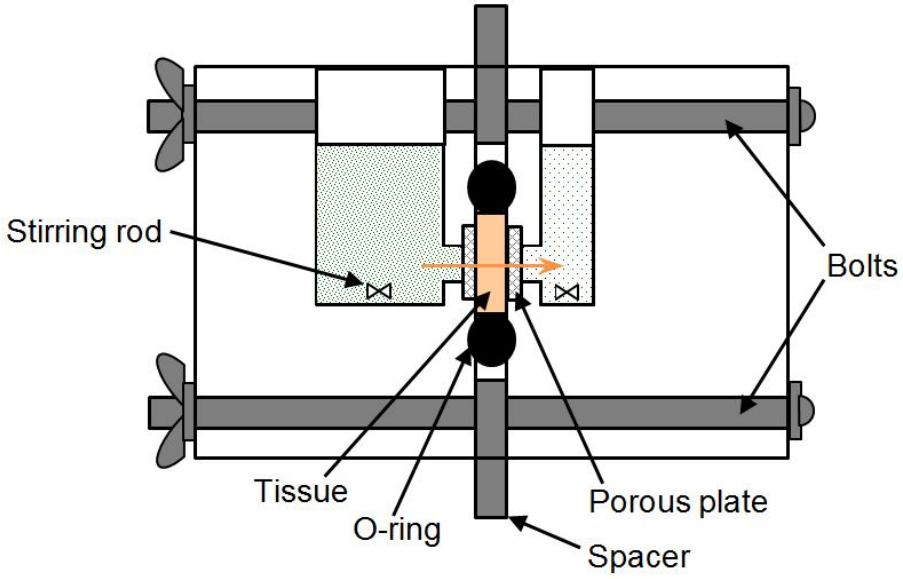

Figure 4-2 Schematic of the diffusion chamber showing the two chambers, the o-ring, metal spacers, porous plates, tissue sample, bolts, and stirring rods.

4.3.2 Specimen Preparation

Lateral and medial menisci were harvested from both left and right cadaveric knees of Yorkshire pigs (99.7 ± 6.1 kg, range: 89.4 kg – 108.0 kg, ~20-25 weeks, both male and females) obtained from a local slaughterhouse within 1 hour of death. A total of 22

menisci were harvested from 11 pigs. Cylindrical specimens (6 mm diameter and ~0.5 mm thickness) were prepared using a stainless steel corneal trephine (Biomedical Research Instruments, Inc., Malden, MA) and sledge microtome (Model SM2400, Leica Instruments, Nussloch, Germany) with freezing stage (Model BFS-30, Physitemp Instruments Inc., Clifton, NJ). The height was measured using a custom current-sensing micrometer that works using a capacitive sensor to read the height of the tissue sample and is precise to 0.001mm. Samples were excised in the axial and circumferential directions, see **Figure 4-3.**

Samples from both medial and lateral menisci from both left and right knees were pooled. In the axial direction, samples were taken from both the horn and the central regions, as shown in **Figure 4-3**, while circumferential samples were only taken from the central region. A total of three groups of specimens were tested: axial horn (AH) (n=30), axial central (AC) (n=30), and circumferential central (CC) (n=30). Three tests, corresponding to three levels of compressive strain (0%, 10%, 20%), were performed on each sample specimen. In this study, the samples were compressed 10% and 20%, as these strain levels have been previously studied and are known to be in the range of physiological meniscal strains occurring in daily activity (Chia and Hull, 2008; Eckstein et al., 2000; Martin Seitz et al., 2013; Quinn et al., 2000; Quinn et al., 2001; Yang et al., 2010).

4.3.3 Water Content Measurement

The water volume fraction of the tissues was measured using the same methods as the hydraulic permeability study in **Chapter 3** using a buoyancy method published in literature (Gu et al., 1996; Gu et al., 1997).

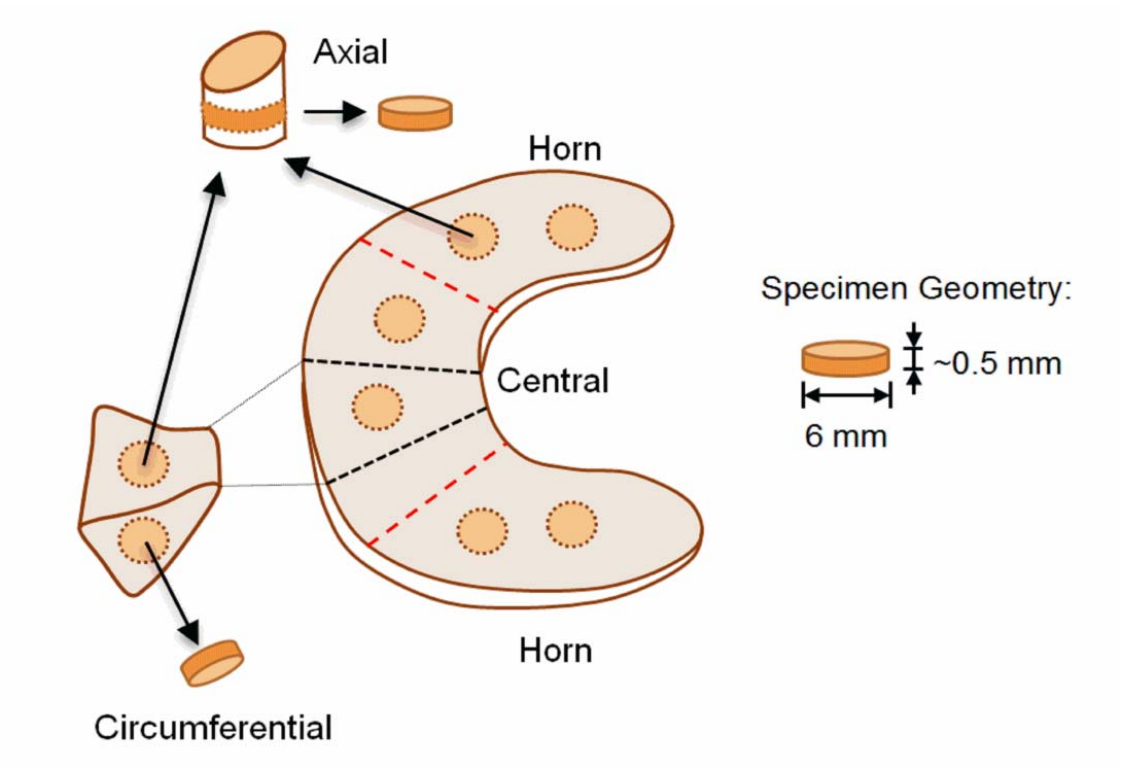

Figure 4-3 Schematic drawing of the meniscus tissue and the locations, directions, and sizes of the specimens used. Tissues were taking in both the axial and circumferential directions and from both the horn and central regions (axial direction only). Specimens were approximately 0.5mm thick with a diameter of 6mm.

4.3.4 Measurement of Glucose Diffusivity

A 1-D steady-state diffusion experiment was employed to measure the glucose diffusion coefficient in meniscus as seen in previous studies (Jackson et al., 2012; Jackson et al., 2008; Maroudas et al., 1968; Maroudas et al., 1975; Yuan et al., 2009). The specimen was placed in the sealed chamber and allowed to equilibrate for approximately 20 minutes, see **Figure 4-4**. At the start of the experiment, high glucose PBS solution (20g/L, Sigma-Aldrich Co., St. Louis, MO) was added to the upstream chamber, while blank PBS solution was loaded in the downstream chamber. At 15 minute time intervals, all 200μL of the downstream chamber solution was removed and a fresh 200μL of blank PBS solution was added. A sample (1μL) of the extracted 200μL solution was then used to measure the glucose levels in the downstream chamber using a custom-modified diabetic glucose meter (Accu-Chek Aviva, Roche Diagnostics, Indianapolis, IN**)** in concert with a sourcemeter (Keithley SourceMeter, Cleveland, OH) and custom LabView (National Instruments, Austin, TX**)** software, see **Figure 4-5.** A standard calibration curve was used to determine the glucose concentration measurements from recorded current readings; for all experiments, the calibration curve had an $R^2 \geq 0.98$.

Figure 4-4 Photograph of the actual diffusion chamber used during an experiment on a magnetic stirring plate. The metal spacers were used to confine the specimen to its desired thickness and could be increased in order to compress the tissues to 10% or 20%, as needed.

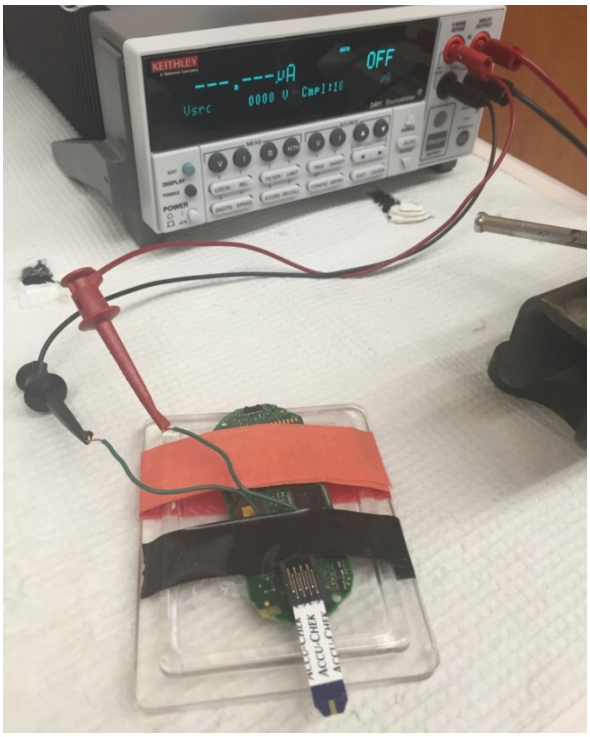

Figure 4-5 Photograph showing the modified glucose meter connected to the Keithley SourceMeter. A customized program and glucose meter made it possible to measure very low levels of glucose in the solution.

Once steady-state (2-3 consecutive measurements within the same (~5%) concentration) was achieved for specimens at 0% compression, the experiment was repeated for 10% and 20% compressive strains. When the downstream concentration reached steady state, the apparent diffusion coefficient, D_{app}, ($= \phi D$, where ϕ is the partition coefficient and D is the effective diffusion coefficient), was calculated from a simplified version of **Equation (4-4)** (Jackson et al., 2012; Jackson et al., 2008; Malda et al., 2004; Yuan et al., 2009):

$$D_{app} = \ln\left(\frac{C_{up}}{C_{up} - C_{down}(t)}\right)\frac{V_{down}h}{A \cdot t}, \quad \textbf{(4-5)}$$

where C_{up} is the solute concentration in the upstream chamber (the high concentration side), C_{down} is the solute concentration in the downstream chamber, V_{down} is the volume in the downstream chamber, t is the time interval (in this case, 15 minutes), and A and h are the diffusion area and diffusion distance (equal to specimen thickness after compression), respectively. Tests were carried out at room temperature (~23°C).

4.3.5 Scanning Electron Microscopy

Scanning electron microscopy (SEM) images of porcine meniscus tissues were obtained in order to compare the collagen fiber structure to the diffusion coefficient results. Axial and circumferential slices of knee meniscus tissues from the central region, prepared as described above, were fixed with a 2% glutaraldehyde (Sigma-Aldrich Co., St. Louis, MO) in PBS solution (Sigma-Aldrich Co., St. Louis, MO). Samples were then dehydrated

in a graded series of ethanol (20%, 50%, 70%, 90%, 100%) and dried by immersion in hexamethyldisilizane (Sigma-Aldrich Co., St. Louis, MO) (Hayat, 1982). The samples were sputter-coated with gold/palladium (Cressington Scientific 108auto Sputter Coater, Redding, CA). High-resolution SEM images were obtained using an Environmental Scanning Electron Microscope (FEI/Phillips XL-30 FEG ESEM, Hillsboro, OR). The fixed tissues can be seen in **Figure 4-6**.

Figure 4-6 Photograph showing the knee meniscus tissue samples prepared for scanning electron microscopy. The samples were fixed with a 2% glutaraldehyde in PBS solution. Samples were then be dehydrated in a graded series of ethanol (20%, 50%, 70%, 90%, 100%) and dried by immersion in hexamethyldisilizane. Tissue specimens were taken in both the axial and circumferential direction in order to compare the collagen alignment.

4.3.6 Statistical Analysis

A total of 30 specimens were tested for each of the nine groups (= 3 location/direction groups x 3 strain levels). Three independent variables were studied: level of compression, direction of diffusion, and regional location. Statistical significance between groups was determined by two 3 x 2 two-way mixed ANOVA analysis of variance tests using IBM SPSS Statistics 22 (International Business Machines Corp., Armonk, NY). One test was performed to compare axial central and axial horn groups, to determine if significant regional variation was present, while another compared axial central and circumferential central, to determine if significant anisotropy was present. The significance level was set at $p<0.025$ (based on the Bonferroni Correction). For both ANOVA tests, effect of compression was investigated using repeated measures. Least Significant Difference (LSD) post-hoc analysis with the Bonferroni Correction was performed using SPSS software to determine between which groups there was a significant difference. All data are given in mean ± standard deviation.

One-way ANOVA was performed to determine if water volume fraction and height measurements differed significantly between the three test groups (AC, AH, and CC). Regression analysis was performed to determine if the relationships between relative diffusion coefficient and water volume fraction, and diffusion coefficient and strain level were statistically significant.

4.4 RESULTS

The results for the glucose diffusion coefficient for the three groups investigated are shown in **Table 4-1** and **Figure 4-7**; data are shown as mean ± standard deviation. A total of thirty specimens (n=30) were measured for each of the nine test groups (axial horn at 0%, 10%, and 20% strain; axial central at 0%, 10%, and 20% strain; and circumferential central at 0%, 10%, and 20% strain). Tests were carried out at room temperature (~23˚C). The mean height and tissue porosity of the specimens under zero compression conditions were 0.51±0.06mm and 0.70±0.03, respectively. The relative diffusivity, D/D_o , [where D_o is the diffusivity of glucose in aqueous solution (D_o= 6.38 × 10^{-6}cm^2/sec)], (Longsworth, 1953) of glucose in porcine meniscus under zero compression was 0.25±0.08 for AH, 0.26±0.08 for AC, and 0.37±0.15 for CC., see **Table 4-1** and **Figure 4-7**. The values determined here are similar to those in the literature for glucose diffusion coefficients in other cartilaginous tissues (e.g., articular cartilage, intervertebral disc) (Allhands et al., 1984; Burstein et al., 1993; Jackson et al., 2008; Maroudas, 1970; Maroudas et al., 1975; Torzilli et al., 1997; Torzilli et al., 1998). Furthermore, the values for relative diffusivity of glucose in meniscus fibrocartilage are similar to results in the literature (Maroudas, 1968, 1970).

	$Strain$	n	φ^w	D_{app} ($\times$ 10^{-6} cm^2/sec)	D_{app}/D_o
AH	0%	30	0.71 ± 0.03	1.60 ± 0.51	0.25 ± 0.08
	10%	30	0.67 ± 0.03	1.18 ± 0.38	0.19 ± 0.06
	20%	30	0.63 ± 0.03	0.84 ± 0.31	0.13 ± 0.05
AC	0%	30	0.70 ± 0.02	1.67 ± 0.52	0.26 ± 0.08
	10%	30	0.67 ± 0.03	1.19 ± 0.47	0.19 ± 0.07
	20%	30	0.62 ± 0.03	0.80 ± 0.39	0.13 ± 0.06
CC	0%	30	0.71 ± 0.03	2.35 ± 0.94	0.37 ± 0.15
	10%	30	0.67 ± 0.03	1.64 ± 0.63	0.26 ± 0.10
	20%	30	0.63 ± 0.03	1.06 ± 0.45	0.17 ± 0.07

Table 4-1 Results for glucose diffusivity in porcine knee meniscus tissues in two directions (and two regions in the axial direction) and at three levels of compressive strain. Results show strain level, sample size, porosity, diffusivity, and relative diffusivity (D/Do). All results are shown as mean ± standard deviation.

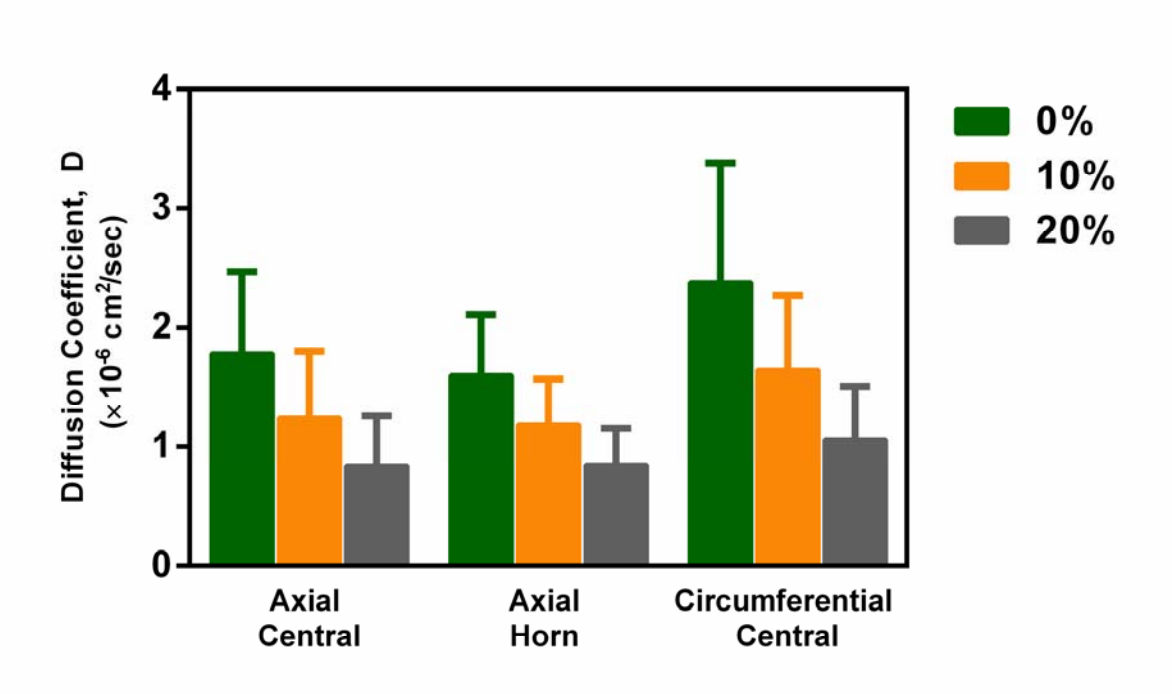

Figure 4-7 Results for glucose diffusivity in porcine meniscus for all three groups investigated (AH, AC, CC) at three levels of compressive strain (0%, 10%, 20%). For each group, n=30. Values for diffusivity are in mean ± standard deviation.

Results show that the diffusion coefficient decreases with increasing level of compressive strain for all groups investigated. On average, 10% compression led to a ~40% decrease in the diffusion coefficient compared to values in uncompressed tissues; 20% compression led to an additional ~48% decrease in the diffusion coefficient (compared to values at 10% compression). We also found that glucose diffusion in the circumferential direction was greater than that in the axial direction in the central region; the ratio of CC to AC was 1.41 at 0% compression, 1.38 at 10% compression, and 1.33 at 20% compression.

Statistical analysis can be found in **Table 4-2**. Two-way mixed ANOVA indicated that the glucose diffusion coefficient was significantly affected by both compression ($p<0.001$) and direction of diffusion ($p<0.025$) when comparing the axial central and circumferential central groups. However, two-way mixed ANOVA showed that the diffusion coefficient was not significantly affected by region in the tissue when comparing axial central and axial horn groups ($p=0.491$), although a significant effect of compression was still seen ($p<0.001$). Tukey HSD post-hoc analysis with the Bonferroni Correction indicated that the diffusion coefficient in the circumferential direction was significantly ($p<0.025$) higher than that in the axial direction at all three levels of compression. Post-hoc analysis also showed that, for each of the three groups investigated, when comparing the diffusion coefficient at 0% and 10% compression and at 10% and 20% compression, results were significantly ($p<0.025$) different.

Figure 4-8 shows regression analysis for the relationship between apparent diffusion coefficient and level of compressive strain. For all three groups, there was a

significant correlation detected between diffusion and strain level, as noted by the p-values, see **Figure 4-8**. This further illustrates the significant effects of compression on transport in meniscus fibrocartilage.

A. ***Strain-Dependent Variation***

	P-values		
0% vs. 10%	0.001*	0.001*	0.001*
10% vs. 20%	0.017*	0.004*	0.008*
0% vs. 20%	2.30e-08*	5.74e-09*	6.77e-09*

B. ***Axial vs. Circumferential Direction***

Direction	0.010*
Compressive Strain	2.04e-20*

C. ***Axial Central vs. Horn Regional Variation***

Regional Location	0.491
Compressive Strain	1.33e-25*

Table 4-2 Significance levels for post-hoc analysis of diffusion data for three comparisons: (A) strain dependent variation (tested in all 3 groups); (B) anisotropic variation: axial vs. circumferential direction (samples taken from central region of meniscus); and (C) regional specific variation: axial horn vs. axial central (samples taken in the axial direction only). Values shown are p-values; significant variation is highlighted and noted with a '*'. 2 × 3 mixed ANOVA and Tukey HSD post-hoc analysis were performed using SPSS software.

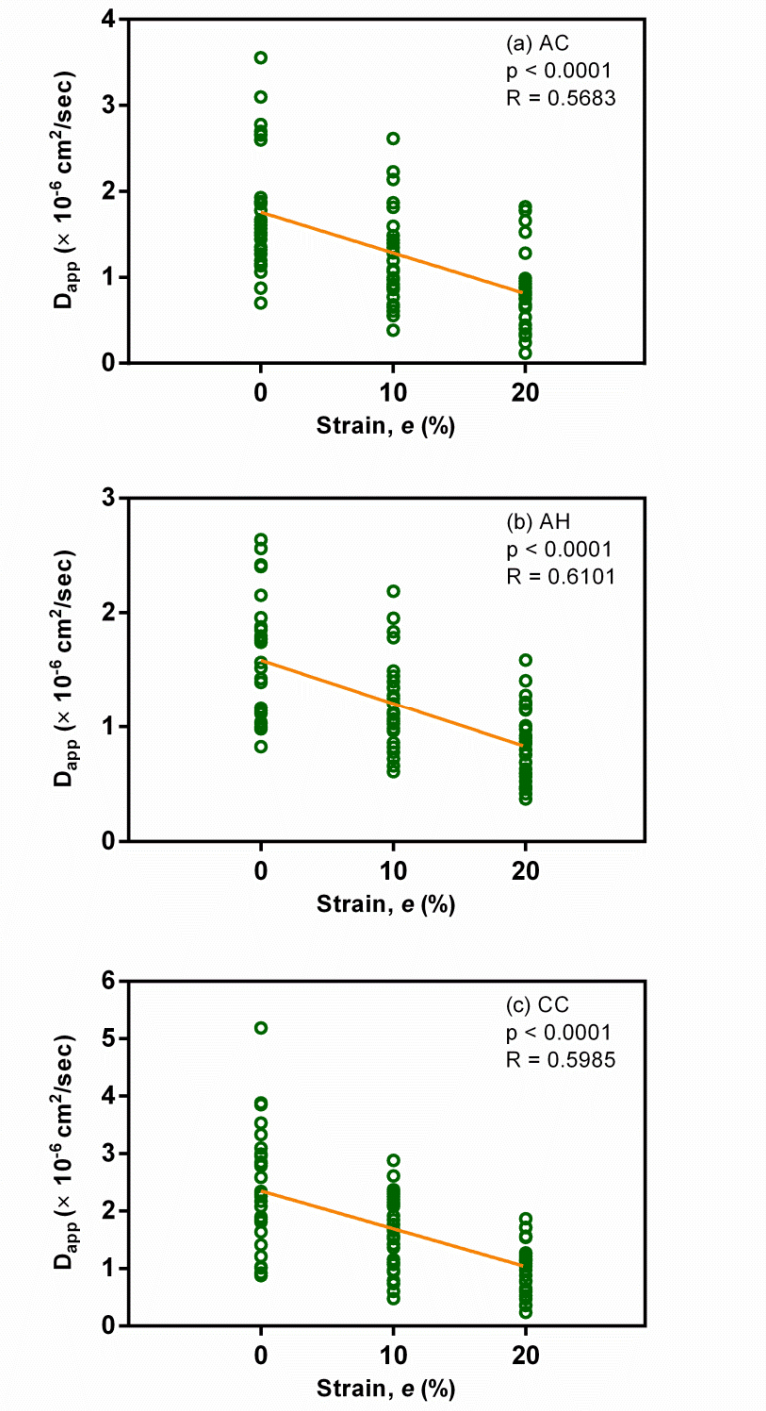

Figure 4-8 Correlation between apparent glucose diffusion coefficient and level of compression for three groups investigated: (a) axial central (AC), (b) axial horn (AC), and (c) circumferential central (CC). Significant correlation was detected for all groups; p-values and R values are shown for each.

The averaged water volume fraction values of the three groups at three levels of compressive strain are shown in **Table 4-1**; there were no significant differences between groups. The mean height of the three groups under zero compression conditions was 0.58 ± 0.06 mm for AH, 0.54 ± 0.08 mm for AC, and 0.54 ± 0.08 mm for CC; again, there were no significant differences between groups. The relative diffusion coefficient, D_{app}/D_o, of glucose in porcine meniscus at three levels of compression are also shown in **Table 4-1**. Statistical significance for relative diffusion data is the same as that for apparent diffusion coefficient discussed above, given that relative diffusion is simply a scaled value.

Given the significant anisotropic findings for the glucose diffusion coefficient determined here (i.e., circumferential diffusivity > axial diffusivity), SEM images were acquired to investigate the relationship between tissue morphology and anisotropic transport; images are shown in **Figure 4-9**. SEM images show the collagen fibers aligned perpendicular to the axial direction, as shown in **Figures 4-9(a) and 4-9(c)**, thereby creating porous channels in the circumferential direction; one such channel is circled in the figure. Note that channels are not present in the axial direction, see **Figures 4-9(b)** and **4-9(d)**.

In addition, we have included scatter plots showing the relationship between tissue water volume fraction, ϕ^w, and relative diffusion, D_{app}/D_o, for each of the three groups tested: AH samples (n=90) [**Figure 4-10(a)**]; AC samples (n=90) [**Figure 4-10(b)**]; and CC samples (n=90) [**Figure 4-10(c)**]. Regression analysis revealed a significant ($p<0.001$) relationship for all three groups investigated when the best fit line

was applied. The values for tissue water volume fraction for compressed samples were calculated at strain levels of 10% ($e = -0.1$) and 20% ($e = -0.2$).

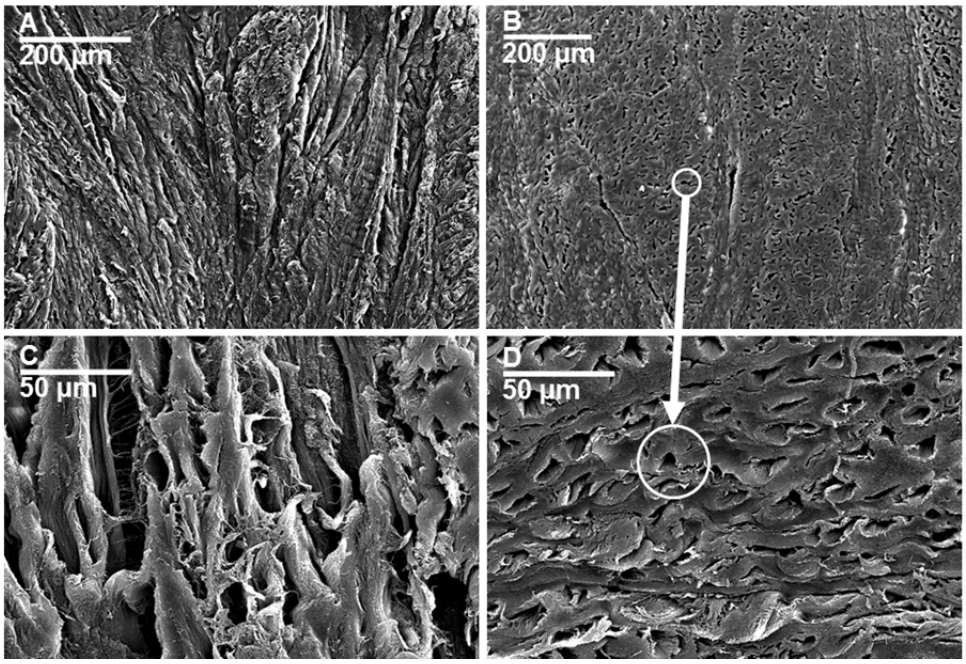

Figure 4-9 Scanning electron microscopy images of both axial (a,c) and circumferential (b,d) porcine meniscus samples. Images (a) and (b) are magnified 250x with scale bars equaling 200µm while (c) and (d) are magnified 1000x with scale bars equaling 50µm. Note the collagen fiber bundles running in the circumferential direction, thereby allowing for the presence of pores in circumferential specimens that are not apparent in axial specimens. The circle on (b) shows an example of a channel in the circumferential direction with the arrow pointing to (d) showing a magnified version of a channel. The samples were fixed using a 2% glutaraldehyde in PBS solution, dehydrated in a graded series of ethanol (20%, 50%, 70%, 90%, 100%) and dried by immersion in hexamethyldisilizane.

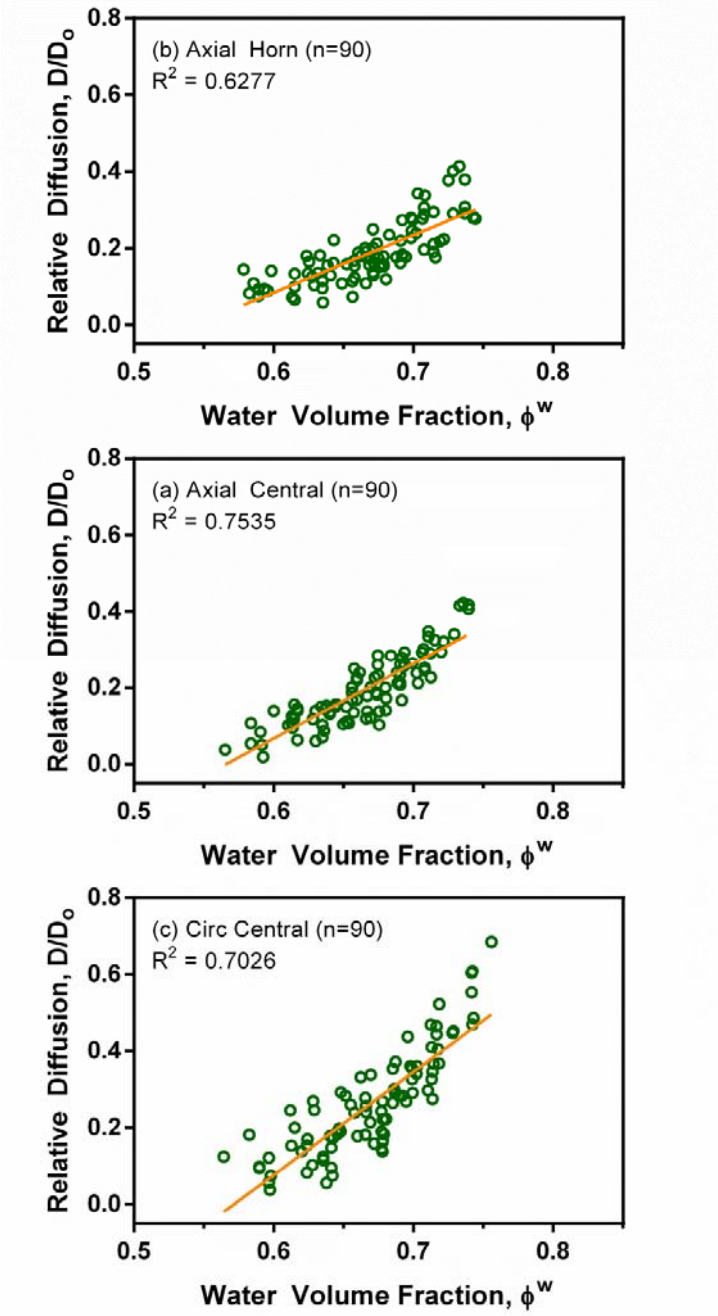

Figure 4-10 Relationship between tissue water volume fraction, ϕ^w, and relative diffusion coefficient, D/D_o, in meniscus tissues for the three groups investigated: (a) axial, central; (b) axial, horn; and (c) circumferential, central. For all groups, n=90. R^2 values from regression analysis are shown for each group.

4.5 DISCUSSION

In this study, we investigated the effects of compression, anisotropy, and tissue region on the apparent diffusion coefficient of glucose in meniscus fibrocartilage using a one-dimensional diffusion experiment. To our knowledge, this is the first study to quantify glucose diffusion in meniscus tissues. The values determined here are similar to those in the literature for glucose diffusion coefficients in other cartilaginous tissues (e.g., articular cartilage, intervertebral disc), which ranged from 0.138 to 6.08 × 10^{-6} cm^2/sec (Allhands et al., 1984; Burstein et al., 1993; Jackson et al., 2012; Jackson et al., 2008; Maroudas, 1968, 1970; Maroudas et al., 1975; Torzilli et al., 1987; Torzilli et al., 1997; Torzilli et al., 1998). Furthermore, the value for relative diffusion of glucose in meniscus fibrocartilage (average of 0.30 ± 0.15 for all groups at 0% compression) is similar to results in the literature, which indicate that it is in the range of 0.3 - 0.38 for articular cartilage (under zero compression conditions) (Maroudas, 1968, 1970).

These experimental results show that the apparent glucose diffusivity in porcine knee meniscus tissues is significantly ($p<0.05$) affected by the level of compressive strain applied. The decrease in diffusivity as the level of compression increases is likely due to the changes in tissue water content caused by the application of compressive strain. The diffusion of solutes in cartilaginous tissues is highly dependent upon tissue water content, generally showing a positive correlation (Fetter et al., 2006; Jackson et al., 2008; Ngwa et al., 2002; Shi et al., 2013; Travascio and Gu, 2007; Travascio et al., 2009a; Travascio et al., 2009b). Indeed, several models for solute diffusion in hydrated porous media, such as meniscus fibrocartilage, show that diffusivity is directly related to tissue water content (or

porosity) (Gu et al., 2004; Mackie and Meares, 1955). According to the equation, with each additional 10% compression, the porosity of the tissue decreases by ~3-4%. Thus, the decreased diffusivity with decreased tissue water content (and increased compressive strain) was anticipated.

4.5.1 Effect of Compression

The experimental results of this study show that the apparent glucose diffusion coefficient in porcine knee meniscus tissues is significantly affected by the level of compressive strain applied. The decrease in diffusion as the level of compression increases is likely due to the changes in tissue water content caused by the application of compressive strain. According to the equation, with each additional 10% compression, the water volume fraction of the tissue decreases by ~3-4%. The diffusion of solutes in cartilaginous tissues is highly dependent upon tissue water content, generally showing a positive correlation (Fetter et al., 2006; Gu et al., 2004; Jackson et al., 2006; Jackson et al., 2008; Kuo et al., 2011; Ngwa et al., 2002; Shi et al., 2013; Travascio and Gu, 2007; Travascio et al., 2009a; Travascio et al., 2009b). Indeed, several models for solute diffusion in hydrated porous media, such as meniscus fibrocartilage, show that the diffusion coefficient is directly related to tissue water volume fraction (Gu et al., 2004; Mackie and Meares, 1955). The relationship between water volume fraction and relative diffusion coefficient is shown in **Figure 4-10**. Regression analysis showed a significant relationship between water volume fraction and relative diffusion coefficient for the circumferential central group. The R^2 values for the correlation between diffusion

coefficient and water volume fraction were 0.6277, 0.7535, and 0.7026 for AH, AC, and CC, respectively.

The strain-dependent behavior of glucose diffusion coefficient found here is similar to results in the literature for diffusion of solutes in other cartilaginous tissues under compression. Numerous investigators have found that static loading results in reduced diffusion of solutes of various sizes in articular cartilage (Arkill and Winlove, 2008; Burstein et al., 1993; Evans and Quinn, 2005; Ngwa et al., 2002; Nimer et al., 2003; Quinn et al., 2000; Quinn et al., 2001). Literature shows that while dynamic loading enhances the transport of large molecules in cartilaginous tissues, it does not improve the transport of small molecules or fluid (Katz et al., 1986; O'Hara et al., 1990; Urban et al., 1982). Previous studies have also found static loading to be detrimental to meniscus cellular activity (Imler et al., 2004; Upton et al., 2003). Therefore, the changes in nutrient transport and availability caused by compression may play a role in mediating cellular response to loading (Quinn et al., 2001).

4.5.2 Effect of Anisotropy

Our results also indicate that diffusion of glucose in meniscus tissues is anisotropic (i.e., direction-dependent). It was found that the apparent glucose diffusion coefficient in the central region in the axial direction was significantly less than that in the circumferential direction at all levels of compressive strain. Travascio *et al.* previously found that the diffusion of fluorescein (MW = 332 Da) in meniscus tissues is anisotropic, with an anisotropic ratio of 3 in the tissue (Travascio et al., 2009b). In the present study, we have

found that the diffusion coefficient in the circumferential direction was ~1.4X that in the axial direction under zero strain conditions. Similar anisotropic results have been found for solute diffusion in cartilaginous tissues (de Visser et al., 2008; Filidoro et al., 2005; Hsu and Setton, 1999; Jackson et al., 2006; Jackson et al., 2012; Jackson et al., 2008; Leddy et al., 2006; Meder et al., 2006; Shi et al., 2013; Travascio et al., 2009a). It should be noted that there were no significant differences in the tissue water volume fraction values for axial and circumferential specimens (values shown in **Table 4-1**), indicating that the difference in the diffusion coefficient found for the two directions is not likely to be attributed to variations in tissue composition alone.

In order to fully understand the anisotropic results found here, SEM images of axial [**Figure 4-9(a)** and **4-9(c)**] and circumferential [**Figure 4-9(b)** and **4-9(d)**] meniscus samples from the central region were obtained. The SEM images show the collagen fibers aligned perpendicular to the axial direction, and thus parallel to the circumferential direction (i.e., collagen fiber bundles are oriented in the circumferential direction). As seen in **Figure 4-9(b)**, the alignment of the collagen fibers in the circumferential direction allow for the presence of pores that are not apparent in the axial direction; see notation in **Figures 4-9(b)** and **4-9(d)**. This pore structure may allow glucose to move more freely in the circumferential direction, parallel to the collagen fiber bundles. Indeed, previous studies have found the diffusion coefficient to be significantly higher in the direction parallel to collagen fibers (i.e., circumferential) in cartilaginous tissues (Leddy et al., 2006; Stylianopoulos et al., 2010). Furthermore, similar pore structure has also been found in other cartilaginous tissues, termed either microtubules or tubules (ap Gwynn et al., 2002; Iatridis and ap Gwynn, 2004; Jackson et al., 2009a; Travascio et al.,

2009a). This is in agreement with our data showing that the particular organization of collagen fibers contributes to the anisotropic transport behavior of glucose in meniscus fibrocartilage. It should be noted that this organization of collagen fibers has been previously established for the deep (interior) layer of the meniscus (Fithian et al., 1990; McDevitt and Webber, 1990); samples for diffusion experiments and imaging studies were both harvested from this deep layer.

4.5.3 Effect of Tissue Region

Additionally, our results indicate that there is no statistically significant variation in the apparent diffusion coefficient when comparing axial diffusion in different tissue regions (i.e., horn versus central regions). This is in agreement with our hypothesis that the glucose diffusion coefficient would not vary with location of the tissue specimen (central vs. horn region). These findings are consistent with results in the literature showing that fluid transport (i.e., hydraulic permeability) in meniscus tissues is homogeneous (Proctor et al., 1989; Sweigart et al., 2004). The lack of statistical significance found in this study may be attributed to several factors. First, only ten samples (n=10) were tested for each of the groups and thus sample size was small. Furthermore, regional variation was only investigated for axially oriented tissue specimens; however, given the anisotropic results found here and the dependence on the particular structure of the tissue, the diffusion coefficient in other directions (e.g., circumferential) may be affected by tissue region and deserves further study.

4.5.4 Experimental Limitations

There are several limitations to this study that should be noted. For example, in order to seal the chamber around the tissues, we utilized porous plates in the custom made diffusion chamber. While we do not anticipate a large change in the results due to the use of these plates, it is possible that there was a stagnant layer formed on the boundary of the porous plates, thus influencing our results. This build-up was minimized by the use of stirring rods and continuous movement of the fluid throughout the experiment. These porous plates were necessary to hold the tissue in place, minimize swelling, and allow for compression. Previous studies by Jackson *et al.* showed a reduction in the diffusion coefficient by 7% with the use of porous plates (Jackson et al., 2008); this was most likely due to the build-up of a stagnant layer at the tissue boundary.

Additionally, in this study, we used samples from both the medial and lateral menisci, but did not study their effects separately, rather pooling all specimens. Future studies should report on the differences between the medial and lateral components for glucose diffusion, as previous studies in the literature have reported inhomogeneous tissue properties (e.g., composition, biomechanics) for meniscus tissues.

Moreover, these diffusion studies took place at room temperature on a magnetic stirring plate. Over time, we found the plates could become heated. Since diffusion is a temperature-dependent process, this change in environment temperature could potentially affect the results. However, we believe that the total change in temperature inside the diffusion chamber was minimal, if any. Nevertheless, in the future, it would be beneficial

to better mimic the environment inside the human body to see if results were indeed, affected.

Finally, as previously stated and discussed further in the future recommendations section of **Chapter 8**, future studies should investigate all three primary directions (axial, radial, and circumferential) in addition to medial and lateral regions and posterior and anterior horns and degenerated tissues. Nonetheless, the results of this study provide important information regarding nutritional supply in the tissue, and serve as a launching point for this work.

4.6 SUMMARY AND CONCLUSIONS

In summary, this study investigated the strain-dependent, anisotropic and region-dependent diffusion of glucose in porcine meniscus fibrocartilage. It was found that the apparent glucose diffusion coefficient is significantly affected by mechanical compression, decreasing as strain is increased. It was also found that diffusion of glucose in the circumferential direction, along the primary direction of the collagen fibers, is significantly higher than in the axial direction. Lastly, there was no statistically significant difference in axial glucose diffusion comparing the central and horn regions of the meniscus. Given the importance of a healthy meniscus in the proper functioning of the knee joint, as well as the unknown role of the tissue in the onset and progression of OA, better understanding of the transport environment within the tissue and the

relationship with tissue pathophysiology is essential in the development of new strategies to treat and/or prevent tissue degeneration and related OA. This study provides baseline information on the structure-function relationships for solute transport properties in the meniscus, and establishes the methods necessary to move toward full characterization of nutritional transport in meniscus fibrocartilage.

CHAPTER 5. MEASUREMENT OF STRAIN-DEPENDENT AND REGION SPECIFIC GLUCOSE PARTITION COEFFICIENT IN KNEE MENISCUS TISSUES

5.1 INTRODUCTORY REMARKS

As previously discussed, in adult meniscus tissues, vasculature is limited to the outer 10-30% of the tissue, leaving the inner tissue avascular, referred to as "white zones" (Danzig et al., 1987; McDevitt and Webber, 1990; Sweigart and Athanasiou, 2001). Meniscus cells, particularly in white zones, therefore rely on transport through the extracellular matrix for essential nutritional supply (Makris et al., 2011). This occurs mainly via diffusion from the vasculature in the adjacent red zones, and from the bathing synovial fluid. Although there is little information in the literature regarding the metabolic requirements of glucose by meniscus cells, several studies of cells from other similar cartilaginous tissues (e.g., articular cartilage, intervertebral disc, temporomandibular joint) show reduced viability and altered anabolic and catabolic activity under low glucose levels, and suggest glucose as the limiting nutrient for cell survival (Bibby and Urban, 2004; Cisewski et al., 2015; Heywood et al., 2006a, b; Holm et al., 1981; Richardson et al., 2003). Thus, elucidating nutrient transport and availability in the tissue is fundamental to understanding tissue homeostasis and pathobiology.

The transport of small, uncharged molecules within cartilaginous tissues is determined by the diffusion coefficient and the partition coefficient (Fetter et al., 2006). This study focuses on the equilibrium partition coefficient, K, which describes the maximum concentration of solute that can enter a tissue, sometimes referred to as its

solubility. The partition coefficient is the ratio of the concentration of a molecule within the tissue, c, relative to the concentration in free solution, c^*, at equilibrium (Maroudas, 1968):

$$K = \frac{c}{c^*} \quad \textbf{(5-1)}$$

When the partition coefficient equals unity ($K = 1$), the solute is evenly distributed between the tissue and the bathing solution, which is generally only the case for small, uncharged solutes. When $K < 1$, the solute is excluded from the tissue; possibly because of the size or the charge of the solute. The partition coefficient of glucose (MW=180Da) in other cartilaginous tissues has been shown to be less than unity (Fetter et al., 2006; Garcia et al., 2003; Maroudas, 1976; Maroudas et al., 1975; Nimer et al., 2003; Quinn et al., 2000; Quinn et al., 2001; Roberts et al., 1996; Schneiderman et al., 1995; Torzilli, 1993; Torzilli et al., 1998), signifying that even a relatively small molecule is sterically excluded. To our knowledge, there is currently no information regarding glucose partitioning in the knee meniscus.

The overall objective of this study is to provide quantitative information regarding equilibrium nutrient partitioning in meniscus tissue. We have hypothesized that the glucose partition coefficient in meniscus tissue is strain-dependent, decreasing with increasing compression. We have also hypothesized that the glucose partition coefficient varies based on location in the tissue, when comparing central vs. horn regions, and medial vs. lateral tissues. Finally, we hypothesized that glucose partition is dependent on tissue composition. To test these hypotheses, we measured the glucose partition coefficient in porcine meniscus under three levels of uniaxial confined compression (0%,

10%, 20%) and in four different locations in the tissue (medial central, medial horn, lateral central, lateral horn). This was accomplished using a series of equilibrating baths, as has been previously employed for cartilaginous tissues (Fetter et al., 2006; Jackson et al., 2012; Quinn et al., 2001). Results were then correlated with tissue water volume fraction and glycosaminoglycan (GAG) content. This study provides new information about nutritional supply and nutrient availability in meniscus tissues, which may have important implications for tissue health and/or degeneration.

Information regarding the glucose partition coefficient is necessary because the partition coefficient is one of the key parameters governing transport properties of a tissue. Additionally, it is useful in order to convert the apparent diffusivity (D_{app}) into the effective diffusivity (D_{eff}) by the equation:

$$D_{app} = KD_{eff} \quad \textbf{(5-2)}$$

5.2 THEORETICAL APPROACH

The partition coefficient is defined as the ratio of the solute concentration in the tissue, c, to that in the bathing solution, c^*:

$$c = Kc^* \quad \textbf{(5-3)}$$

When the partition coefficient equals 1 ($K = 1$), the solute is evenly distributed between the tissue and the bathing solution, which is generally only the case for small, uncharged solutes. When $K < 1$, the solute is excluded from the tissue; possibly because

of the size or the charge of the solute. For the porcine knee meniscus, which has negative fixed charges on the matrix, $K > 1$ for small cations, such as Na^+ and Ca^{2+}.

The partition coefficient of glucose in knee meniscus tissues can be measured by equilibrating the tissue in a series of baths and measuring the equilibrium concentrations, see **Figure 5-1**. Initially, the tissue is equilibrated in a solution containing glucose with the final concentration of solute (at equilibrium) measured. This process is then repeated in a bath containing no glucose and the equilibrium concentration is measured.

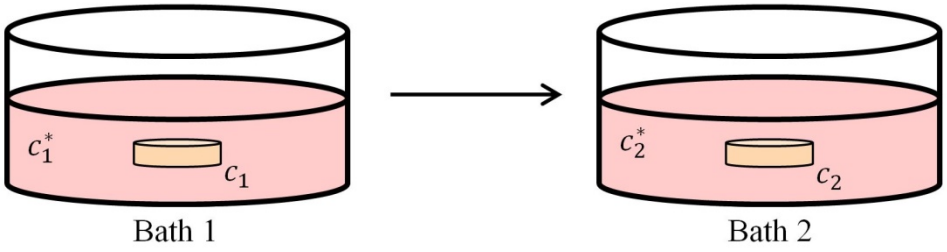

Figure 5-1 Schematic showing a much generalized depiction of the methods for determining the partition coefficient in a tissue specimen. Bath 1 shows the tissue in the high glucose concentration (the first 24 hour equilibration period) while Baths 2-5 show the tissue in the no glucose concentration solution (the final ~42 hours).

Using **Equation (5-3)**, the concentration of solute in bath 1, c_1^*, is related to the concentration of the solute in the tissue equilibrated in bath 1, c_1, by:

$$c_1 = Kc_1^*. \tag{5-4}$$

Likewise, the same relationship holds for bath 2:

$$c_2 = Kc_2^*. \tag{5-5}$$

Using conservation of solute mass after transfer from the first to the second equilibrium bath, we have:

$$\phi^w V(c_1 - c_2) = V_2 c_2^*. \quad \textbf{(5-6)}$$

where ϕ^w is the tissue water volume fraction, V is the tissue specimen volume, and V_2 is the volume of equilibrium bath 2. Using the relationship in **Equations (5-4)** and **(5-5)**, we have:

$$\phi^w V(Kc_1^* - Kc_2^*) = V_2 c_2^*. \quad \textbf{(5-7)}$$

Therefore, by simplifying **Equation (5-7)**, the partition coefficient can be written as (Fetter et al., 2006; Quinn et al., 2001):

$$K = \frac{V_2 c_2^*}{\phi^w V(c_1^* - c_2^*)}. \quad \textbf{(5-8)}$$

where, again, V_2 is the volume in bath 2, c_2^* is the concentration of solute in bath 2, ϕ^w is the water volume fraction of the compressed tissue, V is the volume of the compressed tissue specimen, and c_1^* is the concentration of solute in bath 1. As formerly stated, this method has been previously used to measure partition coefficient of solutes in articular cartilage.

Finally, in order to determine the strain-dependent partition coefficient, the tissue must be compressed to the desired height with equilibrations taking place while the tissue is confined, in order to maintain the proper strain-level. By varying the level of compression, a relationship for the strain-dependent partition coefficient of glucose in knee meniscus tissues can be determined.

5.3 Materials and Methods

5.3.1 Design of Experimental Apparatus

A custom-made chamber was constructed as shown in **Figure 5-2** and **Figure 5-3** to measure the strain-dependent partition coefficient of glucose in meniscus tissue based on previous studies (Fetter et al., 2006; Jackson et al., 2012; Quinn et al., 2001). The device consists of two cylindrical acrylic solution chambers encompassing a specimen chamber in the middle. The chambers allows for confined compression of a specimen during equilibration in a given solution. The specimen fits into a well with the same dimensions as the compressed tissue (i.e., d=8mm, h=2mm). A stainless steel wire mesh was used to confine the specimen, which was sealed with an o-ring. The solution was introduced into the solution chamber above the tissue specimen along with a micro stir bar, and was sealed from the air with a cap. Four bolts were used to hold the two chamber halves together. The compressive strain was determined by the height of the specimen well (i.e., 2mm) with respect to that of the uncompressed tissue specimen.

The chamber was machined out of a 2 inch acrylic rod (Small Parts). The solution chamber was designed to hold 100 μL of solution, in addition to a magnetic stirring bar. The specimen was sealed using an o-ring and a metal screen (Small Parts). The stainless steel screen was chosen over the porous plates, as were used in diffusion measurements, because it could confine the specimen without absorbing any of the bathing solution. The o-ring was used to seal the chamber and confine the equilibrating solution to the chamber above the tissue specimen.

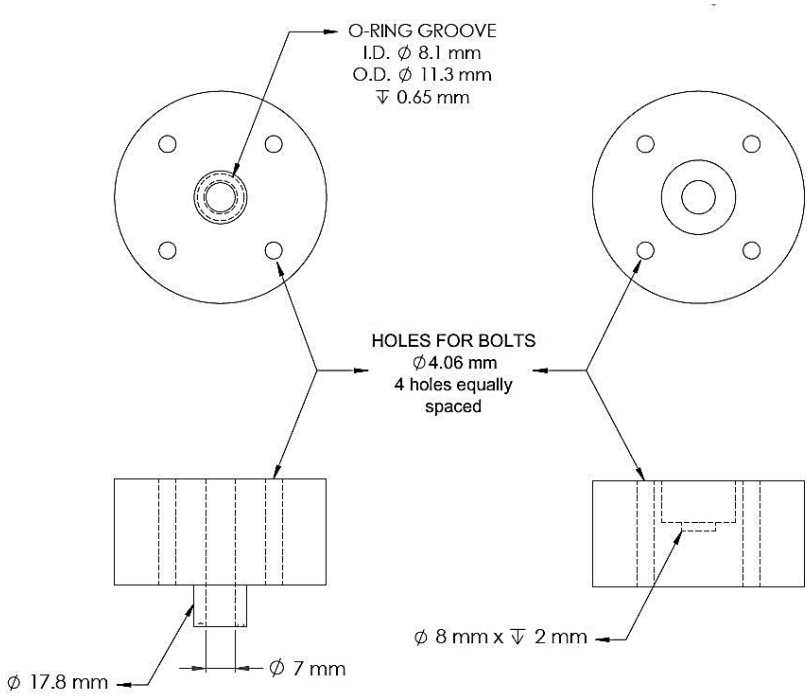

Figure 5-2 Engineering drawing showing the top and front views of the two halves of the custom partition coefficient chamber. See **Figure 5-3** for the schematic of the assembled apparatus.

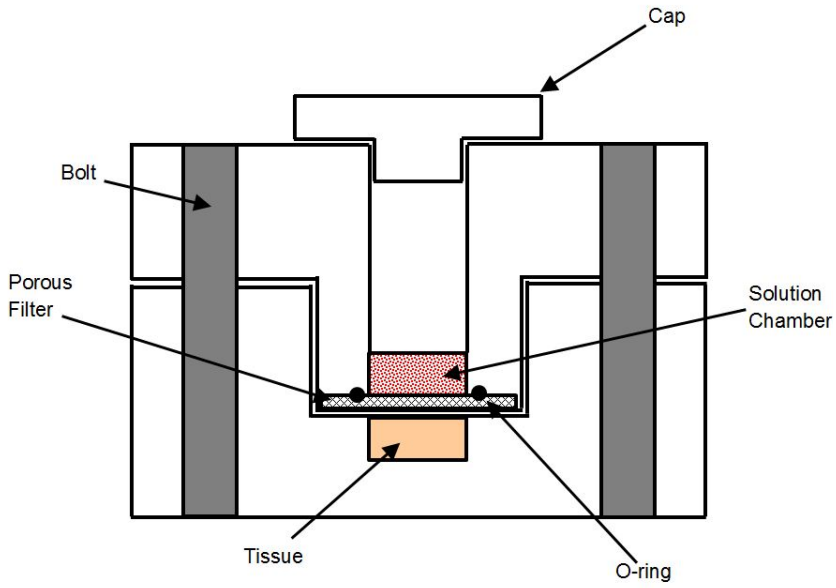

Figure 5-3 Schematic drawing of the partition coefficient chamber including the solution chamber, o-ring, tissue sample, porous filter, bolts, and cap. The chamber was constructed out of acrylic and held together by four bolts with wing nuts and caps.

5.3.2 Specimen Preparation

Four meniscus pairs were harvested from porcine knees obtained from a frozen tissue bank (Advanced Tissue Concepts, LLC, Smithfield, UT); specimens were kept frozen until the day of experimentation, in order to limit changes in tissue properties caused by multiple freeze-thaw cycles (Changoor et al., 2010). Pigs were 10 to 12 months in age, representing skeletally mature, healthy specimens. Cylindrical specimens (8mm in diameter and ~2.0-2.5mm thickness, depending on compression level) were prepared using a stainless steel corneal trephine (Biomedical Research Instruments, Inc., Malden, MA) and trimmed to the desired height using a microtome (Model SM2400, Leica Instruments, Nussloch, Germany) with freezing stage (Model BFS-30, Physitemp Instruments Inc., Clifton, NJ). The height was measured using a custom current-sensing micrometer that works using a capacitive sensor to read the height of the tissue sample and is precise to 0.001mm.

Specimens were harvested from the middle zone of the meniscus from four regions: medial horn, medial central, lateral horn and lateral central, see **Figure 5-4**; the horn region samples were pooled from both anterior and posterior horns**.** In each meniscus, three samples (n=3) were prepared from each region for testing at three levels of uniaxial compression: ~0%, 10% and 20%; thus, a total of six specimens (n=6) were harvested from each meniscus. Because four meniscus pairs were utilized, a total of four specimens (n=4) were prepared in each group for each strain level, for a total of forty-eight (n=48) tissue specimens; only one partition measurement was performed on each sample.

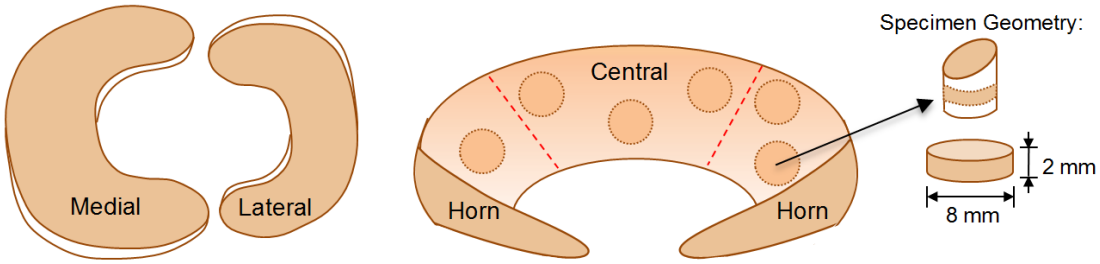

Figure 5-4 Schematic showing the orientation and size of specimens obtained from the porcine knee meniscus tissues. Tissue specimens were taken in the axial direction only, from both the medial and lateral menisci, and from both the horn and central regions. Specimens were approximately 2mm thick (depending on the level of compressive strain) and 8mm in diameter.

Again in this study, the samples were compressed approximately 10% and 20%, as these strain levels have been previously studied and are known to be in the range of physiological meniscal strains occurring in daily activity (Chia and Hull, 2008; Eckstein et al., 2000; Martin Seitz et al., 2013; Quinn et al., 2000; Quinn et al., 2001; Yang et al., 2010).

5.3.3 Water Content Measurement

Tissue water content for partition coefficient specimens was again measured using a buoyancy method (Gu et al., 1996) discussed in **Chapter 3**. However, with this project, the weights were taken following the partition experiment thereby allowing for measurements were taken on compressed tissues, the water volume fraction values reported reflect the reduced fluid content caused by compression.

5.3.4 Measurement of Partition Coefficient

Prior to partition measurements, samples were first compressed in a separate compression apparatus, see **Figure 5-5**, **5-6**, and **5-8**, prior to loading into the measurement chamber. This apparatus consisted of an acrylic confining ring and two porous plates. All specimens were compressed to a final height of 2mm, and the level of compressive strain was calculated based on the initial height measured during specimen preparation. Tissues underwent confined compression at a slow strain rate (~1-2%/min) to a final height of 2mm, and the level of strain was calculated based on the initial height measured during specimen preparation. Both initial and compressed heights were measured using a custom current sensing micrometer, accurate to 0.001mm.

The glucose partition coefficient in meniscus tissues can then be measured by equilibrating the tissue in a series of baths and measuring the equilibrium concentrations. To do this, the tissue was loaded into the chamber, see **Figure 5-7**, and sealed in place with the steel filter and o-ring. The chamber was then tightened with bolts and wing nuts. Initially, the tissue is equilibrated with 100μL of PBS (PBS, concentration = 5g/L glucose in solution) that was added into the solution chamber along with a magnetic micro-stirring rod. The concentration of the bathing solution was chosen to ensure final equilibrium bath concentrations could be reliably measured using our custom device (see below); a previous study in articular cartilage found that partition coefficient is not concentration dependent (Torzilli, 1993). The custom cap was then used to seal the chamber and the entire apparatus was placed on a magnetic stirring plate inside a

refrigerator (T = ~2°C) in order to minimize bacterial production in the bathing solution. The initial equilibration period is 24 hours.

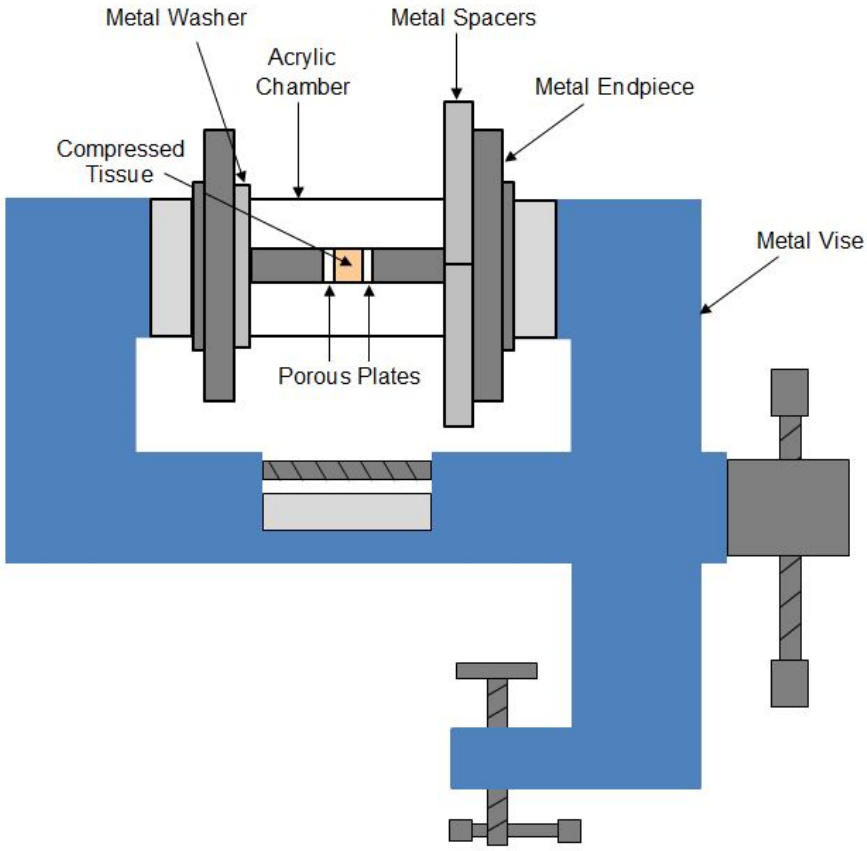

Figure 5-5 Schematic diagram of the compression chamber used to compress tissues to 2mm thickness. A vise clamp was used to hold the tissue confined between two porous plates for approximately 15 minutes to ensure compression. Following compression, specimens were immediately loaded into the partitioning chamber in order to keep them in their compressed state.

Figure 5-6 Photograph showing the compression chamber based on the schematic in **Figure 5-5**. Tissues were loaded between two porous plates in order for the water that is exuded during compression to be absorbed.

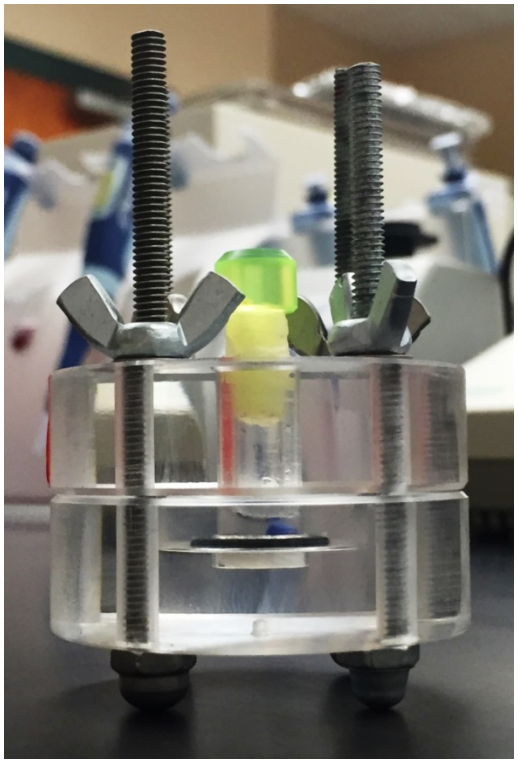

Figure 5-7 Photograph showing the partition coefficient chamber used to calculate glucose partitioning. This chamber was based on the design shown in **Figures 5-2** and **5-3**.

At the end of the first equilibration period, the concentration of glucose in the bathing solution was measured. Concentration measurements were carried out using the modified blood glucose meter used previously in glucose diffusion experiments (**Chapter 4**).

Following this measurement, the solution was removed and the chamber wiped out. This process is then repeated in a bath containing no glucose and the equilibrium concentration is measured. Therefore, 100μL of PBS containing no glucose was added into the solution chamber and allowed to equilibrate for 8 hours in the refrigerator. Following this period, the solution was collected and a fresh 100μL of no glucose PBS added into the chamber for an additional 8 hour period. This was repeated again a third time for an additional 8 hours and a fourth time for a final 18 hours, totaling approximately 42 hours of equilibration. Following this period, the concentration of glucose in the collected bathing solution (a total of 400μL combined and mixed) was measured. The consecutive equilibrations in four solutions were carried out in order to facilitate the diffusion of glucose out of the tissue sample and into solution; that is, by replacing the equilibrating solution with a fresh, blank solution, the concentration gradient remains steep, therefore, allowing for a faster equilibration. This method, that can be seen in **Figure 5-8**, has been previously used to measure partition coefficient of solutes in articular cartilage (Fetter et al., 2006; Jackson et al., 2012; Quinn et al., 2000; Quinn et al., 2001). Here, tissues are equilibrated under confined compression in order to minimize tissue swelling and proteoglycan leaching. Following the final equilibration period, the specimen was removed for water volume fraction measurements and the partition coefficient was calculated using **Equation (5-8)**.

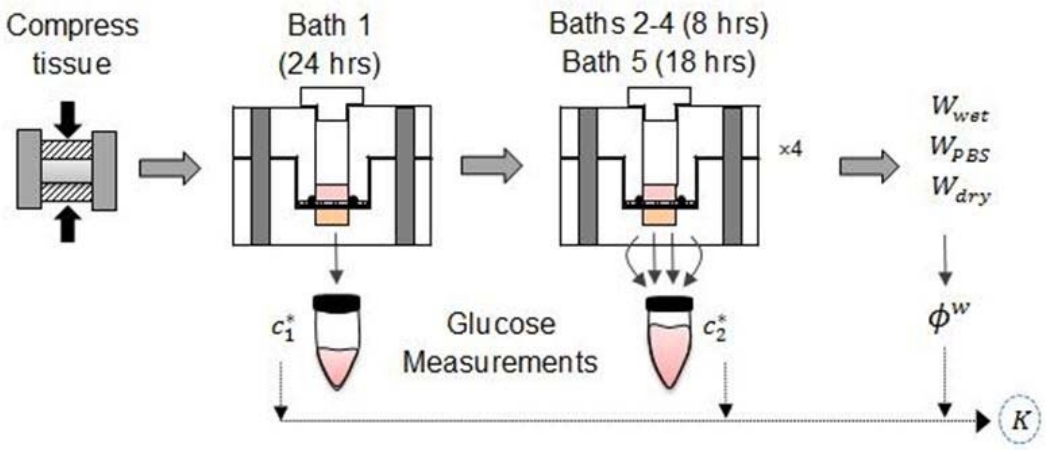

Figure 5-8 Schematic depiction of the flow chart showing the sequence of baths used to calculate the partition coefficient.

5.3.5 GAG CONTENT MEASUREMENT

The GAG content was measured using a 1,9-dimethylmethylene blue (DMMB) (Polysciences Inc., Warrington, PA) binding assay (Farndale et al., 1982). Following lyophilization, the meniscus tissues were digested using papain solution (250µg/ml) (Sigma Aldrich, St. Louis, MO). Once digested, the tissues were mixed with DMMB and the absorbance was measured using a multi-mode microplate reader (Molecular Devices SpectraMax M2 Series, Sunnyvale, CA) at 525nm wavelength. GAG content measurements were normalized by tissue wet weight and compared to the glucose partition coefficient.

5.3.6 STATISTICAL ANALYSES

A total of 4 specimens were tested (n=4) for each of the twelve groups [= 2 locations (central vs. horn) x 2 meniscus components (medial vs. lateral) x 3 strain levels (~0%, 10%, 20%)], for a total of 48 measurements. Three independent variables were studied: level of compression, regional location, and meniscus component. Statistical significance between groups was determined using repeated measures ANOVA analysis of variance tests using IBM SPSS Statistics 22. Tests were performed to determine if significant differences existed between central and horn groups, between 0%, 10%, and 20% compression level groups, and between medial and lateral meniscus groups. The significance level was set at $p<0.05$. Šídák post-hoc analysis was performed to determine between which groups there was a significant difference.

One-way ANOVA was also performed to determine if water volume fraction and tissue thickness differed significantly between the test groups. Regression analysis was performed to determine if the relationships between glucose partition coefficient and strain level, water volume fraction, and GAG content were statistically significant.

5.4 RESULTS

The results of this study can be found in **Tables 5-1**, **5-2**, and **5-3** and **Figures 5-9**, **5-10**, and **5-11**. A total of 48 specimens were measured; for each regional group, at each strain level, n=4, while n=16 for pooled results at each strain level. The relationship between

mechanical compression and partition coefficient for all groups is shown in **Figure 5-9** and **5-10**. Repeated measures ANOVA indicated that partition coefficient significantly decreased with increasing level of compression for all groups ($p<0.001$). Šídák post-hoc analysis showed significant differences when comparing partition coefficient values at 0% and 10% ($p=0.002$), 0% and 20% ($p=0.00006$), and 10% and 20% ($p=0.006$) compressive strain. However, since our experimental setup resulted in a more continuous strain-level (rather than discrete, exact levels at 0%, 20% and 20% compression), we also examined the correlation between strain and partition coefficient for pooled data (**Figure 5-9**) via regression analysis. We found a significant negative correlation between the level of compressive strain and the glucose partition coefficient ($R^2=0.71$, $p<0.001$).

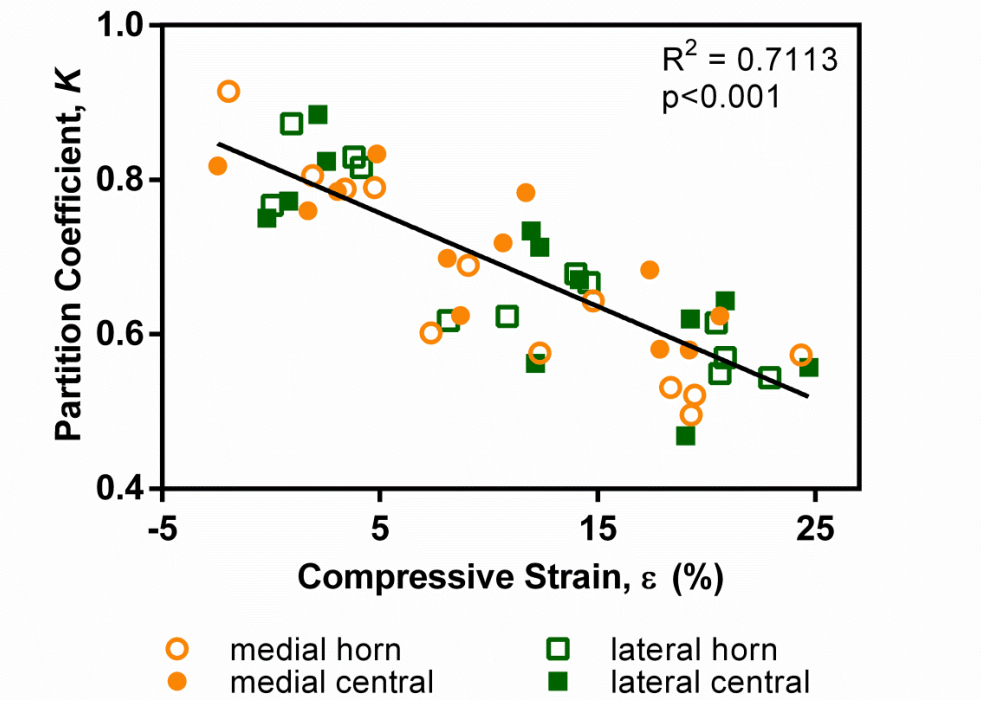

Figure 5-9 Correlation between glucose partition coefficient, *K*, and level of compression for all samples investigated. Significant correlation was detected. Correlation coefficient and p-value is shown.

	Strain (ε) (%)	*K*
Medial horn	2.03 ± 2.89	0.82 ± 0.06
	10.89 ± 3.33	0.63 ± 0.05
	20.36 ± 2.70	0.53 ± 0.03
Medial central	1.79 ± 3.11	0.80 ± 0.03
	9.79 ± 1.68	0.71 ± 0.07
	18.76 ± 1.44	0.62 ± 0.05
Lateral horn	2.24 ± 2.04	0.82 ± 0.04
	11.90 ± 2.99	0.65 ± 0.03
	21.20 ± 1.15	0.57 ± 0.03
Lateral central	1.33 ± 1.26	0.81 ± 0.06
	12.65 ± 1.01	0.67 ± 0.08
	20.96 ± 2.62	0.57 ± 0.08
All Data Pooled	1.84 ± 2.21	0.81 ± 0.05
	11.31 ± 2.45	0.66 ± 0.06
	20.32 ± 2.12	0.57 ± 0.06

Table 5-1 Table showing the results for glucose partition coefficient for each strain level for all four groups and pooled data.

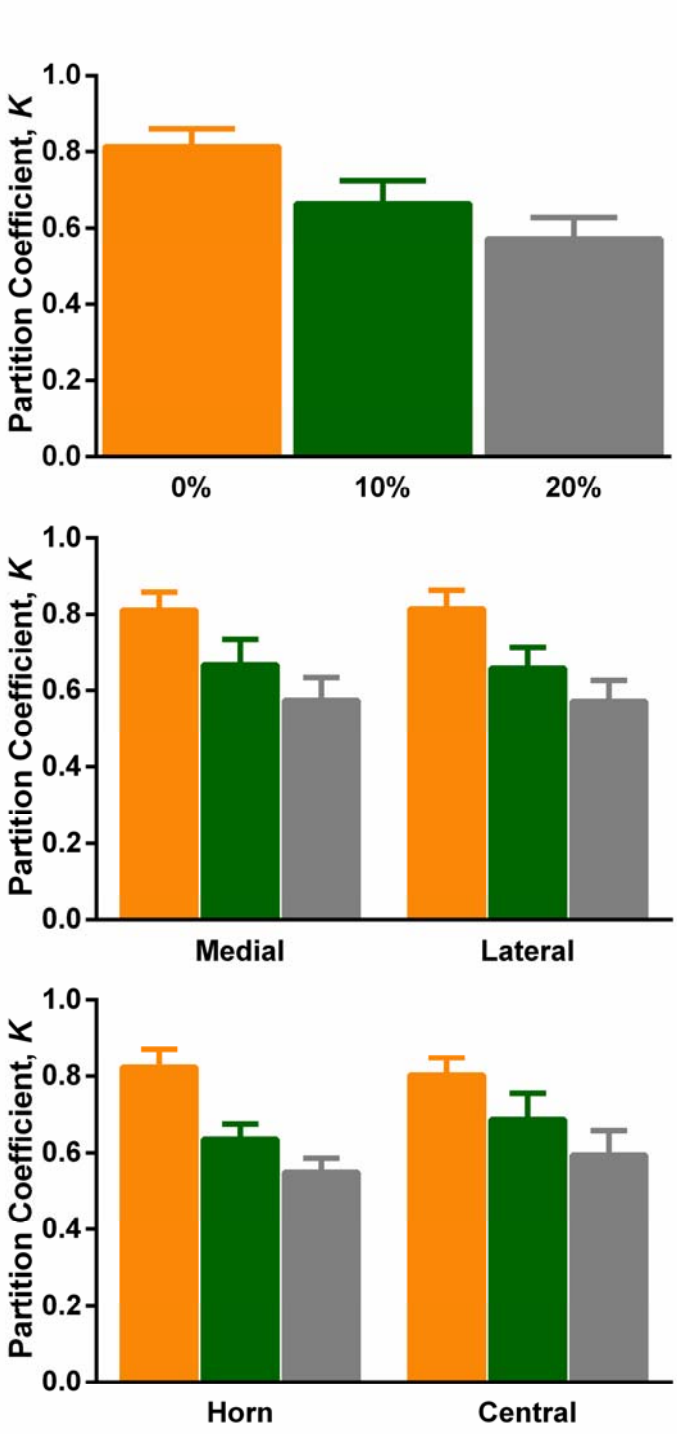

Figure 5-10 Bar graph showing the results from the partition coefficient studies: (a) shows 0%, 10% and 20% compressive strain; (b) shows medial versus lateral at 0%, 10%, and 20% compressive strain; (c) shows horn versus central regions at 0%, 10%, and 20% compressive strain.

Our analysis additionally showed there was no significant effect of region when comparing the partition coefficient for central to horn groups (p=0.181) or medial versus lateral meniscus (p=0.837). In order to investigate the effect of tissue composition on the partitioning of glucose, we correlated our results with tissue water volume fraction and GAG content. Correlation coefficients and p-values for all groups are shown in **Table 5-2**; scatter plots showing the relationship between water volume fraction and GAG content are shown in **Figure 5-11** and **5-12**. There was a significant positive correlation between tissue water volume fraction and partition coefficient (R^2=0.45, p<0.001), but the correlation with GAG content was not significant (R^2=0.054, p=0.11). Note that all four groups are shown in each graph, but best-fit line and regression analysis shown on the figure is for pooled data.

	Strain (ε) (%)	ϕ^w	**GAG Content**
Medial horn	R^2 = 0.81 p<0.001	R^2 = 0.44 p = 0.02	R^2 = 0.059 p = 0.45
Medial central	R^2 = 0.64 p = 0.002	R^2 = 0.43 p = 0.02	R^2 = 0.088 p = 0.35
Lateral horn	R^2 = 0.79 p = 0.0001	R^2 = 0.68 p = 0.001	R^2 = 0.48 p = 0.01
Lateral central	R^2 = 0.65 p = 0.002	R^2 = 0.56 p = 0.005	R^2 = 0.008 p = 0.78
All Data Pooled	R^2 = 0.71 p<0.001	R^2 = 0.45 p<0.001	R^2 = 0.054 p = 0.11

Table 5-2 Regression analysis for correlation between glucose partition coefficient and strain, ε, water volume fraction, ϕ^w, and GAG content.

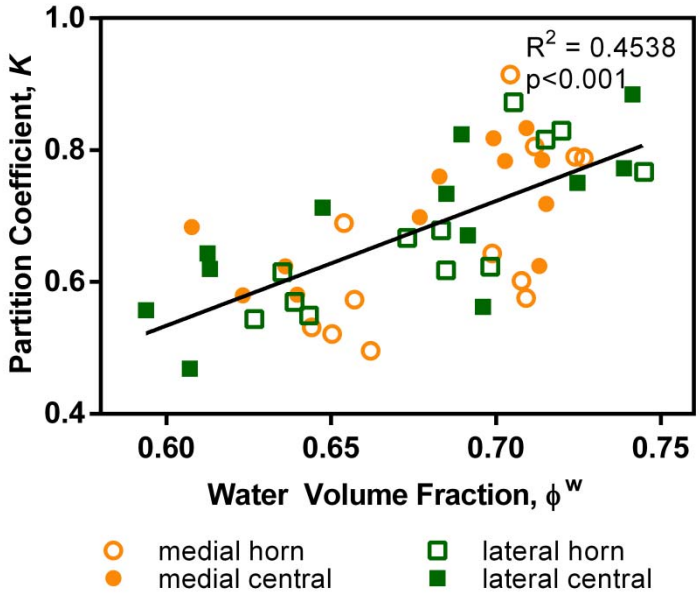

Figure 5-11 Relationship between tissue water volume fraction, ϕ^w, and glucose partition coefficient, K, in meniscus tissues for all samples investigated, n=48. Correlation coefficient and p-value are shown.

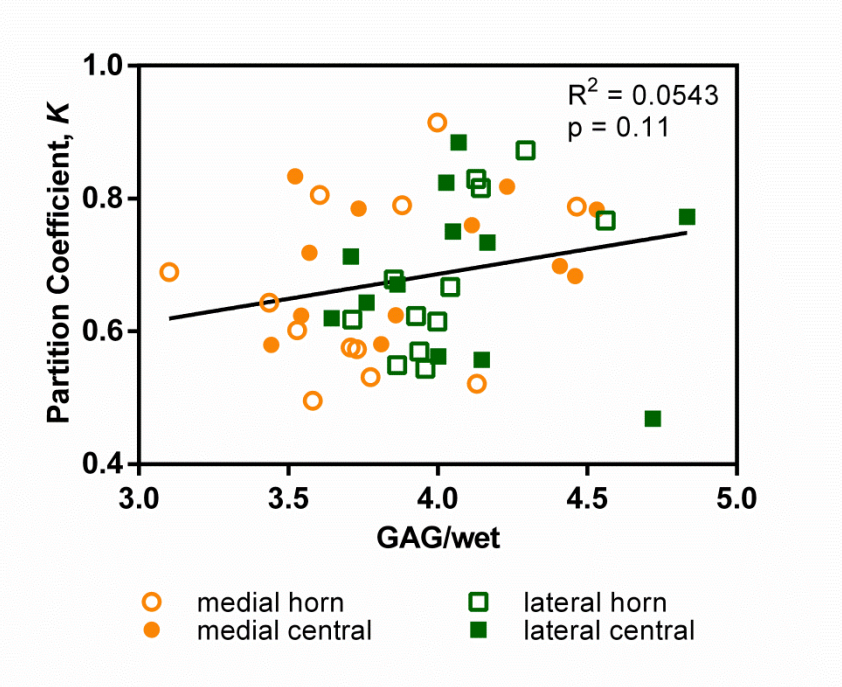

Figure 5-12 Relationship between GAG content in terms of wet weight, and glucose partition coefficient, K, in meniscus tissues for all samples investigated, n=48. Correlation coefficient and p-value are shown.

SIDAK post-hoc analysis showed that, for each group, when comparing partition coefficient at 0% and 10%, 0% and 20%, and 10% and 20% compressive strain, results were significantly ($p<0.01$) different. There was no significant difference between tissue thickness or water volume fraction of any of the groups (ANOVA, $p<0.001$). Statistical analysis results are shown with detail in **Table 5-3**.

5.5 DISCUSSION

In this study, we have investigated the effects of compression and tissue region on the glucose partition coefficient in healthy porcine meniscus fibrocartilage. To our knowledge, this is the first study to quantify glucose partitioning in meniscus tissues. Several previous studies have investigated the partitioning of a variety of small and large solutes in cartilage (Fetter et al., 2006; Garcia et al., 2003; Maroudas, 1976; Maroudas et al., 1975; Nimer et al., 2003; Quinn et al., 2000; Roberts et al., 1996; Schneiderman et al., 1995; Torzilli et al., 1998). The values determined here are similar to those in literature for glucose partition coefficients in other cartilaginous tissues (e.g., articular cartilage and intervertebral disc), which ranged from 0.51 to 0.90 (Maroudas, 1976; Maroudas et al., 1975; Torzilli et al., 1998).

A. ***Strain-Dependent Variation***

	P-values			
	Central	**Horn**	**Medial**	**Lateral**
0% vs. 10%	0.003*	4.6E-08*	0.0002*	2.4E-05*
10% vs. 20%	0.016*	0.001*	0.014*	0.011*
0% vs. 20%	2.0E-06*	4.7E-11*	2.2E-07 *	2.7E-08*

B. ***Axial Horn vs. Central Region***

	P-values
Region	0.181
Compressive Strain	1.07E-8*
Interaction	0.190

C. ***Medial vs. Lateral Component***

	P-values
Component	0.837
Compressive Strain	2.04-8*
Interaction	0.968

Table 5-3 Significance levels for post-hoc analysis of partition coefficient data for three comparisons: (A) strain dependent variation (tested in all 4 groups); (B) regional specific variation: axial horn vs. axial central (samples taken in the axial direction only); and (C) meniscal variation: medial vs. lateral component. Values shown are p-values; significant variation is noted with a '*'. Repeated measures ANOVA with SIDAK post-hoc analysis was performed using SPSS software.

5.5.1 Effect of Compression

The partition coefficient significantly decreased as compressive strain increased, see **Figure 5-9**, which is similar to previous studies examining a variety of solutes in cartilage and intervertebral disc (Jackson and Gu, 2009; Jackson et al., 2012; Nimer et al., 2003; Quinn et al., 2000; Quinn et al., 2001; Travascio et al., 2009a). This strain-dependent behavior is likely due to the decrease in water content during compression, and related decrease in pore size. All specimen groups showed a significant correlation between partitioning and strain, see **Table 5-3**. The effect of compression on glucose partitioning is significant because the tissue undergoes loading throughout the day, including circumferential hoop stresses, radial tension, shear and compression (Makris et al., 2011; Sweigart and Athanasiou, 2001; Walker and Erkman, 1975; Zhu et al., 1994). Our results show that compressive loading leads to a decrease in glucose solubility in the tissue, signifying a decrease in glucose availability for resident cells, especially in the avascular white zones. Although exact knowledge of meniscus cell glucose demand is not known, previous studies have shown that chondrocytes from articular cartilage, which are similar to meniscus cells from the inner, avascular regions (Makris et al., 2011), display reduced viability and poor homeostasis (i.e., reduced anabolic and increased catabolic activity) when exposed to low glucose levels (Heywood et al., 2006a, b; Richardson et al., 2003). If meniscus cells behave similarly, the reduced solubility of glucose in compressed tissues may negatively impact cell behavior and related tissue homeostasis. However, this requires further investigation of the effects of surrounding nutrient levels on meniscus cellular activity.

In this study, we focused on uniaxial, static compression within the range of physiological meniscal strains occurring in daily activity (Chia and Hull, 2008; Eckstein et al., 2000; Martin Seitz et al., 2013; Quinn et al., 2000; Quinn et al., 2001; Yang et al., 2010). Therefore, our results represent the equilibrium partition coefficient under static conditions. As mentioned, the knee and meniscus undergo a variety of loading conditions during normal daily activity, including dynamic compression (Makris et al., 2011). However, it has been shown that while dynamic loading enhances the transport of large molecules in cartilaginous tissues, it does not improve the transport of small molecules (Katz et al., 1986; O'Hara et al., 1990; Urban et al., 1982). Additionally, an earlier study found that continuous passive motion of the knee joint did not enhance nutrient transport in the meniscus (Danzig et al., 1987). Previous studies have also found static loading to be detrimental to meniscus cellular activity (Imler et al., 2004; Upton et al., 2003). The changes in nutrient transport and availability caused by compression may play a role in mediating cellular response to loading (Quinn et al., 2001).

5.5.2 Effect of Regional Variations

Our results did not show any significant regional variation in glucose partitioning when comparing central and horn regions, or medial and lateral menisci. Previous studies investigating mechanical properties in meniscus have found mixed results regarding the inhomogeneous nature of the tissue, see review (Makris et al., 2011). Our earlier studies on glucose diffusion and ion transport in porcine meniscus fibrocartilage also did not show any significant regional variation in transport in the tissue (Kleinhans et al., 2015;

Kleinhans et al., 2016). Furthermore, several previous studies, including our own discussed in **Chapter 3**, found that the hydraulic permeability (i.e., fluid transport) in porcine meniscus did not vary by region (anterior vs. central vs. posterior medial meniscus); in fact, the same study found that permeability only varied significantly by region in one (lapine) out of six species investigated (Sweigart et al., 2004). Nonetheless, the regional dependence of transport properties in meniscus deserves further investigation, particularly in human tissues.

5.5.3 Effect of Biochemical Content

We found a significant correlation between tissue water volume fraction and glucose partition coefficient for all groups investigated, see **Table 5-3** and **Figure 5-10**. This is in agreement with previous studies who have found that small solute transport in cartilaginous tissues depends primarily on tissue water content (Jackson and Gu, 2009). This relationship also helps to explain the strain-dependent behavior of glucose partitioning in the tissue, given that compression causes reduced tissue water content. On the other hand, our results did not show a significant correlation between tissue GAG content and glucose partition coefficient for pooled samples, see **Figure 5-12**. Previous studies on articular cartilage have found the transport of small solutes is less strongly influenced by GAG content than larger solutes (Burstein et al., 1993; Maroudas, 1970; Torzilli et al., 1997). Overall, the GAG content of meniscus tissue is much lower than that of other cartilaginous tissues (i.e., articular cartilage, intervertebral disc), and therefore may provide less interaction, especially for transport of small solutes (Almarza

and Athanasiou, 2004). However, we found a significant positive correlation between GAG content and the partition coefficient in only the lateral horn region, see **Table 5-2**. We believe the significant correlation in this region alone may be due to the particular distribution of GAG in the tissue. That is, the GAG content in the lateral horn tended to be higher than in other regions (no significant difference; data not shown), which may indicate that it plays a stronger role in transport. This should be further investigated to determine if differences exist for anterior and posterior horn regions, and for inner and outer zones, which have been shown to have different GAG contents (Killian et al., 2010; Sanchez-Adams et al., 2011). Furthermore, it is expected that the partitioning of larger and/or charged solutes in meniscus may be significantly correlated with tissue GAG content, and should be further explored.

5.5.4 Experimental Limitations

There are several limitations to this study that should be addressed. For example, our study divided specimens into horn and central regions, while some previous studies have found that anterior and posterior horns have distinct structure and composition (Di Giancamillo et al., 2014; Killian et al., 2010). Therefore, more investigation is warranted to determine if differences exist in transport properties among these regions.

Additionally, our measurements were carried out at low temperature (2^{o}C, in the refrigerator) in order to minimize bacterial production in the equilibrating baths. Solute transport rates are directly dependent on temperature; therefore, our results may underestimate partitioning at physiological temperature (Torzilli, 1993). In the future,

these studies should be modified to run at body temperature in order for a more realistic environment for experimentation.

Finally, as previously stated and discussed further in the future recommendations of **Chapter 8**, future studies should investigate all three primary directions (axial, radial, and circumferential) in addition to medial and lateral regions and posterior and anterior horns and degenerated tissues. This data would be beneficial for better understanding the homogenous behavior of the meniscus.

5.6 SUMMARY AND CONCLUSIONS

In summary, we have reported, to our knowledge, the first quantitative information on glucose partitioning in meniscus fibrocartilage. We found that glucose partitioning in porcine meniscus tissues is strain-dependent, but did not vary with regional location. The results of this investigation are important for better understanding the nutritional transport pathways and availability in the meniscus. Given the largely avascular nature of the adult meniscus, and the need for nutrition by resident cells, understanding how essential nutrients, like glucose, are supplied to the cells, and how this supply is affected by physiological conditions, is important for elucidating tissue pathophysiology. New knowledge of the mechanisms of meniscus degeneration can provide key insight for developing novel strategies to prevent and/or treat meniscus degeneration and related OA.

CHAPTER 6. EFFECTIVE DIFFUSIVITY OF GLUCOSE IN KNEE MENISCUS TISSUES

6.1 INTRODUCTORY REMARKS

Previously, we determined the apparent diffusion coefficient of glucose in porcine knee meniscus tissues in two directions (axial and circumferential) and in two regions (central and horn). However, the quantity most commonly expressed in literature is the effective diffusion coefficient. With the intention of effectively modeling transport properties in knee meniscus tissues, the knowledge of the effective diffusion coefficients is required in order to accurately predict solute concentrations in tissues. As mentioned previously, the apparent diffusivity can be related to the effective diffusivity by the partition coefficient, see **Equation (6-1)**. Thus, we can apply our results from the apparent glucose diffusion studies from **Chapter 4** with the glucose partition coefficient study from **Chapter 5**.

$$D_{app} = K \times D_{eff}. \quad \textbf{(6-1)}$$

In this chapter, we will be utilizing our results from **Chapters 4** and **5** in order to determine the effective diffusion coefficient of glucose in porcine meniscus fibrocartilage.

6.2 Combination of Diffusivity and Partitioning Results

To begin calculating the effective diffusion coefficient, a relationship between the partition coefficient and tissue water volume fraction was determined from curve-fitting the pooled data in **Chapter 5**:

$$K = 1.887 * \phi^{w} - 0.5985. \quad \textbf{(6-2)}$$

This relationship was then used to relate the apparent diffusion coefficient data to that of the partition coefficient via the tissue water volume fraction for each specimen (i.e., the partition coefficient was calculated based on the porosity of the tissue for each measurement of apparent glucose diffusion coefficient in **Chapter 4**). Then, rearranging **Equation (6-1)**, we were able to calculate the effective diffusivity from:

$$D_{eff} = \frac{D_{app}}{K}. \quad \textbf{(6-3)}$$

The results for the relative diffusion coefficient of glucose in porcine meniscus fibrocartilage are shown in **Figure 6-1**, and are also listed in **Table 6-1**. These results are grouped by the two locations studied, as related to tissue water content. Although there is an obvious correlation, there is still a large amount of scatter in the data. This is likely the result of variation between specimens from different menisci and/or pigs.

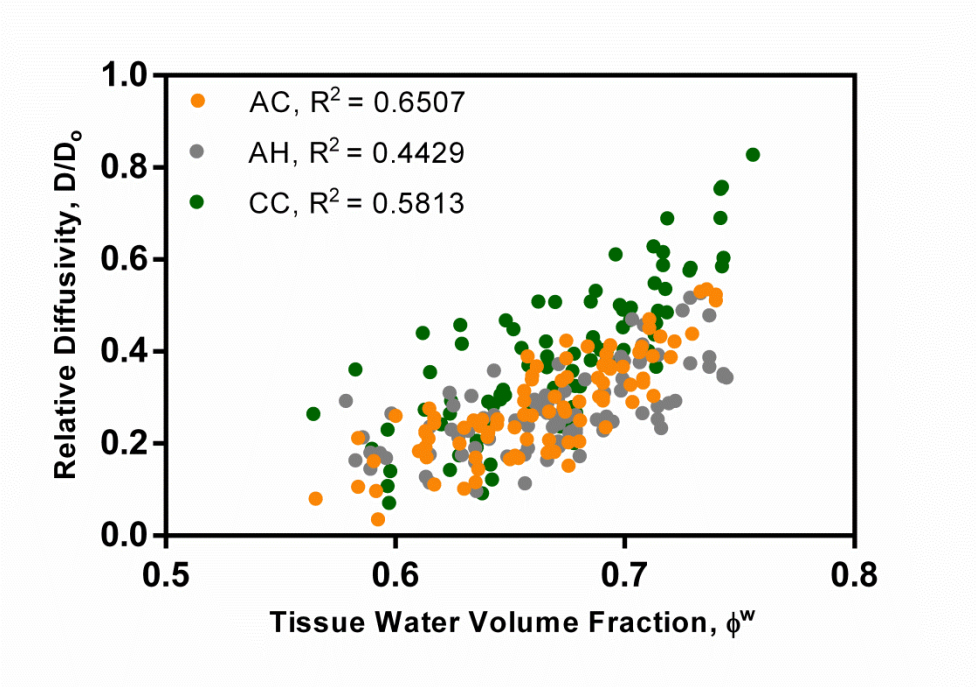

Figure 6-1 Results showing the tissue water volume fraction versus the relative diffusion coefficient for glucose for all three groups and all three strain levels, n=90 per group.

In addition to this data, diffusion coefficients are often expressed relative to the diffusivity of the solute in aqueous solution, known as the relative diffusivity. The diffusivity of glucose in aqueous solution, D_o, at 23°C is 6.382 × 10^{-6} cm^2/sec, which was calculated based on the value at *25°C* (Longsworth, 1953) using the Stokes-Einstein equation:

$$D_o = \frac{k_B T}{6\pi\eta r_s}, \qquad \textbf{(6-4)}$$

where k_B is Boltzmann's constant, T is absolute temperature, η is the solvent viscosity, and r_s is the hydrodynamic radius of the solute.

The relative diffusivities of glucose in porcine meniscus tissue at 0% compressive strain are shown in **Table 6-1**. The average relative diffusivity for all strain levels was 0.28 ± 0.10 for axial specimens, and ranged from 0.035 to 0.536. For circumferential specimens, the average relative diffusivity was 0.38 ± 0.16 at 0% compressive strain, ranging from 0.071 to 0.83.

	Strain (%)	Relative Diffusivity	Effective Diffusivity ($\times 10^{-6}$ cm^2/sec)
AC	1.03 ± 0.11	0.36 ± 0.09	2.29 ± 0.59
AH	1.04 ± 0.12	0.34 ± 0.09	2.16 ± 0.58
CC	1.02 ± 0.11	0.49 ± 0.09	3.15 ± 1.08

Table 6-1 Results showing the effective diffusion coefficient and relative diffusion coefficient for each group at 0% compressive strain, n=30 for each group.

6.3 COMPARISON WITH PREVIOUS STUDIES

Previous studies have investigated the transport of various solutes in other cartilaginous tissues. These results are summarized in **Table 6-2**; it is important to note that the methods and techniques used in these studies vary between one another and our own study. However, in general the diffusivities of small solutes in other cartilaginous tissues have been found to be smaller than their diffusivity in aqueous solution, similar to our results here (Burstein et al., 1993; Gu et al., 2004; Jackson et al., 2006; Jackson et al.,

2008; Maroudas et al., 1975; Quinn et al., 2000; Torzilli et al., 1987; Travascio and Gu, 2007; Travascio et al., 2009b; Urban et al., 1978; Yuan et al., 2009). Furthermore, for small solutes, the relative diffusivities have been found to be in the range of 0.35 to 0.6 (Burstein et al., 1993; Gu et al., 2004; Jackson et al., 2006). The majority of results for our study fall within this range, although some are much smaller. We believe this to be the result of different measurement techniques.

As can be seen in **Table 6-2**, the larger the solute, the lower the diffusion rate; i.e., solute diffusivity decreases as the size of the solute increases. Our results, as well, follow this trend with glucose diffusivity values less than other smaller molecules and higher than those of larger molecules.

6.4 SUMMARY AND CONCLUSIONS

We were successfully able to calculate the effective diffusivity by utilizing our results for apparent diffusivity and partitioning of glucose in porcine knee meniscus tissues. Our results are within the range stated in the literature for the relative diffusivity of small solutes in cartilaginous tissues. Additionally, our results follow the trend of decreasing diffusivity with an increase in solute size and/or molecular weight. The results for effective diffusivity of glucose in porcine knee meniscus tissues are necessary to theoretically model nutrient transport in the meniscus.

Solute	Tissue	D ($\times 10^{-6}$ cm^2/s)	Reference
Na+	Human articular cartilage	4.3-4.9	(Maroudas, 1968)
Cl-	Human articular cartilage	6.6-7.9	(Maroudas, 1968)
K+	Human articular cartilage	7.4	(Maroudas, 1968)
SO_4-	Human articular cartilage	6.8	(Maroudas, 1968)
Water	Bovine cartilage	13.8	(Burstein et al., 1993)
NaCl	Bovine cartilage	7.56	(Burstein et al., 1993)
Glucose	Adult bovine and equine articular cartilage	4.83	(Allhands et al., 1984)
	Human adult cartilage	1.4-2.3	(Maroudas, 1968)
	Human cartilage endplate	2.43	(Maroudas et al., 1975)
	Human articular cartilage	2.1-2.3	(Maroudas, 1970)
	Porcine meniscus	0.22-5.28	Present Study
Sucrose	Human articular cartilage	1.3	(Maroudas, 1970)
Hemoglobin	Human articular cartilage	0.115-0.16	(Maroudas, 1970)
Urea	Human articular cartilage	5.9-6.15	(Maroudas, 1970)
Dextran (10K)	Immature bovine articular cartilage	5.09	(Torzilli et al., 1998)
	Human articular cartilage	0.06-0.147	(Maroudas, 1970)
	Mature bovine cartilage	0.170-5.68	(Torzilli et al., 1987)

Table 6-2 Summary of experimental results for diffusion coefficient, D, in other cartilaginous tissues from literature.

CHAPTER 7. MEASUREMENT OF STRAIN-DEPENDENT AND ANISOTROPIC ELECTRICAL CONDUCTIVITY AND RELATIVE ION DIFFUSION IN KNEE MENISCUS TISSUES

7.1 INTRODUCTORY REMARKS

The fibrocartilaginous meniscus has a composition more similar to temporomandibular joint (TMJ) cartilage than hyaline cartilage, with high water content (~70%), and the remaining comprising mostly collagen (~75% dry weight, primarily type I) with small quantities (2-3% dry weight) of proteoglycans (PGs) (Almarza and Athanasiou, 2004). PGs are large, negatively charged molecules formed by glycosaminoglycans (GAGs) linked to a core protein; the negatively charged anions attached to GAG molecules attract positive cations in the surrounding fluid thus creating the Donnan osmotic pressure. This contributes to tissue hydration and related compressive properties, as well as allowing for the mechano-electrochemical responses in the tissue (Fithian et al., 1990; Hardingham and A., 1992; Mow et al., 1999; Sweigart and Athanasiou, 2001).

Electrical conductivity is an important material property of biological tissues that depends on ion diffusivities and concentrations within the tissues, which are related to tissue composition and structure (Frank et al., 1990; Maroudas, 1968). Previous studies have found that conductivity is directly correlated to tissue water content (Gu and Justiz, 2002; Gu et al., 2002; Gu et al., 2004; Jackson et al., 2009a; Kuo et al., 2011; Wright et al., 2013), and is strain-dependent (Jackson et al., 2009a; Kuo et al., 2011; Wright et al., 2013). Better understanding of electromechanical properties of tissues, including conductivity and ion transport, and their relationship to tissue composition and relevant

loading conditions, can provide essential information about endogenous electrical signals, which play a key role in directing resident cellular activity.

Electrical conductivity can be used to estimate the relative ion diffusivity in a tissue (Gu et al., 2004; Jackson et al., 2006; Kuo et al., 2011; Wright et al., 2013). Elucidating transport properties in meniscus is important given that much of the adult meniscus is avascular (Makris et al., 2011). As a result, essential nutrients are supplied by vasculature in outer tissue regions and surrounding synovial fluid. Solute concentrations in the tissue are related to transport rates through the ECM (i.e., solute diffusivities). Thus, better understanding transport properties in menisci can provide necessary information regarding the chemical environment in the tissue.

Increased knowledge of electromechanical and transport properties in meniscus is important for fully understanding structure-function relations in the tissue. Such information is valuable in developing novel strategies for meniscus repair and/or regeneration (e.g., tissue engineering or drug delivery approaches) and can be employed in theoretical modeling, used to predict the *in vivo* environment in the meniscus. To our knowledge, no previous study has investigated the electrical conductivity and/or ion diffusivity in meniscus fibrocartilage. We hypothesized that electrical conductivity and ion diffusivity in porcine meniscus are strain-dependent, anisotropic, and region-dependent. Therefore, our objective was to measure the electrical conductivity of porcine meniscus from two tissue regions, in two directions, and under three levels of compression. This information was then used to estimate relative ion diffusivity in the tissue.

7.2 THEORETICAL APPROACH

A charged porous material has an electrical conductivity (χ) which is related to the diffusivity of its intrinsic cations and anions (D^i, $i = +, -$). Under zero fluid flow conditions, the measured electrical conductivity of a tissue in ionic solution can be found by **Equation (7-1)** (Frank et al., 1990; Gu et al., 2004; Helfferich, 1962; Maroudas, 1968):

$$\chi = \frac{F_c^2 \phi^w (c^+ D^+ + c^- D^-)}{RT} \tag{7-1}$$

where F_c is the Faraday constant, R is the gas constant, T is the absolute temperature, $\phi^w$is the water volume fraction, c^+ is the cation concentration, and c^- is the anion concentration. Because the ECM of cartilaginous tissues is negatively charged, the cation and anion concentrations can be determined using the electroneutrality condition (Katchalsky and Curran, 1975; Lai et al., 1991) in **Equation (7-2)** for a negatively charged tissue:

$$c^+ = c^- + c^F \tag{7-2}$$

where c^F is the absolute value of the negative fixed charged density (FCD). At equilibrium, the chemical potential inside the tissue is equal to that of the bathing solution. As a result (Maroudas, 1975, 1979):

$$(c^+)(c^-) = (c^*)^2 \tag{7-3}$$

where c^* is the concentration of salt in the bathing solution. **Equations (7-2)** and **(7-3)** can be solved for the cation and anion concentrations to give the ideal Donnan equation:

$$c^{+} = \frac{c^{F} + \sqrt{(c^{F})^{2} + 4(c^{*})^{2}}}{2} \quad \textbf{(7-4)}$$

$$c^{-} = \frac{-c^{F} + \sqrt{(c^{F})^{2} + 4(c^{*})^{2}}}{2} \quad \textbf{(7-5)}$$

Thus, the electrical conductivity of a tissue is dependent upon the diffusivity of anions and cations in the tissue (i.e., D^{-} and D^{+}), tissue water content, and fixed charge density. In this study, we used electrical conductivity measurements to investigate ion diffusion coefficients, thereby providing important information about small solute transport in the tissue. The relative diffusion coefficient (D/D_o) can be estimated using **Equation (7-6)**, where D is the mean ion diffusivity of Na^{+} and Cl^{-} in tissue, D_o is the mean ion diffusivity in the bathing solution, χ is the electrical conductivity of the tissue, ϕ^{w} is the tissue water volume fraction, and χ_o is the conductivity of the bathing solution.(Gu et al., 2004)

$$\frac{D}{D_o} = \frac{\chi}{\phi^{w}\chi_o} \quad \textbf{(7-6)}$$

In our analysis, Na^{+} and Cl^{-} were assumed to carry the electrical current because these ions are the primary ionic components of PBS (0.15 M NaCl).

7.3 Materials and Methods

7.3.1 Design of Experimental Apparatus

A custom-made electrical conductivity apparatus was constructed as shown in **Figure 7-1** and **Figure 7-2** to measure the conductivity of meniscus tissue based on previous studies

(Gu and Justiz, 2002; Gu et al., 2002; Jackson et al., 2009a; Jackson et al., 2009b). The device consists of two stainless steel current electrodes, two Polyester-coated Ag/AgCl voltage electrodes, a metal spacer, and a nonconductive acrylic chamber. A four-wire method was applied using a sourcemeter (Keithley SourceMeter, Cleveland, OH). The resistance, Ω, across the tissue sample was measured at a low constant current of 10 μA.

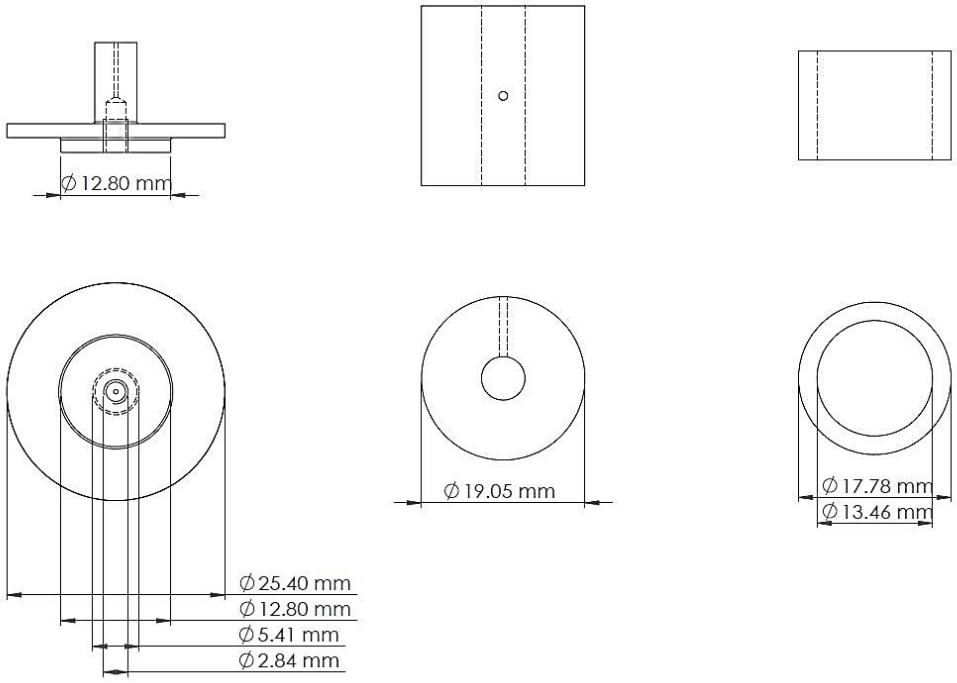

Figure 7-1 Engineer drawing of the electrical conductivity chamber parts including: (a) metal electrode, (b) acrylic chamber and tissue holder, and (c) plastic endcaps.

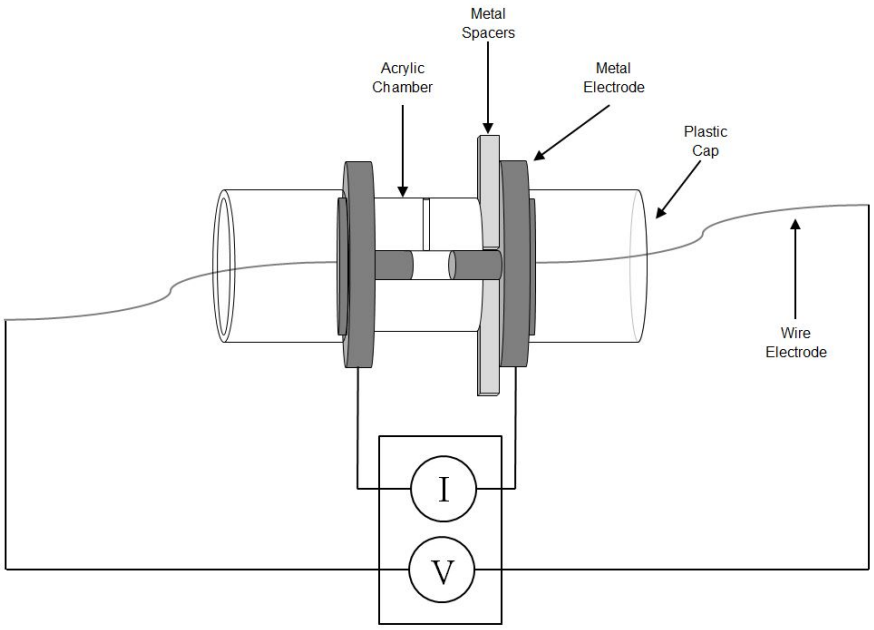

Figure 7-2 Schematic of the custom-designed chamber for measuring the electrical conductivity. The metal spacers between the chamber and one of the metal electrodes are used to control the amount of uniaxial confined compression on the specimen; that is, the spacer matches the desired compressed height of the tissue (i.e., for a 3.00mm thick specimen at 0% strain, the spacer is used to make a 3.00mm space in the chamber).

To prepare the Ag/AgCl wire electrodes, ions were passed using an electric current through KCl in a process known as electrolysis. A silver wire was used as an anode in a solution of 0.1M KCl and separated from a large stainless steel rod in 1M NaCl by a salt bridge (**Figure 7-3** and **7-4**). The salt bridge, containing 0.1M KCl in 2% agar, allows the flow of charges but restricts the transfer of solution. The silver wire was insulated by heat-shrink polyester tubing, so only the end of the silver was actually coated with silver chloride. A current density of 1.0 mA/cm^2 for 30 minutes was used (Gu and Justiz, 2002; Gu et al., 2002).

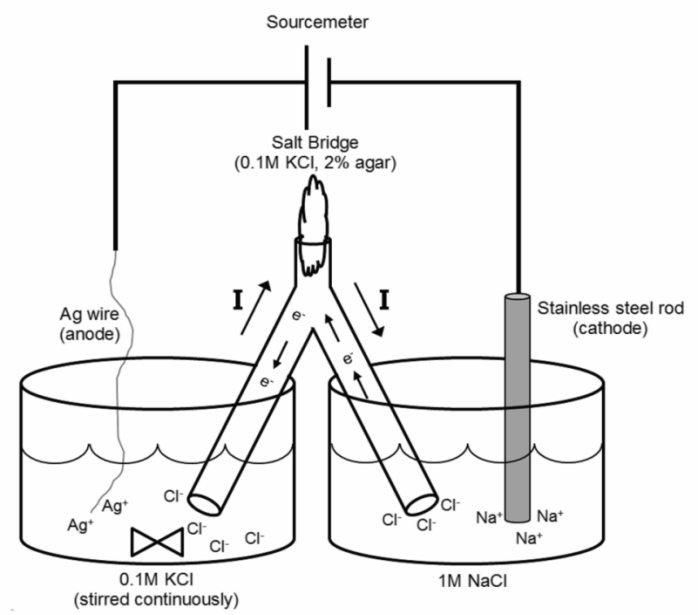

Figure 7-3 Schematic showing the preparation of the Ag/AgCl wire electrodes using a salt bridge. Silver wire is coated with silver chloride at a current density of 1.0 mA/cm2 for 30 minutes.

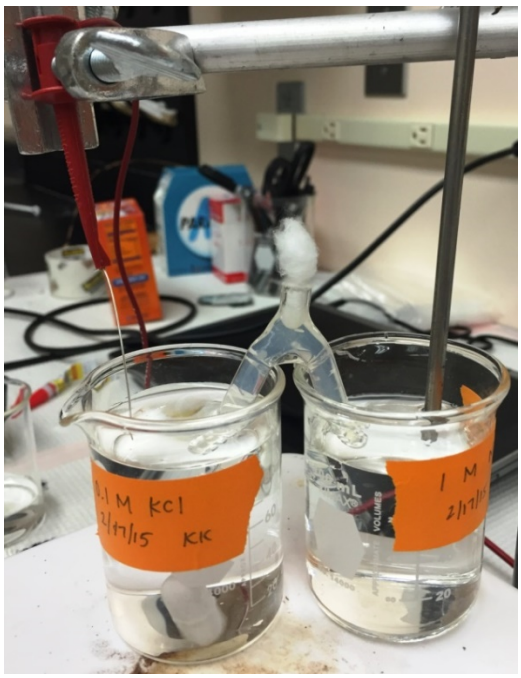

Figure 7-4 Photograph showing the salt-bridge electrolysis system. On the left, the wire is coated with Ag/AgCl and submerged in KCl and the electrons are transferred through the salt bridge to the NaCl on the right side with a metal rod.

7.3.2 Specimen Preparation

Fifteen lateral and medial menisci were harvested from both left and right cadaveric knees of 9 Yorkshire pigs (~20-25 weeks, both male and females) obtained from a local abattoir within one hour of death. Cylindrical specimens (d=5mm and t=3.06±0.27mm) were prepared using a stainless steel corneal trephine (Biomedical Research Instruments, Inc., Malden, MA) and sledge microtome (Model SM2400, Leica Instruments, Nussloch, Germany) with freezing stage (Model BFS-30, Physitemp Instruments Inc., Clifton, NJ). The height was measured using a custom current-sensing micrometer that works by using a capacitive sensor to read the height of the tissue sample and is precise to 0.001 mm. Samples were harvested from either the central or horn region in either the axial and circumferential orientation; see **Figure 7-5.** Samples from both medial and lateral menisci from both left and right knees were pooled. In the axial direction, samples were taken from both the horn and the central regions, as shown in **Figure 7-5**, while circumferential samples were taken only from the central region due to size restraints. A total of nine groups were investigated, including three orientation/regions: [axial horn (AH), axial central (AC), and circumferential central (CC)] and three levels of compressive strain (0%, 10%, 20%). In each group, fifteen (n=15) samples were measured, for a total of 135 tissue specimens; only one electrical conductivity measurement was taken on each sample.

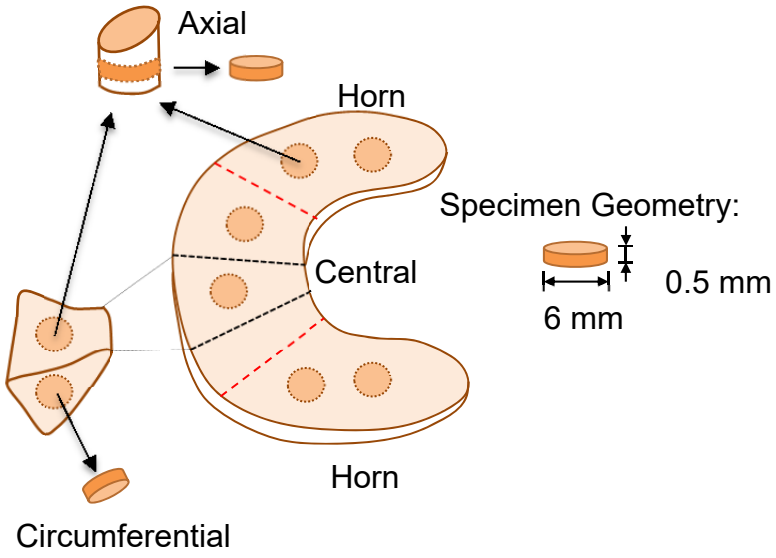

Figure 7-5 Schematic showing locations and sizes of test specimens. The meniscus was divided into central and horn regions (demarcated by larger dashed lines). From the central region, both axial and circumferential specimens were prepared; only axial specimens were prepared from the horn region. All specimens were cylindrical with a height of ~3.0mm and a diameter of 5mm. Samples from both medial and lateral menisci were pooled.

7.3.3 Water Content Measurement

Again, tissue water content for electrical conductivity specimens was measured using the buoyancy method described in **Chapter 3**. Measurements were taken following experimentation, after each specimen was frozen at -20°C and lyophilized.

7.3.4 Tissue Compression

Prior to conductivity measurement, in a separate chamber, the tissue specimens underwent uniaxial confined compression; see **Figure 7-6**. The tissue was compressed between two porous plates in an acrylic chamber with an inner diameter of 5mm. A separate compression chamber was used in order to avoid damage to the Ag/AgCl

electrodes in the conductivity chamber. Unless being studied at 0% strain, each specimen was compressed to either 10% or 20% strain depending on the sample test. Following compression, the specimen was removed and immediately placed in the conductivity chamber in order to measure the resistance, as detailed below.

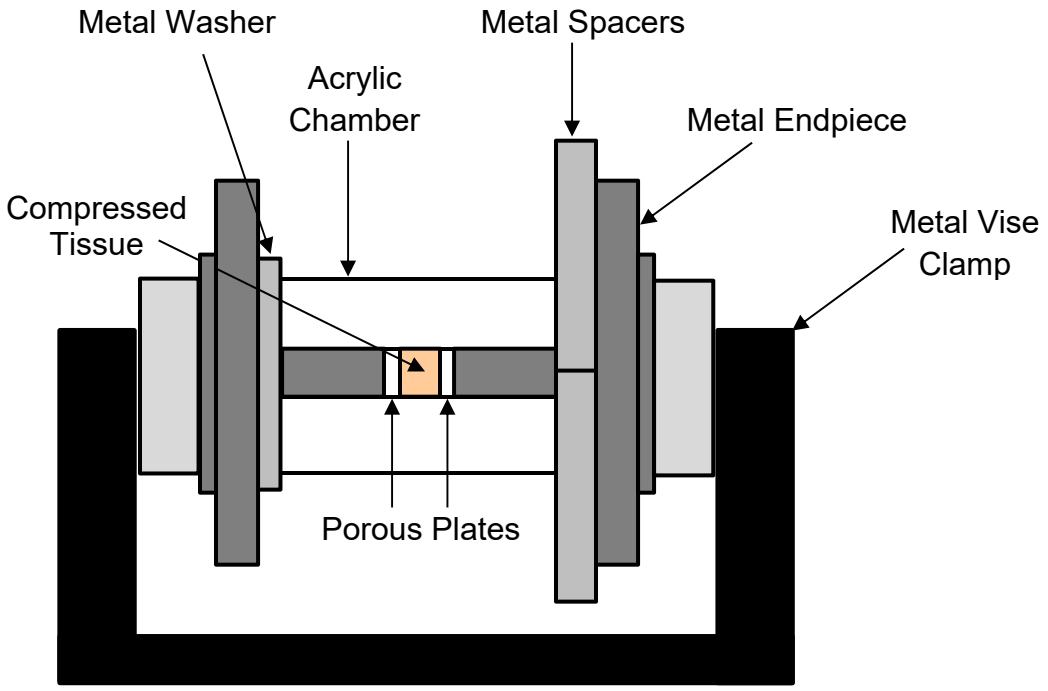

Figure 7-6 Schematic drawing of the specimen compression chamber. A vise clamp was used to hold the tissue in place and slowly compress the chamber until it was flush with the metal spacers.

7.3.5 Measurement of Electrical Conductivity

The custom conductivity apparatus is similar to that in the literature (Gu and Justiz, 2002; Jackson et al., 2009a), see **Figure 7-7**. Briefly, the apparatus consists of two stainless steel current electrodes, two Polyester-coated Ag/AgCl voltage electrodes, a metal spacer, and a non-conductive acrylic chamber. A four-wire method was applied using a

sourcemeter. The resistance, Ω, across the tissue sample was measured at a low constant current of 10μA (current density = 0.051 mA/cm^2). Electrical conductivity (χ) is related to resistance by:

$$\chi = \frac{h}{\Omega \cdot A} \tag{7-7}$$

where A is the cross sectional area and h is the thickness of the sample.

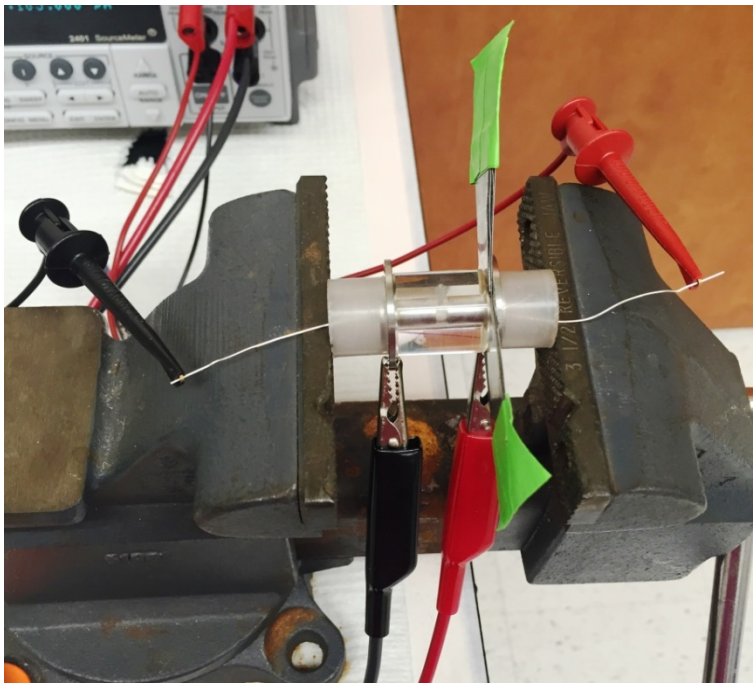

Figure 7-7 Photograph showing the actual electrical conductivity chamber hooked up to the SourceMeter. A four-wire method was used to find the resistance across the tissue and an equation was used to calculate the electrical conductivity of each specimen.

Conductivity measurements were taken at 0%, 10%, or 20% compression. Prior to measurements, tissue specimens were compressed to the desired thickness via uniaxial confined compression between two porous plates in a separate compression chamber based on initial measurement height and desired strain level, see **Figure 7-6**. After

compression and a brief equilibration period, the compressed sample was moved to the custom conductivity apparatus; the level of compression was maintained by controlling the distance between current electrodes using metal spacers. For each experiment, several resistance measurements were obtained at 10 minute intervals to ensure the tissue had reached equilibrium in the chamber; that is, measurements were repeated until the same resistance value (within 5%) was measured for two consecutive readings, signifying equilibrium was reached (i.e., no fluid flow).

7.3.6 Relative Ion Diffusion Calculation

The electrical conductivity of a charged porous material is related to the diffusivity of its intrinsic cations and anions (D^i, $i = +, -$) under zero fluid flow conditions by (Frank et al., 1990; Gu et al., 2004; Helfferich, 1962; Maroudas, 1968) **Equation (7-1)**. Due to the low GAG content (~2-3% dry weight) in meniscus compared to other cartilaginous tissues, it was considered an uncharged tissue. The relative diffusivity (D/D_o) of NaCl can then be related to the conductivity measurements by (Gu et al., 2004; Kuo et al., 2011; Wright et al., 2013) **Equation (7-6)**. This value is the averaged relative diffusivity of Na^+ and Cl^- ions, which were assumed to carry the current as the primary ions in PBS solution (Kuo et al., 2011; Wright et al., 2013).

7.3.7 Proteoglycan Content Measurement

The GAG content was again measured using a 1,9-dimethylmethylene blue (DMMB) (Polysciences Inc., Warrington, PA) binding assay (Farndale et al., 1982) to investigate

whether the electrical conductivity was related to the proteoglycan content. Following lyophilization, the meniscus tissues were digested using papain solution (250 μg/ml). Once digested, the tissues were mixed with DMMB and the absorbance was measured using a multi-mode microplate reader (Molecular Devices SpectraMax M2 Series, Sunnyvale, CA) at 525nm wavelength. The fixed charge density (FCD) could be calculated by:

$$c^F = \left(\frac{2\ mol\ charges}{502.5g\ GAG}\right)\frac{W_{GAG}}{W_{air}}, \quad \textbf{(7-8)}$$

where W_{GAG} is the GAG content (in grams) in the sample and W_{air} is the weight of the wet tissue in air.

For compressed samples, the FCD could be calculated by:

$$c^F = \frac{c_0^F(1-\phi^w)\phi_o^w}{(1-\phi_0^w)\phi^w} \quad \textbf{(7-9)}$$

where c_o^F is the FCD of the sample calculated in **Equation (7-8)**, ϕ^w is the compressed tissue water volume fraction calculated, and ϕ_o^w is the water volume fraction of the undeformed tissue.

7.3.8 Statistical Analyses

A total of 9 pigs were tested (n=9) with three factors (location: AC, AH, and CC) and three levels per factor (compression level: 0%, 10%, 20%). The total measurements taken were 135. Three independent variables were studied for each sample: level of compression, direction of diffusion, and regional location. Statistical significance

between groups was determined by two-way repeated measures ANOVA analysis of variance tests using IBM SPSS Statistics 22 with multiple pairwise comparisons using SIDAK post-hoc methods to control for the alpha level, which was set at $p<0.05$; sample size was set to $n=9$.

One-way ANOVA was also performed to determine if water volume fraction and height measurements differed significantly between the three test groups (AC, AH, CC). Regression analysis was performed to determine if relationships between electrical conductivity or ion diffusivity and water volume fraction and strain level were statistically significant.

7.4 RESULTS

A total of 135 specimens were measured, with an average uncompressed water volume fraction of 0.70 ± 0.04. The results for this study for all nine groups investigated are shown in **Figure 7-8** and **Table 7-1**; data are shown as mean ± standard deviation. Results show that the electrical conductivity decreases with increasing level of compressive strain for all groups investigated.

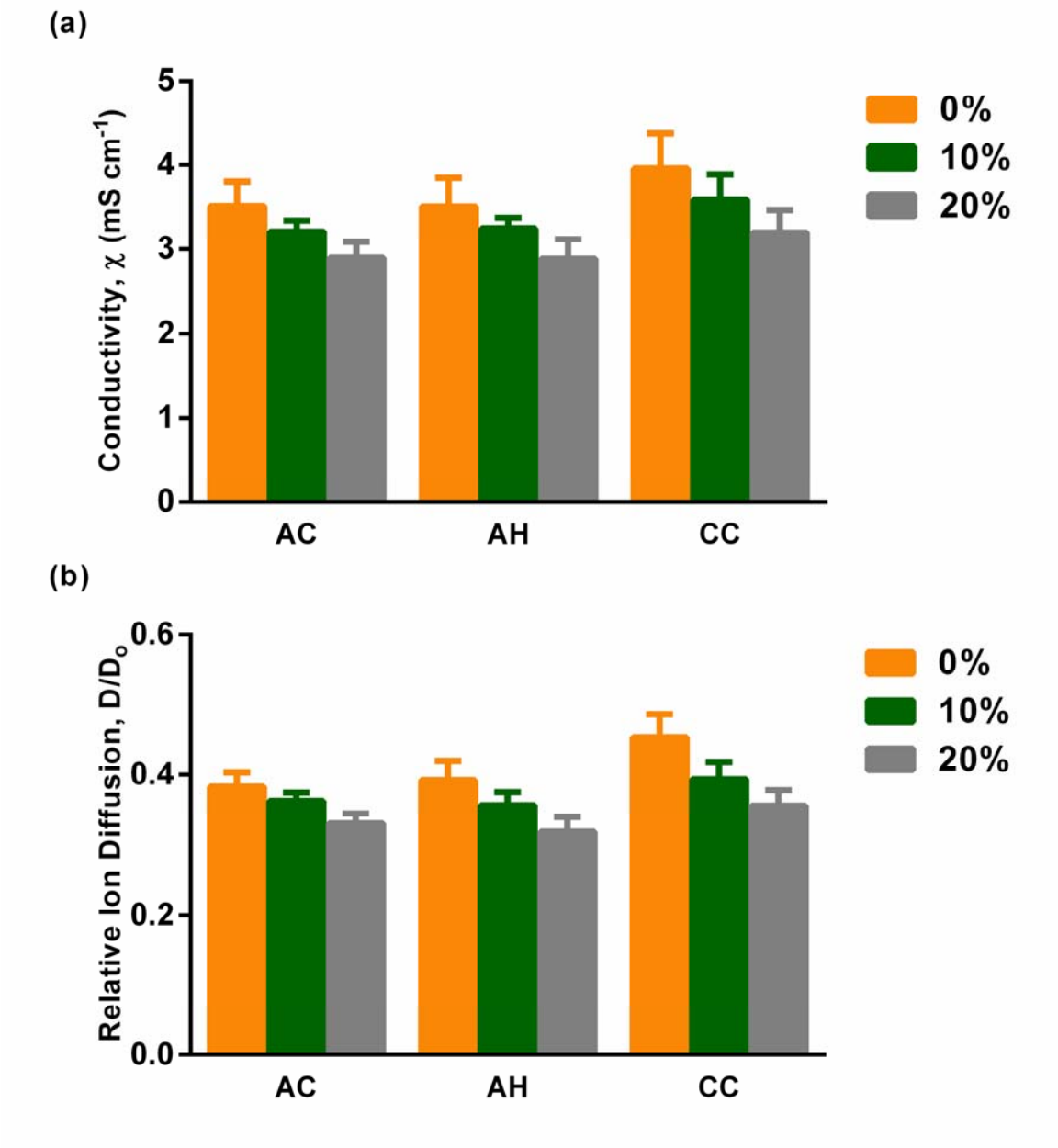

Figure 7-8 Graph showing the electrical conductivity, χ, and the relative ion diffusion coefficient, D/D_o, for each of the three groups studied (i.e., axial central, axial horn, and circumferential central) at 0%, 10%, and 20% compressive strain. Data is shown as mean ± standard deviation; for each group, n=15.

	Strain (%)	N	h	ϕ^w
AH	0	15	3.06 ± 0.26	0.69 ± 0.04
	10	15	2.96 ± 0.20	0.68 ± 0.05
	20	15	3.22 ± 0.27	0.63 ± 0.04
AC	0	15	2.95 ± 0.22	0.71 ± 0.04
	10	15	3.05 ± 0.31	0.65 ± 0.03
	20	15	3.09 ± 0.35	0.60 ± 0.05
CC	0	15	2.94 ± 0.23	0.68 ± 0.03
	10	15	3.08 ± 0.20	0.68 ± 0.04
	20	15	3.15 ± 0.28	0.62 ± 0.05

Table 7-1 Results for tissue thickness and tissue water volume fraction in porcine knee meniscus tissues for the three groups tested [axial horn (AH), axial central (AC), circumferential central (CC)] and at three levels of compressive strain. All results are shown as mean ± standard deviation.

Figure 7-9 shows the regression analysis for the relationship between both the electrical conductivity and the relative ion diffusion coefficient and mechanical compression. Electrical conductivity and ion diffusivity significantly decreased with increasing level of compression for all three regions/direction groups ($p<0.001$). In addition, both conductivity and relative ion diffusion in the circumferential direction were made significantly greater than that in the axial direction in the central region. For all

groups, there was a significant correlation detected between conductivity and diffusion and strain level, as noted by the p-values and R^2 values.

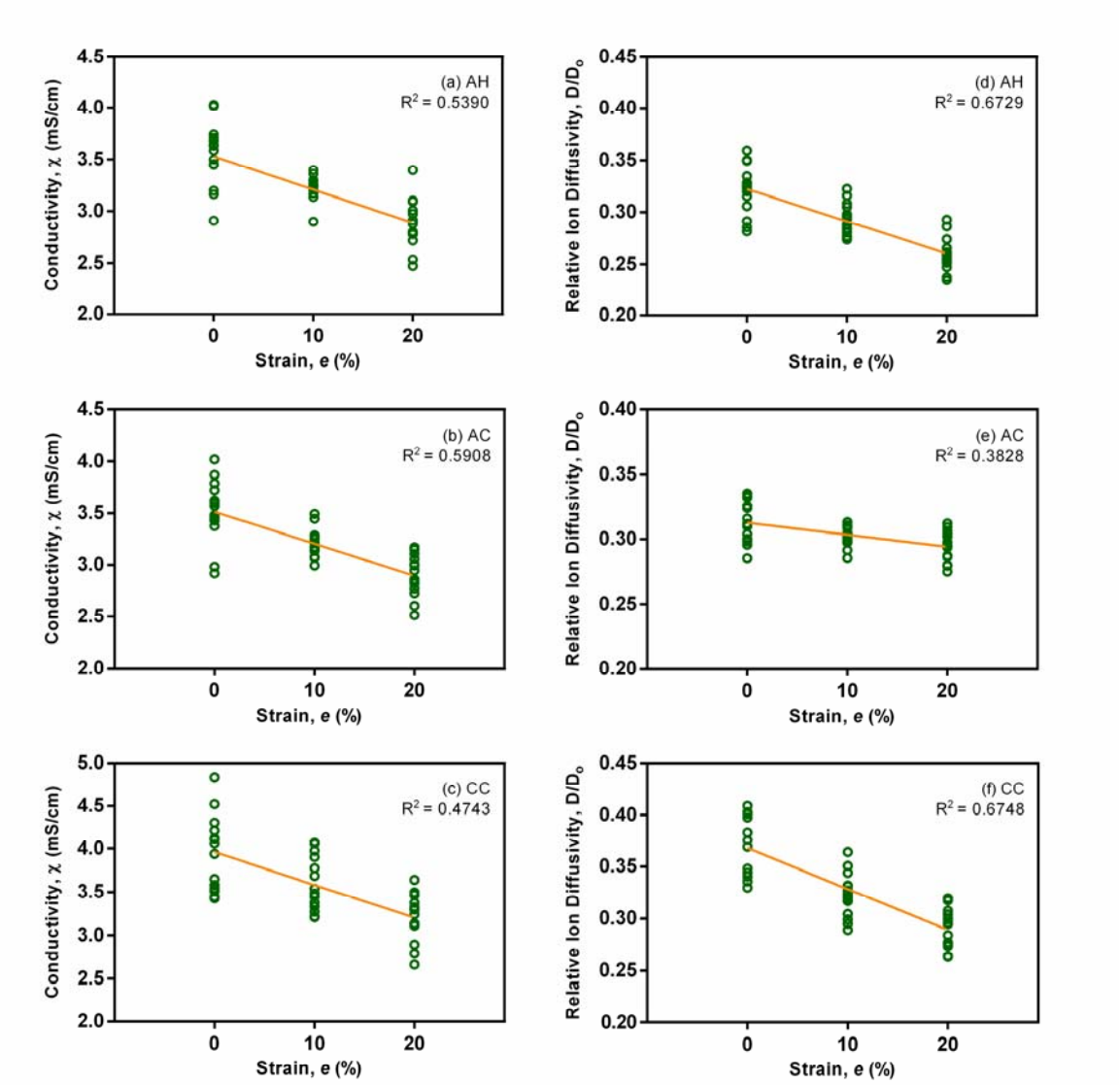

Figure 7-9 Correlation between both the electrical conductivity, χ, and the relative ion diffusion coefficient, D/D_o, and level of compressive strain, e, for three groups investigated: (a,d) Axial Horn (AH); (b,e) Axial Central (AC); and (c,f) Circumferential Central (CC). Significant correlation was detected for all groups; R^2 values are shown for each. For all groups, n=45.

The average tissue water volume fraction values of the nine groups are shown in **Table 7-1**. It should be noted that there were no significant differences in the tissue water volume fraction values or for tissue thickness levels for all specimens (values shown in **Table 7-1**), indicating that the difference in the diffusion coefficients found is not likely to be attributed to variations in tissue preparation.

In addition, we have included scatter plots (**Figure 7-10**) showing the relationship between tissue water volume fraction, ϕ^w, and both electrical conductivity, χ, and relative ion diffusion, D/D_o, for each of the three groups tested. Regression analysis revealed significant ($p<0.001$) relationships for all groups investigated. R^2 values are shown for each group in **Figure 7-10**. The values for tissue water volume fraction for compressed samples were calculated at strain levels of 10% ($e = -0.1$) and 20% ($e = -0.2$).

The average GAG content per dry weight of meniscus tissue specimens under zero compression was 14.65 ± 3.31 μg/mg; the calculated average FCD for uncompressed tissues was 0.021 ± 0.004 mEq/g wet weight. **Figure 7-11** shows scatter plots with the relationship between the estimated fixed charge density and the electrical conductivity for each group. R^2 values are shown for each of the three groups (i.e., axial horn, axial central, and circumferential central). The values for FCD were calculated based on the GAG content of the tissue samples using **Equations (7-8)** and **(7-9)**. There was a weak correlation showing an increase in fixed charge density resulting in a decreased electrical conductivity.

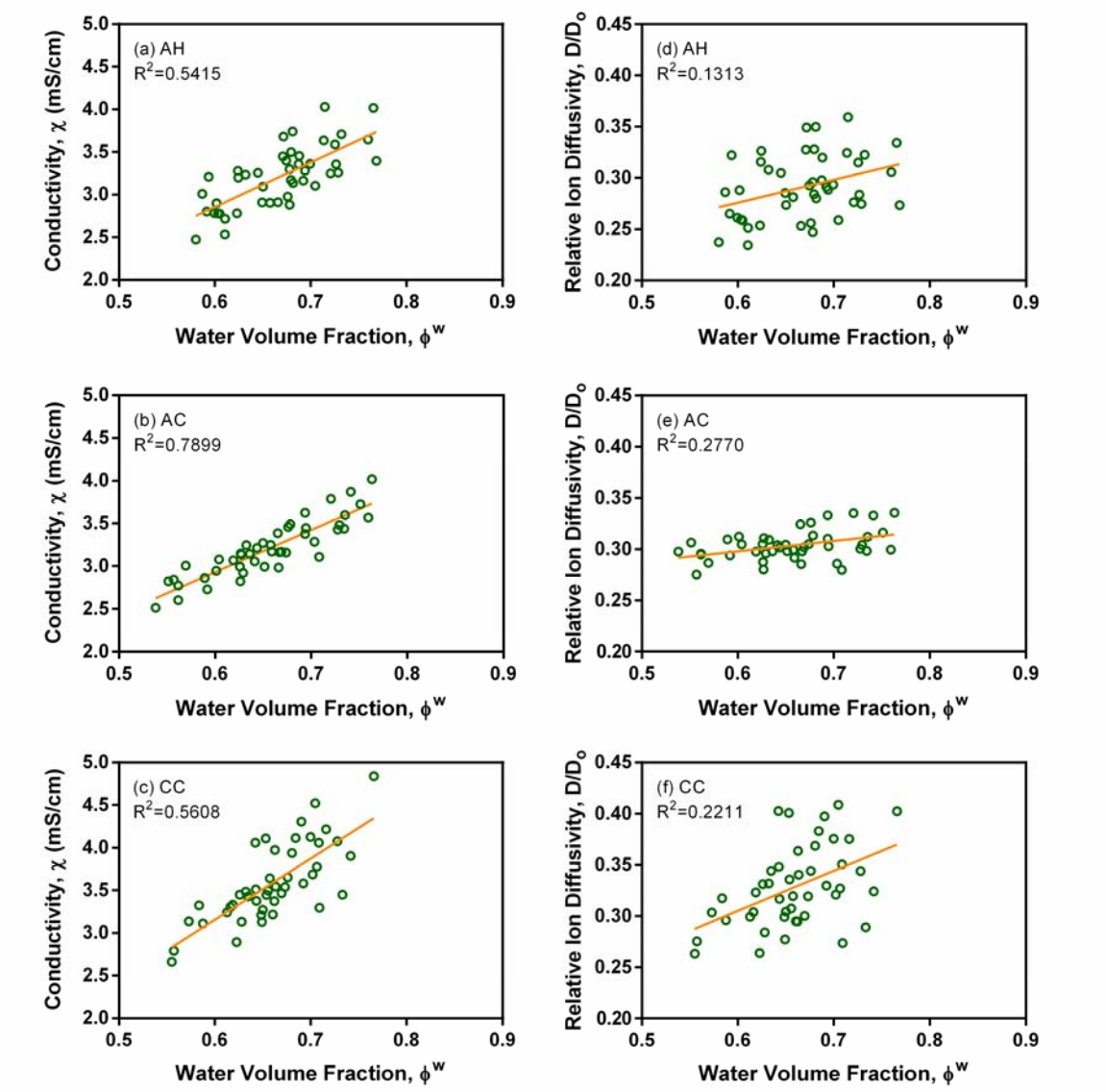

Figure 7-10 Relationship between tissue porosity, ϕ^w, and both electrical conductivity, χ, and relative ion diffusion coefficient, D/D_o, in meniscus tissues for the three groups investigated: (a,d) Axial Horn (AH); (b,e) Axial Central (AC); and (c,f) Circumferential Central (CC). Significant correlation was detected for all groups; R^2 values are shown for each. For all groups, n=45.

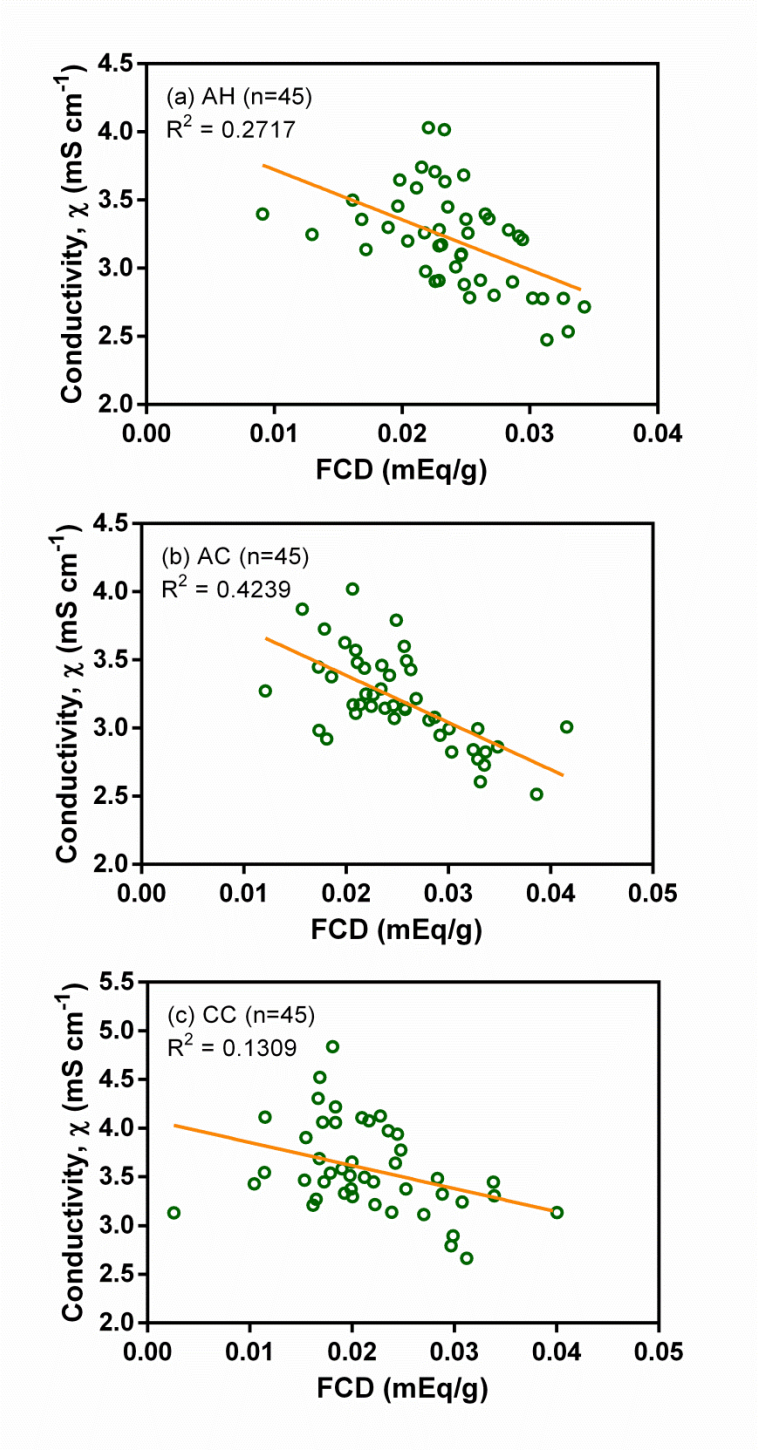

Figure 7-11 Correlation between the electrical conductivity and fixed charged density (FCD) for three groups investigated: (a) Axial Horn (AH); (b) Axial Central (AC);, and (c) Circumferential Central (CC). Significant correlation was detected for all groups; R^2 values are shown for each. For all groups, n=45.

Statistical analysis of this study is presented in **Table 7-2**, below. Two-way repeated measures ANOVA indicated that the electrical conductivity and ion diffusivity were significantly affected by both compression ($p<0.001$) and direction of diffusion ($p<0.001$) when comparing the axial central and circumferential central groups. However, two-way repeated measures ANOVA showed no significant effect of region when comparing axial central and axial horn groups ($p>0.05$), although a significant effect of compression was still seen ($p<0.001$). SIDAK post-hoc analysis indicated that the conductivity and diffusion coefficient in the circumferential direction was significantly ($p<0.001$) higher than that in the axial direction at all three levels of compression. SIDAK post-hoc analysis also showed that, for each of the groups investigated, when comparing both the electrical conductivity and ion diffusivity at 0% and 10%, 0% and 20%, and at 10% and 20% compression, results were significantly ($p<0.05$) different.

7.5 DISCUSSION

The goal of this study was to determine the effect of compressive strain, anisotropy, and tissue region on the electrical conductivity and ion diffusivity in porcine meniscus. We found significant strain-dependent and anisotropic behaviors, while no significant regional variation for conductivity or ion diffusivity in meniscus tissues was seen. Overall, our values for conductivity and ion transport are comparable to those in the literature for other cartilaginous tissues, and are most similar to values for porcine TMJ

(**Table 7-3**). This is likely because meniscus composition is most like that of TMJ tissue, which also has a relatively low GAG content as compared to articular cartilage or intervertebral disc (Almarza and Athanasiou, 2004).

7.5.1 Effect of Compression and Tissue Water Volume Fraction

The strain-dependent behavior of electrical conductivity and relative ion diffusivity found here is similar to results in the literature for other cartilaginous tissues (i.e., meniscus, articular cartilage, intervertebral disc, TMJ), which showed that static compression leads to reduced solute diffusivity and/or electrical conductivity (Jackson et al., 2009a; Jackson et al., 2008; Kleinhans et al., 2015; Kuo et al., 2011; Quinn et al., 2000; Quinn et al., 2001; Wright et al., 2013; Yuan et al., 2009). This change is likely due to reduced tissue water content caused by fluid exudation during compression. In fact, we found a significant positive correlation between conductivity and ion diffusivity and tissue water volume fraction, see **Figure 7-10**; previous studies have found similar correlations (Gu and Justiz, 2002; Gu et al., 2002; Gu et al., 2004; Jackson et al., 2009a; Kuo et al., 2011; Wright et al., 2013). Overall, these findings indicate that solute transport through the tissue is hindered by mechanical loading.

A. ***Strain-Dependent Variation***

Electrical Conductivity	**P-values**		
	AC	**AH**	**CC**
0% vs. 10%	0.001*	0.02*	0.01*
10% vs. 20%	0.0008*	0.0004*	0.009*
0% vs. 20%	8.4E-09*	4.1E-08*	7.3E-07*
Relative Ion Diffusion	**P-values**		
	AC	**AH**	**CC**
0% vs. 10%	0.003*	0.0003*	0.000002*
10% vs. 20%	0.000005*	0.00003*	0.002*
0% vs. 20%	5.2E-09*	5.1E-09*	5.1E-09*

B. ***Axial vs. Circumferential Direction***

	P-values	
Direction	1.35E-08*	2.94E-13*
Compressive Strain	8.51E-14*	1.76E-19*
Interaction	0.632*	0.001*

C. ***Axial Central vs. Horn Regional Variation***

	P-values	
Regional Location	0.933	0.381
Compressive Strain	6.11E-16*	1.26E-20*
Interaction	0.852	0.068

Table 7-2 Significance levels for post-hoc analysis of electrical conductivity and relative ion diffusion data for three comparisons: (A) strain dependent variation (tested in all 3 groups); (B) anisotropic variation: axial vs. circumferential direction (samples taken from central region of meniscus); and (C) regional specific variation: axial horn vs. axial central (samples taken in the axial direction only). Values shown are p-values; significant variation is highlighted and noted with a '*'. Two-way repeated measures ANOVA and SIDAK post-hoc analysis were performed using SPSS software.

Tissue	Direction	Conductivity (mS/cm)	Water Volume Fraction	References
Porcine meniscus	Axial	3.51 ± 0.29	0.71 ± 0.04	Present Study
	Circumferential	3.96 ± 0.42	0.68 ± 0.04	
Human TMJ disc	Axial	5.49 ± 0.97	0.77 ± 0.01	(Wright et al., 2013)
Porcine TMJ disc	Axial	3.10 ± 0.68	0.73 ± 0.02	(Kuo et al., 2011; Wright et al., 2013)
Human articular cartilage		6-10	~0.8	(Hasegawa et al., 1983)
Porcine annulus fibrosis	Axial	5.60 ± 0.89	0.74 ± 0.03	(Gu et al., 2002)
Human annulus fibrosis	Axial	7.53 ± 0.72	0.80 ± 0.02	(Jackson et al., 2009a)
	Circumferential	7.46 ± 0.9	0.79 ± 0.02	

Table 7-3 Comparison of electrical conductivity and tissue water volume fraction in uncompressed tissues between porcine meniscus and other cartilaginous tissues from the literature. Results were found at 0% compressive strain and are shown as mean ± standard deviation.

According to the equation, with each additional 10% compression, the water volume fraction of the tissue decreases by ~3-4%. The strain-dependent behavior of both conductivity and ion diffusivity indicates that mechanical loading impedes solute transport in meniscus tissues. Since the meniscus, which relies on diffusive transport for nutritional supply to resident cells, undergoes a variety of loading conditions *in vivo,* understanding how physiological loading conditions affect transport behavior in meniscus tissues may provide valuable insight into the mechanically driven causes of meniscal degeneration.

7.5.2 Effect of Anisotropy

Electrical conductivity and ion diffusivity in porcine meniscus was also found to be significantly anisotropic (i.e., direction-dependent). Both parameters were found to be significantly less in the axial direction than in the circumferential direction at all levels of compressive strain. Results also found that the electrical conductivity and relative ion diffusion coefficient in the circumferential direction was approximately respectively 1.1× and 1.2× that in the axial direction under zero strain conditions. Similar anisotropic results have been found for ion diffusion in other cartilaginous tissues.(Jackson et al., 2009a; Jackson et al., 2006) We believe this behavior is a result of the particular organization of the tissue ECM; that is, collagen fibers in meniscus are aligned along the circumferential direction, allowing for pores that are not apparent in the axial direction. This pore structure, similar to that found for other cartilaginous tissues (ap Gwynn et al., 2002; Iatridis and ap Gwynn, 2004; Jackson et al., 2009a; Kleinhans et al., 2015;

Travascio et al., 2009a), may allow ions to move more freely in the circumferential direction, parallel to the collagen fiber bundles, resulting in higher conductivity and ion transport rates. Other studies have also found the diffusion coefficient to be significantly higher in the direction parallel to collagen fibers (i.e., circumferential) in other cartilaginous tissues (Leddy et al., 2006; Stylianopoulos et al., 2010). These trends are similar to earlier findings for glucose diffusivity in porcine meniscus (Kleinhans et al., 2015).

7.5.3 Effects of Tissue Region

Our results showed no statistically significant effect when looking at the variation in the electrical conductivity and ion diffusion coefficient between axial conductivity in different tissue regions (i.e., horn versus central regions). We previously hypothesized that the electrical conductivity and relative ion diffusivity would not vary with location of the tissue specimen based on our previous study on small solute transport in the tissue (Kleinhans et al., 2015). The results are in agreement with this hypothesis and with results in the literature showing that fluid and solute transport (i.e., hydraulic permeability and glucose diffusion coefficient) in meniscus tissues is homogeneous (Kleinhans et al., 2015; Proctor et al., 1989; Sweigart et al., 2004).

Previous studies investigating mechanical properties, solute diffusivity, and fluid transport (i.e., hydraulic permeability) in meniscus have found mixed results regarding the inhomogeneity of tissue properties, see review (Makris et al., 2011). While there was no evidence of a significant difference between axial horn and axial central regions, these

findings may be attributed to several factors. Although our sample size (n=15 for each group) was large enough to see significant effects of other parameters, it is still a small collection of samples. Furthermore, regional variation was only investigated for axially oriented tissue specimens. However, because of the anisotropic trend found between axial and circumferential specimens and the dependence on the collagen structure of the tissue, conductivity and relative ion diffusivity in other directions (e.g., circumferential) may be affected by tissue region and deserves further study.

7.5.4 Relationship Between Fixed Charge Density and Conductivity

We also found a significant relationship between tissue fixed charge density and electrical conductivity (**Figure 7-11**) based on estimated values from GAG content measurements. This trend was anticipated since FCD increases when the tissue is compressed (due to reduced tissue volume). Maroudas (1968) previously noted a slight decrease in solute diffusion coefficients and tissue conductivity with increase in fixed charge density in articular cartilage; the same study also found a strong negative correlation between hydraulic permeability and FCD in articular cartilage (Maroudas, 1968). Hasegawa et al. (1983) found the opposite trend in articular cartilage, with conductivity increasing with FCD in the tissue (Hasegawa et al., 1983). Differences in results may be attributed to variable measurement techniques. Our values for GAG content of the meniscus tissues are similar to those in the literature for human meniscus tissues (Herwig et al., 1984).

7.5.6 Experimental Limitations

There are several limitations to this study that should be addressed. For example, while uniaxial confined compression does not precisely mimic the *in vivo* strain configurations in the meniscus, the data and trends gained here can be incorporated into computational models of the tissue to better understand *in vivo* conditions and predict the overall impact of mechanical loading on the tissue chemical environment.

Moreover, in order to measure the resistance across the tissues using this conductivity study, we were required to calibrate the device setup prior to measurement. To do so, we calibrated the setup by moving the wire electrodes closer to or farther from one another while the chamber was filled with a conductivity solution of known resistance. By moving the wire electrodes, we were able to calibrate the system to ensure the perfect distance between electrodes. However, when taking the chamber apart and putting it back together with a tissue inside, there was always a chance of moving the wires from their original position. While this would have changed our results, we do not believe this was a major source of error that needs additional testing. We took several measurements using the chamber before reporting the final measurement, therefore, ensuring that the chamber was properly set up and working appropriately.

Finally, as previously stated and discussed further in the future recommendations of **Chapter 8**, future studies should investigate all three primary directions (axial, radial, and circumferential) in addition to medial and lateral regions and posterior and anterior horns and degenerated tissues. This data would be beneficial for better understanding the homogenous behavior of the meniscus. Overall, the findings of this study provide

important insight and baseline quantitative information regarding the strain-dependent, anisotropic, and region-dependent behavior of electromechanical and transport properties in meniscus fibrocartilage, and establish the methods necessary to move toward full characterization of the tissue.

7.6 Summary and Conclusions

To summarize, the anisotropic, strain-dependent, and region-specific electrical conductivity and relative ion diffusion coefficient in porcine meniscus fibrocartilage was investigated. Our results suggest that the dominant contributing factor to electrical conductivity and estimated ion diffusivity in meniscus tissue is the water volume fraction, based on the significant linear correlation.

Additionally, we found that the electrical conductivity is significantly affected by tissue anisotropy, with results in the circumferential direction having a significantly higher conductivity and relative ion diffusivity values than the axial direction. Furthermore, we determined that the electrical conductivity and ion diffusivity are strain-dependent, decreasing with increasing levels of compressive strain. Lastly, there was no statistically significant difference in axial conductivity or diffusivity between the central and horn regions of the meniscus, suggesting transport behavior in meniscus tissue is homogeneous. The knee meniscus is very important to the proper function of the knee joint and plays an unknown role in the onset and progression of OA. Thus, better

understanding of both the transport environment within the tissue and the relationship with tissue structure and composition is essential in the development and treatment of tissue degeneration and related OA.

Overall, the findings of this study provide important insight and baseline quantitative information regarding the strain-dependent, anisotropic, and region-dependent behavior of electromechanical and transport properties in meniscus fibrocartilage, and establish the methods necessary to move toward full characterization of the tissue.

CHAPTER 8. CONCLUSIONS AND RECOMMENDATIONS FOR FUTURE WORK

8.1 SUMMARY AND CONCLUDING REMARKS

Every year millions of individuals are affected by osteoarthritis and must deal with both the physical pain and financial suffering involved. Degeneration of the knee meniscus is thought to play a role and may be the leading cause of pain in the knee leading to OA. Due to the avascular nature of the meniscus, poor nutritional supply is thought to be a primary etiological factor causing these degenerative changes. Knowing this, it is surprising that transport properties of the meniscus and its cells have not been adequately studied and their roles remain to be fully elucidated. Glucose, in particular, is known to be a critical nutrient necessary for cellular survival and has not yet been fully characterized in terms of transport throughout the meniscus.

Therefore, the major objectives of this dissertation were as follows: (**1**) better understand the pathophysiology involved in the development of knee meniscus injury and degeneration; and (**2**) identify effective treatment solutions for OA. In order to achieve these aims, five studies were carried out: (**1**) measurement of the anisotropic and region-specific hydraulic permeability of porcine knee meniscus (**Chapter 3**); (**2**) measurement of strain-dependent and anisotropic diffusivity of glucose in porcine meniscus (**Chapter 4**); (**3**) measurement of strain-dependent, region-specific partitioning of glucose in porcine meniscus (**Chapter 5**); (**4**) calculation of the effective diffusion coefficient based on the results from the previous glucose diffusion and glucose partition studies (**Chapter**

6); and (**5**) measurement of the strain-dependent electrical conductivity of porcine meniscus (**Chapter 7**).The most important findings from these investigations are summarized below.

8.1.1 Strain-Dependent Transport Properties in Knee Meniscus

First, a chamber was customized to measure the hydraulic permeability in porcine meniscus tissue. We have found that the permeability decreases with increasing static compression, again similar to our findings in previous studies and of other studies published in literature. These findings are all important for understanding transport pathways and mechanisms in the knee meniscus, and their relation to OA.

Next, a one-dimensional steady-state diffusion experiment was carried out to measure the apparent diffusivity of glucose in porcine meniscus. Our results indicate that diffusivity decreases as the level of static compressive strain increases. Furthermore, we have found that glucose diffusivity in porcine knee meniscus is anisotropic, being higher in the circumferential direction as compared with the axial direction. This trend was true for all areas of the meniscus (i.e., horn and central) and all directions (i.e., axial and circumferential).

The strain-dependent partition coefficient of glucose in porcine meniscus tissue was also determined using a custom-designed chamber. We have found that the partition coefficient decreases with increasing static compression, similar to our findings for glucose diffusivity. Furthermore, we found there to be no statistically significant

differences between the axial central and horn regions, nor the medial versus lateral meniscus tissues.

Finally, a one-dimensional electrical conductivity experiment was carried out to measure the ion transport in porcine meniscus. Ours results indicate that conductivity decreases as the level of compressive strain increases. Additionally, we did not find statistically significant differences between the axial horn and central regions.

8.1.2 Anisotropic Transport Properties in Knee Meniscus

Results from our studies indicated that transport properties in knee meniscus tissues are anisotropic. As our studies have shown, the alignment of collagen fibers seems to play a large role in the transporting of solutes such as nutrients and ions. With fibers running in the circumferential direction, properties of tissues cut from this direction seem to have a greater aptitude for transport than those cut in the axial direction which would be against the fiber alignment.

These results were verified in all experiments (i.e., glucose diffusion coefficient, electrical conductivity, and hydraulic permeability). Statistically significant results were found for all studies when comparing the axial central to the circumferential central region.

8.2 Recommendations for Future Work

Overall, the goal of this research was to develop strategies for the treatment and prevention of meniscal degeneration leading to OA. While the research described in this dissertation provides valuable insight into transport properties in meniscus tissues, there remains a great deal of information necessary to fully understand nutrition in the meniscus and its relation to degeneration. Here, recommendations for future work are described.

Transport properties in both the axial and circumferential directions were investigated. However, due to size restrictions, certain parameters were unable to be measured in the circumferential direction (i.e., glucose partitioning, and therefore, effective diffusion coefficient) and no studies were completed in the radial direction. Given the importance of the collagen fiber structure in the meniscus tissue for support, these studies should be investigated in the axial, circumferential, and radial directions. This would allow a more thorough understanding of transport in the meniscus and nutritional supply to the center of the tissue. Therefore, in the future, all three principal directions (i.e., axial, radial, and circumferential) should be investigated, in order to fully understand the anisotropic behavior of fluid and solute transport in the tissue. In addition, given that there are some mixed findings in previous studies as to the inhomogeneity of properties of meniscus tissues (Bursac et al., 2009; Fithian et al., 1990; Proctor et al., 1989; Sanchez-Adams et al., 2011; Sweigart et al., 2004), we should further investigate regional variations. Although we did not find any significant effect of region in any of the studies here, we were not able to distinguish between anterior and posterior horn, and we

were not able to measure properties in different directions outside the central region of the tissue. Therefore, in future studies, a more comprehensive characterization of the regional and anisotropic effects should be investigated.

Although the use of human tissues to calculate the transport properties of meniscus is preferred, we were only able to obtain porcine samples for these studies due to the easy availability of porcine knee joints. However, while we would have preferred using human tissues, it has been found that porcine meniscus tissues have similar properties to human meniscus tissues (Joshi et al., 1995; Sweigart and Athanasiou, 2005; Sweigart et al., 2004). A study by Chu *et al.* found porcine specimens to be good models for human cartilage studies, showing similarities in joint size, structure, and cartilage thickness (Chu et al., 2010). Therefore, our results using porcine tissues are expected to be indicative of trends in human meniscus, if not exact quantities. In the future, human tissues should be investigated to ensure trends in the porcine menisci match those found in human subjects.

Samples used in this dissertation came from similarly aged pigs and were considered healthy tissue. Further studies are necessary in order to understand the effects of tissue degeneration on transport behaviors in meniscus fibrocartilage. These future studies will help provide a full characterization of the nutritional transport environment within the meniscus under numerous physiologically relevant conditions.

These recommended studies would greatly enhance the results detailed in this investigation and would enable us to achieve the long-term goals of our research: to

better understand the pathophysiology involved in the development of knee meniscus injury and degeneration and to identify effective treatment solutions for osteoarthritis.

In total, we have provided the first quantitative characterization of fluid and solute transport properties in meniscus fibrocartilage. Given the importance of a healthy meniscus in the proper functioning of the knee joint, as well as the unknown role of the tissue in the onset and progression of OA, better understanding the transport environment within the tissue and the relationship with tissue pathophysiology is essential in the development of new strategies to treat and/or prevent tissue degeneration and related OA. This study provides baseline information on the structure-function relationships for fluid and solute transport properties in the meniscus and establishes the methods necessary to move toward full characterization of nutritional transport in meniscus fibrocartilage. The information herein can be used to advance the field of meniscus research, treatment, and regeneration. Our quantitative data will be useful for developing new computational models of the meniscus, which can be employed to better understand tissue functioning and pathophysiology, and may also serve as design criteria for developing novel tissue engineered approaches to treating or regenerating the tissue that closely mimic native tissue.

REFERENCES

Aagaard, H., Verdonk, R., 1999. Function of the normal meniscus and consequences of meniscal resection. Scand J Med Sci Sports 9, 134-140.

Abraham, A.C., Donahue, T.L., 2013. From meniscus to bone: a quantitative evaluation of structure and function of the human meniscal attachments. Acta Biomater 9, 6322-6329.

Allhands, R.V., Torzilli, P.A., Kallfelz, F.A., 1984. Measurement of diffusion of uncharged molecules in articular cartilage. Cornell Vet 74, 111-123.

Almarza, A.J., Athanasiou, K.A., 2004. Design characteristics for the tissue engineering of cartilaginous tissues. Annals of biomedical engineering 32, 2-17.

Andriacchi, T.P., Mundermann, A., Smith, R.L., Alexander, E.J., Dyrby, C.O., Koo, S., 2004. A framework for the in vivo pathomechanics of osteoarthritis at the knee. Annals of biomedical engineering 32, 447-457.

ap Gwynn, I., Wade, S., Ito, K., Richards, R.G., 2002. Novel aspects to the structure of rabbit articular cartilage. Eur Cell Mater 4, 18-29.

Arendt, E.A., Agel, J., Dick, R., 1999. Anterior cruciate ligament injury patterns among collegiate men and women. Journal of athletic training 34, 86-92.

Arkill, K.P., Winlove, C.P., 2008. Solute transport in the deep and calcified zones of articular cartilage. Osteoarthritis and cartilage / OARS, Osteoarthritis Research Society 16, 708-714.

Armstrong, C.G., Mow, V.C., 1982. Variations in the intrinsic mechanical properties of human articular cartilage with age, degeneration, and water content. J Bone Joint Surg 64A, 88-94.

Ateshian, G.A., Warden, W.H., Kim, J.J., Grelsamer, R.P., Mow, V.C., 1997. Finite deformation biphasic material properties of bovine articular cartilage from confined compression experiments. Journal of biomechanics 30, 1157-1164.

Athanasiou, K.A., Agarwal, A., Dzida, F.J., 1994. Comparative study of the intrinsic mechanical properties of the human acetabular and femoral head cartilage. Journal of orthopaedic research : official publication of the Orthopaedic Research Society 12, 340-349.

Athanasiou, K.A., Niederauer, G.G., Schenck, R.C., Jr., 1995. Biomechanical topography of human ankle cartilage. Ann.Biomed.Eng 23, 697-704.

Baker, B.E., Peckham, A.C., Pupparo, F., Sanborn, J.C., 1985. Review of meniscal injury and associated sports. The American journal of sports medicine 13, 1-4.

Barbour, K.E., Helmick, C.G., Boring, M., Brady, T.J., 2017. Vital signs: prevalence of doctor-diagnosed arthritis and arthritis-attributable activity limitation - United States, 2013-2015. MMWR Morb Mortal Wkly Rep 66, 246-253.

Barrett, G.R., Field, M.H., Treacy, S.H., Ruff, C.G., 1998. Clinical results of meniscus repair in patients 40 years and older. Arthroscopy : the journal of arthroscopic & related surgery : official publication of the Arthroscopy Association of North America and the International Arthroscopy Association 14, 824-829.

Bedi, A., Kelly, N.H., Baad, M., Fox, A.J., Brophy, R.H., Warren, R.F., Maher, S.A., 2010. Dynamic contact mechanics of the medial meniscus as a function of radial tear, repair, and partial meniscectomy. The Journal of bone and joint surgery. American volume 92, 1398-1408.

Berthiaume, M.J., Raynauld, J.P., Martel-Pelletier, J., Labonte, F., Beaudoin, G., Bloch, D.A., Choquette, D., Haraoui, B., Altman, R.D., Hochberg, M., Meyer, J.M., Cline, G.A., Pelletier, J.P., 2005. Meniscal tear and extrusion are strongly associated with progression of symptomatic knee osteoarthritis as assessed by quantitative magnetic resonance imaging. Annals of the rheumatic diseases 64, 556-563.

Bhattacharyya, T., Gale, D., Dewire, P., Totterman, S., Gale, M.E., McLaughlin, S., Einhorn, T.A., Felson, D.T., 2003. The clinical importance of meniscal tears demonstrated by magnetic resonance imaging in osteoarthritis of the knee. The Journal of bone and joint surgery. American volume 85-A, 4-9.

Bibby, S.R., Urban, J.P., 2004. Effect of nutrient deprivation on the viability of intervertebral disc cells. Eur Spine J 13, 695-701.

Brindle, T., Nyland, J., Johnson, D.L., 2001. The meniscus: review of basic principles with application to surgery and rehabilitation. Journal of athletic training 36, 160-169.

Bursac, P., Arnoczky, S., York, A., 2009. Dynamic compressive behavior of human meniscus correlates with its extra-cellular matrix composition. Biorheology 46, 227-237.

Bursac, P.M., Obitz, T.W., Eisenberg, S.R., Stamenovic, D., 1999. Confined and unconfined stress relaxation of cartilage: appropriateness of a transversely isotropic analysis. Journal of biomechanics 32, 1125-1130.

Burstein, D., Gray, M.L., Hartman, A.L., Gipe, R., Foy, B.D., 1993. Diffusion of small solutes in cartilage as measured by nuclear magnetic resonance (NMR) spectroscopy and imaging. Journal of orthopaedic research : official publication of the Orthopaedic Research Society 11, 465-478.

Cannon, W.D., Jr., Vittori, J.M., 1992. The incidence of healing in arthroscopic meniscal repairs in anterior cruciate ligament-reconstructed knees versus stable knees. The American journal of sports medicine 20, 176-181.

Chammas, P., Federspiel, W.J., Eisenberg, S.R., 1994. A microcontinuum model of electrokinetic coupling in the extracellular matrix: perturbation formulation and solution. Journal of Colloid and Interface Science 168, 526-538.

Changoor, A., Fereydoonzad, L., Yaroshinsky, A., Buschmann, M.D., 2010. Effects of refrigeration and freezing on the electromechanical and biomechanical properties of articular cartilage. Journal of biomechanical engineering 132, 064502.

Chen, A.C., Bae, W.C., Schinagl, R.M., Sah, R.L., 2001. Depth- and strain-dependent mechanical and electromechanical properties of full-thickness bovine articular cartilage in confined compression. Journal of biomechanics 34, 1-12.

Chia, H.N., Hull, M.L., 2008. Compressive moduli of the human medial meniscus in the axial and radial directions at equilibrium and at a physiological strain rate. Journal of orthopaedic research : official publication of the Orthopaedic Research Society 26, 951-956.

Chu, C.R., Szczodry, M., Bruno, S., 2010. Animal models for cartilage regeneration and repair. Tissue engineering. Part B, Reviews 16, 105-115.

Cisewski, S.E., Zhang, L., Kuo, J., Wright, G.J., Wu, Y., Kern, M.J., Yao, H., 2015. The effects of oxygen level and glucose concentration on the metabolism of porcine TMJ disc cells. Osteoarthritis and cartilage / OARS, Osteoarthritis Research Society 23, 1790-1796.

Clark, C.R., Ogden, J.A., 1983. Development of the menisci of the human knee joint. Morphological changes and their potential role in childhood meniscal injury. The Journal of bone and joint surgery. American volume 65, 538-547.

Cooper, C., McAlindon, T., Snow, S., Vines, K., Young, P., Kirwan, J., Dieppe, P., 1994. Mechanical and constitutional risk factors for symptomatic knee osteoarthritis: differences between medial tibiofemoral and patellofemoral disease. J Rheumatol 21, 307-313.

Danso, E.K., Honkanen, J.T., Saarakkala, S., Korhonen, R.K., 2014. Comparison of nonlinear mechanical properties of bovine articular cartilage and meniscus. Journal of biomechanics 47, 200-206.

Danzig, L.A., Hargens, A.R., Gershuni, D.H., Skyhar, M.J., Sfakianos, P.N., Akeson, W.H., 1987. Increased transsynovial transport with continuous passive motion. Journal of orthopaedic research : official publication of the Orthopaedic Research Society 5, 409-413.

de Visser, S.K., Crawford, R.W., Pope, J.M., 2008. Structural adaptations in compressed articular cartilage measured by diffusion tensor imaging. Osteoarthritis cartilage 16, 83-89.

Di Giancamillo, A., Deponti, D., Addis, A., Domeneghini, C., Peretti, G.M., 2014. Meniscus maturation in the swine model: changes occurring along with anterior to posterior and medial to lateral aspect during growth. J Cell Mol Med 18, 1964-1974.

Eckstein, F., Lemberger, B., Stammberger, T., Englmeier, K.H., Reiser, M., 2000. Patellar cartilage deformation in vivo after static versus dynamic loading. Journal of biomechanics 33, 819-825.

Eggli, S., Wegmuller, H., Kosina, J., Huckell, C., Jakob, R.P., 1995. Long-term results of arthroscopic meniscal repair. An analysis of isolated tears. The American journal of sports medicine 23, 715-720.

Eisenberg, S.R., Grodzinsky, A.J., 1988. Electrokinetic micromodel of extracellular-matrix and other poly-electrolyte networks. Physicochemical hydrodynamics 10, 517-539.

Englund, M., Niu, J., Guermazi, A., Roemer, F.W., Hunter, D.J., Lynch, J.A., Lewis, C.E., Torner, J., Nevitt, M.C., Zhang, Y.Q., Felson, D.T., 2007. Effect of meniscal damage on the development of frequent knee pain, aching, or stiffness. Arthritis and rheumatism 56, 4048-4054.

Evans, R.C., Quinn, T.M., 2005. Solute diffusivity correlates with mechanical properties and matrix density of compressed articular cartilage. Arch Biochem Biophys 442, 1-10.

Fairbank, T.J., 1948. Knee joint changes after meniscectomy. J Bone Joint Surg Br 30B, 664-670.

Farndale, R.W., Sayers, C.A., Barrett, A.J., 1982. A direct spectrophotometric microassay for sulfated glycosaminoglycans in cartilage cultures. Connect.Tissue Res 9, 247-248.

Fetter, N.L., Leddy, H.A., Guilak, F., Nunley, J.A., 2006. Composition and transport properties of human ankle and knee cartilage. Journal of orthopaedic research : official publication of the Orthopaedic Research Society 24, 211-219.

Filidoro, L., Dietrich, O., Weber, J., Rauch, E., Oerther, T., Wick, M., Reiser, M.F., Glaser, C., 2005. High-resolution diffusion tensor imaging of human patellar cartilage: feasibility and preliminary findings. Magnetic resonance in medicine : official journal of the Society of Magnetic Resonance in Medicine / Society of Magnetic Resonance in Medicine 53, 993-998.

Fithian, D.C., Kelly, M.A., Mow, V.C., 1990. Material properties and structure-function relationships in the menisci. Clinical orthopaedics and related research, 19-31.

Frank, E.H., Grodzinsky, A.J., 1987. Cartilage electromechanics--I. Electrokinetic transduction and the effects of electrolyte pH and ionic strength. J.Biomech. 20, 615-627.

Frank, E.H., Grodzinsky, A.J., Phillips, S.L., Grimshaw, P.E., 1990. Physiochemical and bioelectrical determinants of cartilage material properties, in: Mow, V.C., Wood, D.O., Woo, S.L. (Eds.), Biomechanics of Diarthrodial Joints. Spring-Verlag, New York, pp. 261-282.

Froimson, M.I., Ratcliffe, A., Gardner, T.R., Mow, V.C., 1997. Differences in patellofemoral joint cartilage material properties and their significance to the etiology of cartilage surface fibrillation. Osteoarthritis cartilage 5, 377-386.

Gabrion, A., Aimedieu, P., Laya, Z., Havet, E., Mertl, P., Grebe, R., Laude, M., 2005. Relationship between ultrastructure and biomechanical properties of the knee meniscus. Surgical and radiologic anatomy : SRA 27, 507-510.

Garcia, A.M., Szasz, N., Trippel, S.B., Morales, T.I., Grodzinsky, A.J., Frank, E.H., 2003. Transport and binding of insulin-like growth factor I through articular cartilage. Arch Biochem Biophys 415, 69-79.

Ghadially, F.N., Thomas, I., Yong, N., Lalonde, J.M., 1978. Ultrastructure of rabbit semilunar cartilages. Journal of anatomy 125, 499-517.

Greis, P.E., Bardana, D.D., Holmstrom, M.C., Burks, R.T., 2002. Meniscal injury: I. Basic science and evaluation. The Journal of the American Academy of Orthopaedic Surgeons 10, 168-176.

Grodzinsky, A.J., 1983. Electromechanical and physicochemical properties of connective tissue. Crit Rev.Biomed.Eng 9, 133-199.

Gu, W.Y., Justiz, M.A., 2002. Apparatus for measuring the swelling dependent electrical conductivity of charged hydrated soft tissues. J Biomech Engng 124, 790-793.

Gu, W.Y., Justiz, M.A., Yao, H., 2002. Electrical conductivity of lumbar annulus fibrosis: Effects of porosity and fixed charge density. Spine 27, 2390-2395.

Gu, W.Y., Lai, W.M., Mow, V.C., 1993. Transport of fluid and ions through a porous-permeable charged-hydrated tissue, and streaming potential data on normal bovine articular cartilage. Journal of biomechanics 26, 709-723.

Gu, W.Y., Lai, W.M., Mow, V.C., 1998. A mixture theory for charged-hydrated soft tissues containing multi- electrolytes: passive transport and swelling behaviors. Journal of Biomechanical Engineering 120, 169-180.

Gu, W.Y., Lewis, B., Lai, W.M., Ratcliffe, A., Mow, V.C., 1996. A technique for measuring volume and true density of the solid matrix of cartilaginous tissues. Advances in Bioengineering, ASME BED33, 89-90.

Gu, W.Y., Lewis, B., Saed-Nejad, F., Lai, W.M., Ratcliffe, A., 1997. Hydration and true denstiy of normal and PG-depleted bovine articular cartilage. Trans Orthop Res Soc 22, 826.

Gu, W.Y., Mao, X.G., Foster, R.J., Weidenbaum, M., Mow, V.C., Rawlins, B.A., 1999. The anisotropic hydraulic permeability of human lumbar anulus fibrosus. Influence of age, degeneration, direction, and water content. Spine 24, 2449-2455.

Gu, W.Y., Yao, H., 2003. Effects of hydration and fixed charge density on fluid transport in charged hydrated soft tissue. Annals of biomedical engineering 31, 1162-1170.

Gu, W.Y., Yao, H., Huang, C.Y., Cheung, H.S., 2003a. New insight into deformation-dependent hydraulic permeability of gels and cartilage, and dynamic behavior of agarose gels in confined compression. Journal of biomechanics 36, 593-598.

Gu, W.Y., Yao, H., Vega, A.L., 2003b. Effect of water volume fraction on electrical conductivity and ion diffusivity in agarose gels, Mechanics of Physicochemical and Electromechanical Interactions in Porous Media. Kluwer Academic Publishers, p. (in press).

Gu, W.Y., Yao, H., Vega, A.L., Flagler, D., 2004. Diffusivity of ions in agarose gels and intervertebral disc: Effect of porosity Annals of biomedical engineering 32, 1710-1717.

Hardingham, T.E., A., F., 1992. Proteoglycans: many forms and many functions. FASEB J, 143-183.

Hasegawa, I., Kuriki, S., Matsuno, S., Matsumoto, G., 1983. Dependence of electrical conductivity on fixed charge density in articular cartilage. Clin Orthop, 283-288.

Hayat, M.A., 1982. Fixation for electron microscope. Academic Press, New York.

Helfferich, F., 1962. Ion exchange. McGraw Hill Book Company, Inc, New York.

Herwig, J., Egner, E., Buddecke, E., 1984. Chemical-changes of human knee-joint menisci in various stages of degeneration. Annals of the rheumatic diseases 43, 635-640.

Heywood, H.K., Bader, D.L., Lee, D.A., 2006a. Glucose concentration and medium volume influence cell viability and glycosaminoglycan synthesis in chondrocyte-seeded alginate constructs. Tissue engineering 12, 3487-3496.

Heywood, H.K., Bader, D.L., Lee, D.A., 2006b. Rate of oxygen consumption by isolated articular chondrocytes is sensitive to medium glucose concentration. J.Cell Physiol 206, 402-410.

Holm, S., Maroudas, A., Urban, J.P., Selstam, G., Nachemson, A., 1981. Nutrition of the intervertebral disc: solute transport and metabolism. Connect.Tissue Res 8, 101-119.

Hsu, E.W., Setton, L.A., 1999. Diffusion tensor microscopy of the intervertebral disc anulus fibrosus. Magnetic resonance in medicine : official journal of the Society of Magnetic Resonance in Medicine / Society of Magnetic Resonance in Medicine 41, 992-999.

Iatridis, J.C., ap Gwynn, I., 2004. Mechanisms for mechanical damage in the intervertebral disc annulus fibrosus. Journal of biomechanics 37, 1165-1175.

Imler, S.M., Doshi, A.N., Levenston, M.E., 2004. Combined effects of growth factors and static mechanical compression on meniscus explant biosynthesis. Osteoarthritis cartilage 12, 736-744.

Jackson, A.R., Gu, W.Y., 2009. Transport properties of cartilaginous tissues. Curr Rheum Rev 5, 40-50.

Jackson, A.R., Travascio, F., Gu, W.Y., 2009a. Effect of mechanical loading on electrical conductivity in human intervertebral disk. J Biomech Eng 131, 054505-054501-054505-054505.

Jackson, A.R., Yao, H., Brown, M.D., Gu, W.Y., 2006. Anisotropic ion diffusivity in intervertebral disc: an electrical conductivity approach. Spine 31, 2783-2789.

Jackson, A.R., Yuan, T.Y., Huang, C.Y., Brown, M.D., Gu, W.Y., 2012. Nutrient transport in human annulus fibrosus is affected by compressive strain and anisotropy. Annals of biomedical engineering 40, 2551-2558.

Jackson, A.R., Yuan, T.Y., Huang, C.Y., Gu, W.Y., 2009b. A conductivity approach to measuring fixed charge density in intervertebral disc tissue. Annals of biomedical engineering 37, 2566-2573.

Jackson, A.R., Yuan, T.Y., Huang, C.Y., Travascio, F., Gu, W.Y., 2008. Effect of compression and anisotropy on the diffusion of glucose in annulus fibrosus. Spine 33, 1-7.

Johnson, R.J., Kettelkamp, D.B., Clark, W., Leaverton, P., 1974. Factors effecting late results after meniscectomy. The Journal of bone and joint surgery. American volume 56, 719-729.

Jones, J.C., Burks, R., Owens, B.D., Sturdivant, R.X., Svoboda, S.J., Cameron, K.L., 2012. Incidence and risk factors associated with meniscal injuries among active-duty US military service members. Journal of athletic training 47, 67-73.

Joshi, M.D., Suh, J.K., Marui, T., Woo, S.L., 1995. Interspecies variation of compressive biomechanical properties of the meniscus. J Biomed Mater Res 29, 823-828.

Jurvelin, J.S., Buschmann, M.D., Hunziker, E.B., 2003. Mechanical anisotropy of the human knee articular cartilage in compression. Proceedings of the Institution of Mechanical Engineers. Part H, Journal of engineering in medicine 217, 215-219.

Katchalsky, A., Curran, P.F., 1975. Nonequilibrium thermodynamics in biophysics. Harvard University Press, Cambridge, MA.

Katz, M.M., Hargens, A.R., Garfin, S.R., 1986. Intervertebral disc nutrition. Diffusion versus convection. Clin.Orthop, 243-245.

Killian, M.L., Lepinski, N.M., Haut, R.C., Haut Donahue, T.L., 2010. Regional and zonal histo-morphological characteristics of the lapine menisci. Anat Rec (Hoboken) 293, 1991-2000.

Kleinhans, K.L., Jackson, A.R., 2017. Effect of strain, region, and tissue composition on glucose partitioning in meniscus fibrocartilage. Journal of biomechanical engineering 139, 034502-034502-034506.

Kleinhans, K.L., Jaworski, L.M., Schneiderbauer, M.M., Jackson, A.R., 2015. Effect of static compressive strain, anisotropy, and tissue region on the diffusion of glucose in meniscus fibrocartilage. Journal of biomechanical engineering 137, 101004-101004.

Kleinhans, K.L., McMahan, J.B., Jackson, A.R., 2016. Electrical conductivity and ion diffusion in porcine meniscus: effects of strain, anisotropy, and tissue region. Journal of biomechanics 49, 3041-3046.

Kohn, D., Moreno, B., 1995. Meniscus insertion anatomy as a basis for meniscus replacement: a morphological cadaveric study. Arthroscopy : the journal of arthroscopic & related surgery : official publication of the Arthroscopy Association of North America and the International Arthroscopy Association 11, 96-103.

Korhonen, R.K., Laasanen, M.S., Toyras, J., Rieppo, J., Hirvonen, J., Helminen, H.J., Jurvelin, J.S., 2002. Comparison of the equilibrium response of articular cartilage in unconfined compression, confined compression and indentation. Journal of biomechanics 35, 903-909.

Kotlarz, H., Gunnarsson, C.L., Fang, H., Rizzo, J.A., 2009. Insurer and out-of-pocket costs of osteoarthritis in the US: evidence from national survey data. Arthritis and rheumatism 60, 3546-3553.

Krause, W.R., Pope, M.H., Johnson, R.J., Wilder, D.G., 1976. Mechanical changes in the knee after meniscectomy. The Journal of bone and joint surgery. American volume 58, 599-604.

Kuo, J., Wright, G.J., Bach, D.E., Slate, E.H., Yao, H., 2011. Effect of mechanical loading on electrical conductivity in porcine TMJ discs. J Dent Res 90, 1216-1220.

Kurosawa, H., Fukubayashi, T., Nakajima, H., 1980. Load-bearing mode of the knee joint: physical behavior of the knee joint with or without menisci. Clin Orthop Relat Res, 283-290.

Kusayama, T., Harner, C.D., Carlin, G.J., Xerogeanes, J.W., Smith, B.A., 1994. Anatomical and biomechanical characteristics of human meniscofemoral ligaments. Knee Surg Sports Traumatol Arthrosc 2, 234-237.

Lai, W.M., Hou, J.S., Mow, V.C., 1991. A triphasic theory for the swelling and deformation behaviors of articular cartilage. J Biomech Eng 113, 245-258.

Lai, W.M., Mow, V.C., 1980. Drag-induced compression of articular cartilage during a permeation experiment. Biorheology 17, 111-123.

Lange, A.K., Fiatarone Singh, M.A., Smith, R.M., Foroughi, N., Baker, M.K., Shnier, R., Vanwanseele, B., 2007. Degenerative meniscus tears and mobility impairment in women with knee osteoarthritis. Osteoarthritis cartilage 15, 701-708.

Leddy, H.A., Haider, M.A., Guilak, F., 2006. Diffusional anisotropy in collagenous tissues: fluorescence imaging of continuous point photobleaching. Biophysical journal 91, 311-316.

LeRoux, M.A., Setton, L.A., 2002. Experimental and biphasic FEM determinations of the material properties and hydraulic permeability of the meniscus in tension. J Biomech Eng 124, 315-321.

Leslie, B.W., Gardner, D.L., McGeough, J.A., Moran, R.S., 2000. Anisotropic response of the human knee joint meniscus to unconfined compression. Proceedings of the Institution of Mechanical Engineers. Part H, Journal of engineering in medicine 214, 631-635.

Longsworth, L.G., 1953. Diffusion measurements, at 25 o C, of aqueous solutions of amino acids, peptides, and sugars. J Am Chem Soc 75, 5705-5709.

Mackie, J.S., Meares, P., 1955. The Diffusion of Electrolytes in a Cation-Exchange Resin Membrane .1. Theoretical. Proc R Soc Lon Ser-A 232, 498-509.

Makris, E.A., Hadidi, P., Athanasiou, K.A., 2011. The knee meniscus: structure-function, pathophysiology, current repair techniques, and prospects for regeneration. Biomaterials 32, 7411-7431.

Malda, J., Rouwkema, J., Martens, D.E., Le Comte, E.P., Kooy, F.K., Tramper, J., van Blitterswijk, C.A., Riesle, J., 2004. Oxygen gradients in tissue-engineered PEGT/PBT cartilaginous constructs: measurement and modeling. Biotechnol.Bioeng. 86, 9-18.

Mansour, J.M., Mow, V.C., 1976. The permeability of articular cartilage under compressive strain and at high pressures. J Bone Joint Surg Am. 58, 509-516.

Maroudas, A., 1968. Physicochemical properties of cartilage in the light of ion exchange theory. Biophys.J 8, 575-595.

Maroudas, A., 1970. Distribution and diffusion of solutes in articular cartilage. Biophysical journal 10, 365-379.

Maroudas, A., 1975. Biophysical chemistry of cartilaginous tissues with special reference to solute and fluid transport. Biorheology 12, 233-248.

Maroudas, A., 1976. Transport of solutes through cartilage: permeability to large molecules. Journal of anatomy 122, 335-347.

Maroudas, A., 1979. Physicochemical properties of articular cartilage, in: Freeman, M.A.R. (Ed.), Adult Articular Cartilage. Pitman Medical, pp. 215-290.

Maroudas, A., Bullough, P., Swanson, S.A., Freeman, M.A., 1968. The permeability of articular cartilage. J Bone Joint Surg Br. 50, 166-177.

Maroudas, A., Stockwell, R.A., Nachemson, A., Urban, J., 1975. Factors involved in the nutrition of the human lumbar intervertebral disc: cellularity and diffusion of glucose in vitro. J Anat. 120, 113-130.

Martin Seitz, A., Galbusera, F., Krais, C., Ignatius, A., Durselen, L., 2013. Stress-relaxation response of human menisci under confined compression conditions. Journal of the mechanical behavior of biomedical materials 26, 68-80.

McAlindon, T.E., Cooper, C., Kirwan, J.R., Dieppe, P.A., 1993. Determinants of disability in osteoarthritis of the knee. Annals of the rheumatic diseases 52, 258-262.

McDermott, I.D., Sharifi, F., Bull, A.M., Gupte, C.M., Thomas, R.W., Amis, A.A., 2004. An anatomical study of meniscal allograft sizing. Knee Surg Sports Traumatol Arthrosc 12, 130-135.

McDevitt, C.A., Webber, R.J., 1990. The ultrastructure and biochemistry of meniscal cartilage. Clinical orthopaedics and related research, 8-18.

McGonagle, D., Tan, A.L., Carey, J., Benjamin, M., 2010. The anatomical basis for a novel classification of osteoarthritis and allied disorders. Journal of anatomy 216, 279-291.

Meder, R., de Visser, S.K., Bowden, J.C., Bostrom, T., Pope, J.M., 2006. Diffusion tensor imaging of articular cartilage as a measure of tissue microstructure. Osteoarthritis and cartilage / OARS, Osteoarthritis Research Society 14, 875-881.

Morgan, C.D., Wojtys, E.M., Casscells, C.D., Casscells, S.W., 1991. Arthroscopic meniscal repair evaluated by second-look arthroscopy. The American journal of sports medicine 19, 632-637; discussion 637-638.

Morrison, J.B., 1969. Function of the knee joint in various activities. Biomed Eng 4, 573-580.

Mow, V.C., Holmes, M.H., Lai, W.M., 1984. Fluid transport and mechanical properties of articular cartilage: a review. Journal of biomechanics 17, 377-394.

Mow, V.C., Kuei, S.C., Lai, W.M., Armstrong, C.G., 1980. Biphasic creep and stress relaxation of articular cartilage in compression: Theory and experiments. J Biomech Eng 102, 73-84.

Mow, V.C., Wang, C.C., Hung, C.T., 1999. The extracellular matrix, interstitial fluid and ions as a mechanical signal transducer in articular cartilage. Osteoarthritis.Cartilage. 7, 41-58.

Newman, A.P., Anderson, D.R., Daniels, A.U., Dales, M.C., 1989. Mechanics of the healed meniscus in a canine model. The American journal of sports medicine 17, 164-175.

Nguyen, A.M., Levenston, M.E., 2012. Comparison of osmotic swelling influences on meniscal fibrocartilage and articular cartilage tissue mechanics in compression and shear. Journal of orthopaedic research : official publication of the Orthopaedic Research Society 30, 95-102.

Ngwa, W., Geier, O., Stallmach, F., Naji, L., Schiller, J., Arnold, K., 2002. Cation diffusion in cartilage measured by pulsed field gradient NMR. Eur Biophys J 31, 73-80.

Nimer, E., Schneiderman, R., Maroudas, A., 2003. Diffusion and partition of solutes in cartilage under static load. Biophycal Chemistry 106, 125-146.

O'Hara, B.P., Urban, J.P., Maroudas, A., 1990. Influence of cyclic loading on the nutrition of articular cartilage. Annals of the rheumatic diseases 49, 536-539.

Pai, Y.C., Rymer, W.Z., Chang, R.W., Sharma, L., 1997. Effect of age and osteoarthritis on knee proprioception. Arthritis and rheumatism 40, 2260-2265.

Proctor, C.S., Schmidt, M.B., Whipple, R.R., Kelly, M.A., Mow, V.C., 1989. Material properties of the normal medial bovine meniscus. Journal of orthopaedic research : official publication of the Orthopaedic Research Society 7, 771-782.

Quinn, T.M., Kocian, P., Meister, J.J., 2000. Static compression is associated with decreased diffusivity of dextrans in cartilage explants. Arch Biochem Biophys 384, 327-334.

Quinn, T.M., Morel, V., Meister, J.J., 2001. Static compression of articular cartilage can reduce solute diffusivity and partitioning: implications for the chondrocyte biological response. Journal of biomechanics 34, 1463-1469.

Reynaud, B., Quinn, T.M., 2006. Anisotropic hydraulic permeability in compressed articular cartilage. Journal of biomechanics 39, 131-137.

Richardson, S., Neama, G., Phillips, T., Bell, S., Carter, S.D., Moley, K.H., Moley, J.F., Vannucci, S.J., Mobasheri, A., 2003. Molecular characterization and partial cDNA cloning of facilitative glucose transporters expressed in human articular chondrocytes; stimulation of 2-deoxyglucose uptake by IGF-I and elevated MMP-2 secretion by glucose deprivation. Osteoarthritis and cartilage / OARS, Osteoarthritis Research Society 11, 92-101.

Roberts, S., Urban, J.P., Evans, H., Eisenstein, S.M., 1996. Transport properties of the human cartilage endplate in relation to its composition and calcification. Spine 21, 415-420.

Sanchez-Adams, J., Willard, V.P., Athanasiou, K.A., 2011. Regional variation in the mechanical role of knee meniscus glycosaminoglycans. J Appl Physiol 111, 1590-1596.

Schneiderman, R., Snir, E., Popper, O., Hiss, J., Stein, H., Maroudas, A., 1995. Insulin-like growth factor-I and its complexes in normal human articular cartilage: studies of partition and diffusion. Arch.Biochem.Biophys., 159-172.

Seedhom, B.B., Dowson, D., Wright, V., 1974. Proceedings: Functions of the menisci. A preliminary study. Ann Rheum Dis 33, 111.

Setton, L.A., Zhu, W.B., Mow, V.C., 1993. The biphasic poroviscoelastic behavior of articular cartilage: Role of the surface zone in governing the compressive behavior. J Biomechanics 26, 581-592.

Shaffer, B., Kennedy, S., Klimkiewicz, J., Yao, L., 2000. Preoperative sizing of meniscal allografts in meniscus transplantation. The American journal of sports medicine 28, 524-533.

Shi, C., Wright, G.J., Ex-Lubeskie, C.L., Bradshaw, A.D., Yao, H., 2013. Relationship between anisotropic diffusion properties and tissue morphology in porcine TMJ disc. Osteoarthritis and cartilage / OARS, Osteoarthritis Research Society 21, 625-633.

Skaggs, D.L., Warden, W.H., Mow, V.C., 1994. Radial tie fibers influence the tensile properties of the bovine medial meniscus. Journal of orthopaedic research : official publication of the Orthopaedic Research Society 12, 176-185.

Soltz, M.A., Ateshian, G.A., 2000. Interstitial fluid pressurization during confined compression cyclical loading of articular cartilage. Ann.Biomed.Eng 28, 150-159.

Spilker, R.L., Donzelli, P.S., Mow, V.C., 1992. A transversely isotropic biphasic finite element model of the meniscus. Journal of biomechanics 25, 1027-1045.

Stylianopoulos, T., Diop-Frimpong, B., Munn, L.L., Jain, R.K., 2010. Diffusion anisotropy in collagen gels and tumors: the effect of fiber network orientation. Biophysical journal 99, 3119-3128.

Sweigart, M.A., Athanasiou, K.A., 2001. Toward tissue engineering of the knee meniscus. Tissue Eng 7, 111-129.

Sweigart, M.A., Athanasiou, K.A., 2005. Biomechanical characteristics of the normal medial and lateral porcine knee menisci. Proceedings of the Institution of Mechanical Engineers. Part H, Journal of engineering in medicine 219, 53-62.

Sweigart, M.A., Zhu, C.F., Burt, D.M., DeHoll, P.D., Agrawal, C.M., Clanton, T.O., Athanasiou, K.A., 2004. Intraspecies and interspecies comparison of the compressive properties of the medial meniscus. Annals of biomedical engineering 32, 1569-1579.

Tissakht, M., Ahmed, A.M., 1995. Tensile stress-strain characteristics of the human meniscal material. Journal of biomechanics 28, 411-422.

Tissakht, M., Ahmed, A.M., Chan, K.C., 1996. Calculated stress-shielding in the distal femur after total knee replacement corresponds to the reported location of bone loss. Journal of orthopaedic research : official publication of the Orthopaedic Research Society 14, 778-785.

Torzilli, P.A., 1993. Effects of temperature, concentration and articular surface removal on transient solute diffusion in articular cartilage. Medical & biological engineering & computing 31 Suppl, S93-98.

Torzilli, P.A., Adams, T.C., Mis, R.J., 1987. Transient solute diffusion in articular cartilage. Journal of biomechanics 20, 203-214.

Torzilli, P.A., Arduino, J.M., Gregory, J.D., Bansal, M., 1997. Effect of proteoglycan removal on solute mobility in articular cartilage. Journal of biomechanics 30, 895-902.

Torzilli, P.A., Grande, D.A., Arduino, J.M., 1998. Diffusive properties of immature articular cartilage. J Biomed Mater.Res 40, 132-138.

Travascio, F., Gu, W.Y., 2007. Anisotropic diffusive transport in annulus fibrosus: experimental determination of the diffusion tensor by FRAP technique. Ann Biomed Eng 35, 1739-1748.

Travascio, F., Jackson, A.R., Brown, M.D., Gu, W.Y., 2009a. Relationship between solute transport properties and tissue morphology in human annulus fibrosus. Journal of orthopaedic research : official publication of the Orthopaedic Research Society 27, 1625-1630.

Travascio, F., Zhao, W., Gu, W.Y., 2009b. Characterization of anisotropic diffusion tensor of solute in tissue by video-FRAP imaging technique. Annals of Biomed Engng 37, 813-823.

Upton, M.L., Chen, J., Guilak, F., Setton, L.A., 2003. Differential effects of static and dynamic compression on meniscal cell gene expression. Journal of orthopaedic research : official publication of the Orthopaedic Research Society 21, 963-969.

Urban, J.P., 2000. Present perspectives on cartilage and chondrocyte mechanobiology. Biorheology 37, 185-190.

Urban, J.P., Holm, S., Maroudas, A., 1978. Diffusion of small solutes into the intervertebral disc: as in vivo study. Biorheology 15, 203-221.

Urban, J.P., Holm, S., Maroudas, A., Nachemson, A., 1982. Nutrition of the intervertebral disc: Effect of fluid flow on solute transport. Clin Orthop 170, 296-302.

Urban, J.P.G., Holms, S., Maroudas, A., Nachemson, A., 1977. Nutrition of the intervertebral disc: An in vivo study of solute transport. Clin Orthop 129, 101-114.

Walker, P.S., Erkman, M.J., 1975. The role of the menisci in force transmission across the knee. Clin Orthop Relat Res, 184-192.

Weiss, J.A., Maakestad, B.J., 2006. Permeability of human medial collateral ligament in compression transverse to the collagen fiber direction. Journal of biomechanics 39, 276-283.

White, A.G., Birnbaum, H.G., Janagap, C., Buteau, S., Schein, J., 2008. Direct and indirect costs of pain therapy for osteoarthritis in an insured population in the United States. Journal of occupational and environmental medicine / American College of Occupational and Environmental Medicine 50, 998-1005.

Wright, G.J., Kuo, J., Shi, C., Bacro, T.R., Slate, E.H., Yao, H., 2013. Effect of mechanical strain on solute diffusion in human TMJ discs: an electrical conductivity study. Annals of biomedical engineering 41, 2349-2357.

Wu, Y., Cisewski, S.E., Sachs, B.L., Pellegrini, V.D., Jr., Kern, M.J., Slate, E.H., Yao, H., 2015. The region-dependent biomechanical and biochemical properties of bovine cartilaginous endplate. Journal of biomechanics 48, 3185-3191.

Yang, N.H., Canavan, P.K., Nayeb-Hashemi, H., Najafi, B., Vaziri, A., 2010. Protocol for constructing subject-specific biomechanical models of knee joint. Computer methods in biomechanics and biomedical engineering 13, 589-603.

Yuan, T.Y., Huang, C.Y., Yong Gu, W., 2011. Novel technique for online characterization of cartilaginous tissue properties. J Biomech Eng 133, 094504.

Yuan, T.Y., Jackson, A.R., Huang, C.Y., Gu, W.Y., 2009. Strain-dependent oxygen diffusivity in bovine annulus fibrosus. J Biomech Eng 131, 074503-074501-074503-074504.

Zhu, W., Chern, K.Y., Mow, V.C., 1994. Anisotropic viscoelastic shear properties of bovine meniscus. Clinical orthopaedics and related research, 34-45.